UNIVERSITY OF CALIFORNIA
RIVERSIDE

Secondary Aerosol Formation from the Oxidation of Amines and Reduced Sulfur Compounds

A Dissertation submitted in partial satisfaction
of the requirements for the degree of

Doctor of Philosophy

in

Chemical & Environmental Engineering

by

Paul Steven Van Rooy

September 2019

Dissertation Committee:
Dr. David R. Cocker III
Dr. Kelley Barsanti
Dr. Kathleen Purvis-Roberts

The Dissertation of Paul Steven Van Rooy is approved:

_____

_____

_____

_____

Committee Chairperson

University of California, Riverside

Acknowledgements:

Looking back at the past five years of trial and error, set back after set back, constant troubleshooting, non-stop experimentation, and finally the sweet taste of accomplishment, one quotation comes to mind that best summarizes my current mental state:

I decided I was a lemon for a couple of weeks. I kept myself amused all the time jumping in and out of a gin and tonic.

-Douglas Adams, Life, the Universe and Everything

Conducting this research has been a weird journey. There were times when I questioned the importance of what I was doing. There have been times when it felt like I was not making any progress in my research. There were times when I felt burnt-out. There were even times when I doubted my intelligence and my ability to complete the task at hand. The amount of useless information I have learned, or stumbled across, in the past five years can only be exceeded (ever so slightly) by the amount of useful information I have taken in. Despite all of this, I never stopped having fun and I never stopped loving what I was working on. I hope future generations of researchers find comfort in these remarks (does anyone actually read these things?). You do not have to be the most intelligent student in your class to be a successful PhD candidate. You need to have a drive to succeed, a good work ethic, and you need to love what you are doing. And I guess you need to be at least kind of smart.

There are many people I owe a great deal of gratitude to as this chapter of my life comes to a close. Most importantly, I need to thank my beautiful wife, who is graciously pouring me a cup of coffee as I write this. Abbey, I could not have gotten through this

process without your support. Your flexibility and willingness to put your dreams on hold so I can follow mine is not lost on me. Our time spent together eating tacos at Tuxies, buying unnecessary old things at estate sales and thrift stores, enjoying beers at Hangar 24, digging through old vinyl, taking trips with the dogs, and talking about anything besides atmospheric chemistry has served as a much needed escape from the world of research. You've made me a well-rounded person. Thanks for putting up with me.

I also need to thank our two dogs, Lyla and Mulder, who kept me as close to stress-free as possible. There are very few things that feel better than coming home after a long, frustrating day and being greeted with kisses by two over-excited little pups.

A major reason this process has been so much fun for me is because of my excellent research advisor, Dr. David Cocker. David, the amount you have taught me about instruments, atmospheric chemistry, and experimentation over the course of my PhD research is almost unbearable. I truly appreciate the freedom and flexibility you have provided that has allowed me to be creative, try new things, and really make this project my own. The trust you have put in me to take charge of the lab has transformed me from a passive bystander into a confident leader. I honestly could not have asked for a better PhD advisor.

I would also like to thank Dr. Katie Purvis-Roberts, who has been encouraging and supportive throughout every peak and valley of my PhD career. Your confidence in me and my work has motivated me to do my very best. Your optimism has been contagious. Thanks for always being on my team and keeping my best interests in mind.

Additionally, I need to thank my third committee member, Dr. Kelley Barsanti. I appreciate the times I was able to talk with you at length about your academic journey; these conversations were quite impactful for me. You have been a source of guidance to me and supplied me with pleasant alternate point of view. Your endless hard work, selflessness, and drive is an inspiration. I am very excited to be working with you in the coming years. I am grateful for the opportunity.

A big thank you to my family. To my mother, who has provided unconditional support as I have gone through this rigorous process. Thanks for always being there to talk and listen. To my father who instilled in me a love of science fiction at a very young age, which, to this day, allows my imagination to run wild. I have come to believe that a strong imagination is a very important trait in any good researcher. To Grandpa and Grandma Day: your world view is rare and welcome at this day and age. You have opened my eyes to many future possibilities and encouraged me to dream. You have taught me the importance of hard work (if it is to be, it is up to me). Your relationship has been an inspiration to me and Abbey. To my brothers, John and Tom, and my sisters, Sarah and Mary: what an oddly diverse family we are! I have learned so much from each of you. Your experiences, and my experiences with you, have shaped me into the person I am today (for better or worse).

I would also like to thank the CE-CERT faculty, specifically Kurt Bumiller, who knows everything and can do anything, in addition to my current and former group members: Patrick, Mary, Derek, Chen, Weihan, Xinze, and others. To my former boss and

mentor, Dr. Michael Olson: you are proof that grunge is dead. Thanks for all the beer and rock n roll.

Funding for this research was primarily provided by the National Science Foundation under Grant No. NSF-ATM-1460389 with supplemental funding from the Esther F. Hays Graduate Fellowship. Chapter 2, 3, 4, and 5 are expected to be submitted, in part or in full, to academic journals in the near future.

The soundtrack that kept me glued to my computer chair as I worked on this for the past three months includes music by Uncle Acid and the Deadbeats, Kraftwerk, Stonefield, Neil Young, Ty Segall, Earth, Black Flag, Tom Petty and the Heartbreakers, Otis Redding, Iggy and the Stooges, Meat Puppets, Thee Oh Sees, Ravi Shankar, Feels, The Paranoyds, Mudhoney, Bob Dylan, Hawkwind, Funkadelic, Frank Zappa, Love, Kikagaku Moyo, George Harrison, and The West Coast Pop Art Experiment Band.

Dedicated to:

My wonderful wife, Abbey, and two pups Lyla and Mulder.

ABSTRACT OF THE DISSERTATION

Secondary Aerosol Formation from the Oxidation of Amines and Reduced Sulfur Compounds

by

Paul Steven Van Rooy

Doctor of Philosophy, Graduate Program in Chemical & Environmental Engineering
University of California, Riverside, September 2019
Dr. David R. Cocker III, Chairperson

Gas-phase reduced sulfur compounds (dimethylsulfide, dimethyldisulfide) and amines (trimethylamine, diethylamine, butylamine, ammonia) are both present in relatively high concentrations over agricultural land and are both thought to be important to new particle formation and particle growth. Despite this, there is a lack of knowledge on how amines oxidize in the atmosphere, there are discrepancies in results from studies focused on determining the oxidation products of reduced sulfur compounds, and there have been no investigations into how these co-emitted compounds interact to form aerosol. This thesis will begin to fill these information gaps. First, the major difficulties involved in running experiments on reduced sulfurs and amines is discussed. The methodology by which these compounds can be successfully oxidized in a 37.5 cubic meter Teflon environmental chamber is laid out. Next, results are presented from oxidation (OH, $O(^3P)$, and NO_3) of reduced sulfur compounds under extreme dry conditions. The importance of NO_x was also

probed. This marks the very first investigation of these compounds under dry conditions. The subsequent study is focused on these same oxidation experiment under humid conditions. These studies provide insight into the importance of water vapor to the mass concentration and composition of secondary aerosol. Results from both of these studies are used to update existing oxidation mechanisms as well as aerosol yields for dimethylsulfide and dimethyldisulfide. To date, this represents the most atmospherically relevant reduced sulfur oxidation study. Next, the physical and chemical properties of secondary aerosol formed through the oxidation of amines under both dry and humid conditions are discussed. Finally, results are discussed from interaction experiments involving the oxidation of an amine in the presence of a reduced sulfur compound. This study is the first of its kind and provides a more realistic look at how these compounds react in the atmosphere to form secondary aerosol. Chemical and physical aerosol properties measured during multiple precursor experiments are compared to results from individual precursor experiments to determine if the two compounds are interacting. Furthermore, when it is determined that an interaction occurred, the nature of this interaction is investigated and a mechanism by which aerosol forms is developed.

Table of Contents

List of Tables:

List of Figures:

Chapter 1: Background on and Motivation to Conduct Research Focused on Oxidation of Amines and Reduced Sulfur Compounds

1.1 Motivation and Background

Air pollution, by definition, is detrimental to the health and welfare of humans, animals, and the environment. The adverse effects of air pollution events have been recognized for over a century. One such event happened in Los Angeles during World War II on July 26, 1943 (SCAQMD 1997, McNally 2010). The air pollution event was initially mistaken by some to be chemical warfare; this was quickly corrected and blamed on the industrial boom occurring in southern California as well as in the increase in population, and therefore vehicles and energy use. Similar events have occurred around the world, perhaps most famously in London during the winter of 1952. The Great Smog of London peaked for five days, from December 5-9, and is estimated to have resulted in 12,000 excess deaths (Bell et al., 2001).

Major air pollution events like these resulted in a push for regulations on industries and a fight against smog. In 1947, Los Angeles County created the Air Pollution Control District, which set out to crack down on smog by requiring permits for all major industries (Cone 1999). Twenty years later, in 1970, the US Environmental Protection Agency finally responded to the increasing air quality issues by passing legislation known as the Clean Air Act (US EPA 1971). The Clean Air Act originally defined and set limits on seven criteria pollutants (lead, nitrogen dioxide, carbon monoxide, ozone, sulfur dioxide, and particulate matter) that were known to cause adverse human and environmental health issues. The

Clean Air Act was amended in 1977 and again in 1990 in order to mitigate acid rain and stop the depletion of stratospheric ozone (US Senate 1977, US EPA 1990).

Despite the implementation of regulations, there are still areas in the US are struggling with air quality. More importantly, the world as a whole is struggling with air pollution issues. The World Health Organization (WHO) estimated that 6.5 million deaths were caused by air pollution in 2012, making it the largest single environmental health risk (WHO 2016). Additionally, global climate change remains a paramount issue. A recent report released by the Intergovernmental Panel on Climate Change suggests that, if changes are not made, global warming is likely to reach 1.5 degrees Celsius in approximately 10 to 30 years (IPCC 2018). The detrimental effects of a global temperature change of 1.5 degrees are likely to include changes in extreme weather patterns (drought and heavy precipitation), decrease in biodiversity, species extinction, and food and water scarcity. Clearly, further research in atmospheric air pollution is necessary.

Particulate matter (PM) is an important component of air pollution that can impact human health as well as the climate. When microscopic PM is suspended in a gas it is known as an aerosol. Atmospheric aerosols fall in to two broad categories: primary and secondary. Primary aerosols are emitted directly as particles. Secondary aerosols are emitted as a gas and, after oxidizing in the atmosphere, can condense on to existing particles or, in the absence of sufficient surface area to condense on to, can create new particles, which is known as particle nucleation (Seinfeld et al., 2003). Both primary and secondary aerosols are known to impact climate change as well as visibility (IPCC 2013, Horvath 1993). Secondary Aerosols, which make up a bulk of total submicron aerosol,

can travel deep into the human lung, causing respiratory and cardiovascular health issues (Hallquist 2009, Pope et al., 2006).

Two potentially important sources of secondary aerosol that are currently not well understood and severely understudied are amines and reduced sulfurs. Both amines and reduced sulfur compounds have been detected in the ambient atmosphere around agricultural land and marine environments (Trabue et al., 2008, van Pinxteren et al., 2019, Schade et al., 1995, Ge et al. 2011, Fitzgerald et al. 1991). Reduced sulfur compounds, like dimethylsulfide, dimethyldisulfide, and methanethiol, have been measured in the part per billion (ppb) levels around agricultural land, with sources thought to be animal waste products, and ppt levels over the ocean, with phytoplankton decomposition thought to be the primary source (Trabue et al., 2008, Berresheim et al., 1990., Liss et al., 1997). Dimethylsulfide and dimethyldisulfide have also been measured in ppb levels during a biomass burning study in Australia (Meinardi et al., 2003). In 2010, a pesticide which contains up to 98.8% dimethyldisulfide was designated as an alternative to methyl bromide, a compound responsible for ozone depletion (US EPA 2010). The EPA allows a maximum application of 455 pounds per acre of this pesticide. The EPA did not include a study of the secondary aerosol formation potential when conducting a risk assessment on this pesticide.

Environmental chamber as well as flow tube studies have been conducted in the past to determine the hydroxyl radical oxidation products of reduced sulfur compound, with a primary focus on dimethylsulfide. Both flow tube and chamber studies have concluded that major oxidation products of dimethylsulfide include dimethylsulfoxide,

dimethylsulfone, methanesulfinic acid, methanesulfonic acid, and sulfuric acid; dimethyldisulfide is thought to form sulfur dioxide, methanesulfonic acid, and sulfuric acid (Arsene et al., 2001, Barnes et al, 1994, 1988, Yin et al. 1990 (II), Patroescu et al., 1999, Chen et al., 2012, Hatakeyama et al., 1982). Methane sulfonic acid is considered to be important to particle growth (Berresheim et al., 2002). Sulfuric acid is thought to be important to new particle formation (Doyle 1961, Shaw 1989, Kulmala et al., 2000, McMurry et al., 2005). Sulfur dioxide is a criteria pollutant that is harmful to plants and can cause respiratory issues in humans (US EPA 1971, 1977, 1990). These products have all been measured in ambient conditions over the ocean during field studies (Davis et al., 1998, Jefferson et al., 1998, Fitzgerald et al, 1991).

It is important to note that, while many of the major oxidation products are consistent between studies, the yields of these products, and the presence of other products, varies. This variability is not well understood but is likely due to the conditions under which the reduced sulfur was studied. Important conditions to consider may include concentrations of NO_x, the precursor, and the oxidant, as well as the level of humidity and the temperature.

An oxidation mechanism for dimethylsulfide and dimethyldisulfide was developed by Yin et al. (1990 (I)) and later summarized and updated by Barnes et al. (2006). Dimethylsulfide and dimethyldisulfide are thought to primarily oxidize in the atmosphere through an initial reaction with hydroxyl radical, but nitrate radical as well as $O(^3P)$ are other possible atmospheric oxidants (Yin et al. 1990 (I)). Both nitrate radical and $O(^3P)$ are expected to react with the reduced sulfurs to form sulfuric and methanesulfonic acid,

however there have been no adequate laboratory studies focused on these oxidants. Additionally, dimethyldisulfide can photodecompose in the atmosphere and go on to form oxidation products (Sheraton et al., 1981).

Relatively few studies to date have focused on amines because their atmospheric relevance is not well established. Field studies have measured gas-phase amines, like trimethylamine, butylamine, and diethylamine, in the ppb levels around agricultural land; sources of these amines are thought to be hay, silage, and animal rumination and exhalation (Ge et al., 2011, Rabaud et al., 2002, Schade et al., 1995). Amine particulate has also been detected around agricultural areas (Silva et al., 2008). Amines are also detected in marine environments where they are thought to be produced through metabolism of organisms (Ge et al., 2011). Additionally, amines are used to capture carbon dioxide emissions in coal-fired power plants and are therefore present around power plants as well (Azzi et al., 2014). The presence of elevated levels of amines in the atmosphere has been correlated with particle nucleation events (Barsanti et al., 2009).

Laboratory studies on oxidation of select amines (butylamine, trimethylamine, diethylamine) have been conducted in the past and have resulted in aerosol yields between 5 and 50% when reacted with hydroxyl radical (Tang et al., 2013). Nitrate radical oxidation has resulted in aerosol yields up to and over 100% for some amines (Price et al., 2014, Tang et al., 2013, Malloy et al., 2009). The study completed by Tang et al. (2013) suggests that humidity plays a minor role in amine aerosol formation. Aerosol products measured in laboratory studies of amines include amine salts as well as secondary organic aerosol (Price et al., 2014, Malloy et al., 2009, Angelino et al., 2001, Murphy et al., 2007).

Oxidation mechanisms for amines have been purposed in previous studies and will be summarized in Chapter 5 of this thesis. Carcinogenic nitrosamines are thought to be oxidation products of amines as well (Lee et al., 2013).

Studies investigating the interaction between amines and sulfur compounds are limited to salt formation from acid-base reactions between ammonia or an amine and sulfuric or methanesulfonic acid. Several flow tube studies have been conducted and all indicate that amines/ammonia and sulfuric or methanesulfonic acid can directly react to nucleate particles (Chen et al., 2015, 2017, Bork et al., 2014). Furthermore, Dawson et al. (2014) found that more basic amines can displace less basic amines in aminium-methanesulfonate salts.

Both amines and reduced sulfur compounds are thought to be important to particle formation and growth. Additionally, they are both precursors to gas-phase products that are detrimental to human health. Previous studies focused on oxidation of reduced sulfur compounds have general agreement on the particulate products, but disagreement in yields. Flow tube experiments were conducted at ppm level oxidant and precursor concentrations and often times ppm level NO_x concentrations. There have been two known chamber studies focused on oxidation of reduced sulfurs, both of which were done in outdoor chambers, under humid conditions, with precursor concentrations greater than 200 ppb (often 500 ppb or more), and mostly in the presence of high NO_x concentrations (Yin et al., 1990, Tang et al., 2013). In order to obtain a more complete understanding of the mechanism by which reduced sulfurs oxidize to form aerosol, a more controlled chamber study utilizing more atmospherically relevant conditions is necessary.

The few laboratory studies on amines that exist have shown high variability in aerosol yields, dependent on the amine precursor. Additionally, there is a lack of substantial information on the effects of humidity on amine oxidation products and yields. Further investigation of amine oxidation is necessary to validate and elaborate on previous studies. Finally, despite the individual importance of both amines and reduced sulfur compounds to human health, particle formation, and particle growth, and the knowledge that these compounds are often co-emitted in the same environments, particularly around agricultural areas, no laboratory studies have investigated how these compounds oxidize together in the atmosphere. This thesis will begin to fill these information gaps and provide further insight into the oxidation of amines and reduced sulfurs individually as well as together.

Chapter 2 of this theses is focused on the development of a methodology by which these chamber experiments involving amines and reduced sulfurs, or any acidic and basic compounds, must be run. This chapter summarizes the major issues involved in running amines and reduced sulfur compounds in the same chamber, both individually and together. The solutions to these issues are also discussed, including a novel approach to environmental chamber cleaning. Information provided will be useful in future studies of this nature.

Chapters 3 and 4 focus on secondary aerosol formation from oxidation of reduced sulfurs (dimethylsulfide, dimethyldisulfide) under dry and humid conditions, respectively. Hydroxyl radical, nitrate radical, and $O(^3P)$ oxidation are all covered. A study of both dry and humid conditions allows for a more complete understanding of the importance of water

vapor to aerosol yields and the chemistry involved in reduced sulfur oxidation. Results are compared to the accepted mechanism as well as previous studies. New oxidation mechanisms for each reduced sulfur in dry and humid conditions and in the presence and absence of NO_x has been developed based on the information gained through this study. The results of this study are, to date, the most atmospherically relevant that have been recorded.

Chapter 5 briefly covers secondary aerosol formation from oxidation of amines (trimethylamine, butylamine, diethylamine) and ammonia under dry and humid conditions. Chapter 5 primarily focuses on the interactions between these amines/ammonia and the reduced sulfur compounds (dimethylsulfide and dimethyldisulfide). This study represents the first time these co-emitted compounds have been oxidized together. The mass concentration, physical properties, and gas- and particle-phase chemical composition of aerosol that formed during the multiple precursor experiments is compared to that of the individual precursor experiments to determine if and how the two compounds are interaction. When sufficient data is available, yield for both the amine only and the interaction experiments are presented. Furthermore, oxidation mechanisms for amine as well as amine-reduced sulfur interactions are proposed.

1.2 References

Angelino, S., Suess, D. T., Prather, K. A. (2001). Formation of aerosol particles from reactions of secondary and tertiary alkylamines: Characterization by aerosol time-of-flight mass spectrometry. Environmental Science & Technology 35:3130-3138.

Arsene, C., Barnes, I., Becker, K. H., Mocanu, R. (2001). FT-IR product study on the photo-oxidation of dimethyl sulphide in the presence of NOx - temperature dependence. Atmospheric Environment 35:3769-3780.

Azzi, M., Angove, D., Dave, N., Day, S., Do, T., Feron, P., Sharma, S., Attalla, M., Abu Zahra, M. (2014). Emissions to the Atmosphere from Amine-Based Post Combustion CO2 Capture Plant - Regulatory Aspects. Oil & Gas Science and Technology-Revue D Ifp Energies Nouvelles 69:793-803.

Barnes, I., Bastian, V., Becker, K. H. (1988). Kinetics and Mechanisms of the Reaction of OH Radicals with Dimethyl Sulfide. International Journal of Chemical Kinetics 20:415-431.

Barnes, I., Becker, K. H., Mihalopoulos, N. (1994). An FTIR Product Study of the Photooxidation of Dimethyl Disulfide. Journal of Atmospheric Chemistry 18:267-289.

Barnes, I., Hjorth, J., Mihalopoulos, N. (2006). Dimethyl sulfide and dimethyl sulfoxide and their oxidation in the atmosphere. Chemical Reviews 106:940-975.

Barsanti, K. C., McMurry, P. H., Smith, J. N. (2009). The potential contribution of organic salts to new particle growth. Atmospheric Chemistry and Physics 9:2949-2957.

Bell, M. L. and Davis, D. L. (2001). Reassessment of the lethal London fog of 1952: Novel indicators of acute and chronic consequences of acute exposure to air pollution. Environmental Health Perspectives 109:389-394.

Berresheim, H., Andreae, M. O., Ayers, G. P., Gillett, R. W., Merrill, J. T., Davis, V. J., Chameides, W. L. (1990). Airborne Measurements of Dimethyl Sulfide, Sulfur-Dioxide, and Aerosol Ions over the Southern-Ocean South of Australia. Journal of Atmospheric Chemistry 10:341-370.

Berresheim, H., Elste, T., Tremmel, H. G., Allen, A. G., Hansson, H. C., Rosman, K., Dal Maso, M., Makela, J. M., Kulmala, M., O'Dowd, C. D. (2002). Gas-aerosol relationships of H2SO4, MSA, and OH: Observations in the coastal marine

boundary layer at Mace Head, Ireland. Journal of Geophysical Research-Atmospheres 107:12.

Bork, N., Elm, J., Olenius, T., Vehkamaki, H. (2014). Methane sulfonic acid-enhanced formation of molecular clusters of sulfuric acid and dimethyl amine. Atmospheric Chemistry and Physics 14:12023-12030.

Chen, H. H., Ezell, M. J., Arquero, K. D., Varner, M. E., Dawson, M. L., Gerber, R. B., Finlayson-Pitts, B. J. (2015). New particle formation and growth from methanesulfonic acid, trimethylamine and water. Physical Chemistry Chemical Physics 17:13699-13709.

Chen, H. H. and Finlayson-Pitts, B. J. (2017). New Particle Formation from Methanesulfonic Acid and Amines/Ammonia as a Function of Temperature. Environmental Science & Technology 51:243-252.

Chen, T. Y. and Jang, M. (2012). Secondary organic aerosol formation from photooxidation of a mixture of dimethyl sulfide and isoprene. Atmospheric Environment 46:271-278.

Cone, M. (1999). Population Boom FIlled the L.A. Basin -- With Smog, in Los Angeles Times, Los Angeles, CA.

Davis, D., Chen, G., Kasibhatla, P., Jefferson, A., Tanner, D., Eisele, F., Lenschow, D., Neff, W., Berresheim, H. (1998). DMS oxidation in the Antarctic marine boundary layer: Comparison of model simulations and field observations of DMS, DMSO, DMSO2, H2SO4(g), MSA(g), and MSA(p). Journal of Geophysical Research-Atmospheres 103:1657-1678.

Dawson, M. L., Varner, M. E., Perraud, V., Ezell, M. J., Wilson, J., Zelenyuk, A., Gerber, R. B., Finlayson-Pitts, B. J. (2014). Amine-Amine Exchange in Aminium-Methanesulfonate Aerosols. Journal of Physical Chemistry C 118:29431-29440.

Doyle, G. J. (1961). Self-Nucleation in Sulfuric Acid-Water System. Journal of Chemical Physics 35:795.

EPA. (1971). The Clean air act, December 1970. Environmental Protection Agency, Washington.

EPA. (1990). The Clean Air Act of 1990 : a primer on consensus-building. U.S. Environmental Protection Agency, Washington, D.C.

EPA, U. (2010). Pesticide Fact Sheet: Dimethyl Disulfide, U. S. E. P. Agency, ed.

Fitzgerald, J. W. (1991). Marine aerosols: A review. Atmospheric Environment, Part A 25A:533-545.

Ge, X., Wexler, A. S., Clegg, S. L. (2011). Atmospheric amines - Part I. A review. Atmospheric Environment 45:524-546.

Hallquist, M., Wenger, J. C., Baltensperger, U., Rudich, Y., Simpson, D., Claeys, M., Dommen, J., Donahue, N. M., George, C., Goldstein, A. H., Hamilton, J. F., Herrmann, H., Hoffmann, T., Iinuma, Y., Jang, M., Jenkin, M. E., Jimenez, J. L., Kiendler-Scharr, A., Maenhaut, W., McFiggans, G., Mentel, T., Monod, A., Prevot, A. S. H., Seinfeld, J. H., Surratt, J. D., Szmigielski, R., Wildt, J. (2009). The formation, properties and impact of secondary organic aerosol: current and emerging issues. Atmospheric Chemistry and Physics 9:5155-5235.

Hatakeyama, S., Okuda, M., Akimoto, H. (1982). Formation of sulfur dioxide and methanesulfonic acid in the photooxidation of dimethyl sulfide in the air. Geophysical Research Letters, Wash., D.C. 9:583-586.

Horvath, H. (1993). Atmospheric light absorption-a review. Atmospheric Environment. Part A: General Topics, Oxford, England 27A:293-317.

IPCC (2013). Climate Change 2013: The Physical Science Basis. Contribution of Working Group I to the Fifth Assessment Report of the Intergovernmental Panel on Climate Change, T. F. Stocker, D. Qin, G.-K. Plattner, M. Tignor, S. K. Allen, J. Boschung, A. Nauels, Y. Xia, V. Bex, P. M. Midgley, eds., Cambridge, UK and New Yory, NY, USA, 1585.

IPCC (2018). Special Report: Global Warming of 1.5 Degrees C, Intergovernmental Panel on Climate Change.

Jefferson, A., Tanner, D. J., Eisele, F. L., Davis, D. D., Chen, G., Crawford, J., Huey, J. W., Torres, A. L., Berresheim, H. (1998). OH photochemistry and methane sulfonic acid formation in the coastal Antarctic boundary layer. Journal of Geophysical Research. D. Atmospheres 103:1647-1656.

Kulmala, M., Pirjola, U., Makela, J. M. (2000). Stable sulphate clusters as a source of new atmospheric particles. Nature 404:66-69.

Lee, D. and Wexler, A. S. (2013). Atmospheric amines - Part III: Photochemistry and toxicity. Atmospheric Environment 71:95-103.

Liss, P. S., Hatton, A. D., Malin, G., Nightingale, P. D., Turner, S. M. (1997). Marine sulphur emissions. Philosophical Transactions of the Royal Society B-Biological Sciences 352:159-168.

Malloy, Q. G. J., Qi, L., Warren, B., Cocker, D. R., Erupe, M. E., Silva, P. J. (2009). Secondary organic aerosol formation from primary aliphatic amines with NO3 radical. Atmospheric Chemistry and Physics 9:2051-2060.

McMurry, P. H., Fink, M., Sakurai, H., Stolzenburg, M. R., Mauldin, R. L., Smith, J., Eisele, F., Moore, K., Sjostedt, S., Tanner, D., Huey, L. G., Nowak, J. B., Edgerton, E., Voisin, D. (2005). A criterion for new particle formation in the sulfur-rich Atlanta atmosphere. Journal of Geophysical Research-Atmospheres 110:10.

McNally, J. (2010). July 26, 1943: L.A. Gets First Big Smog, in Wired, Conde Nast.

Meinardi, S., Simpson, I. J., Blake, N. J., Blake, D. R., Rowland, F. S. (2003). Dimethyl disulfide (DMDS) and dimethyl sulfide (DMS) emissions from biomass burning in Australia. Geophysical Research Letters 30:4.

Murphy, S. M., Sorooshian, A., Kroll, J. H., Ng, N. L., Chhabra, P., Tong, C., Surratt, J. D., Knipping, E., Flagan, R. C., Seinfeld, J. H. (2007). Secondary aerosol formation from atmospheric reactions of aliphatic amines. Atmospheric Chemistry and Physics 7:2313-2337.

Patroescu, I. V., Barnes, I., Becker, K. H., Mihalopoulos, N. (1999). FT-IR product study of the OH-initiated oxidation of DMS in the presence of NOx. Atmospheric Environment 33:25-35.

Pope, C. A., III and Dockery, D. W. 2006 Critical Review - Health Effects of Fine Particulate Air Pollution: Lines that Connect. Journal of the Air & Waste Management Association.

Price, D. J., Clark, C. H., Tang, X., Cocker, D. R., Purvis-Roberts, K. L., Silva, P. J. (2014). Proposed chemical mechanisms leading to secondary organic aerosol in the reactions of aliphatic amines with hydroxyl and nitrate radicals. Atmospheric Environment 96:135-144.

Rabaud, N. E. Characterization and quantification of airborne ammonia and volatile organic compounds from industrial animal agriculture. ProQuest Dissertations and Theses.

SCAQMD (1997). The Southland's War on Smog: Fifty Years of Progress Toward Clean Air, South Coast Air Quality Management District.

Schade, G. W. and Crutzen, P. J. (1995). Emission of Aliphatic-Amines from Animal Husbandry and their Reactions – Potential Source of N2O and HCN. Journal of Atmospheric Chemistry 22:319-346.

Seinfeld, J. H. and Pankow, J. F. (2003). Organic atmospheric particulate material. Annual Review of Physical Chemistry 54:121-140.

Shaw, G. E. (1989). Production of Condensation Nuclei in Clean-Air by Nucleation of H2SO4. Atmospheric Environment 23:2841-2846.

Sheraton, D. F. and Murray, F. E. (1981). Quantum Yields in the Photolytic Oxidation of some Sulfur-Compounds. Canadian Journal of Chemistry-Revue Canadienne De Chimie 59:2750-2754.

Silva, P. J., Erupe, M. E., Price, D., Elias, J. (2008). Trimethylamine as Precursor to Secondary Organic Aerosol Formation via Nitrate Radical Reaction in the Atmosphere. Environmental Science & Technology 42:4689-4696.

Tang, X. C., Price, D., Praske, E., Lee, S. A., Shattuck, M. A., Purvis-Roberts, K., Silva, P. J., Asa-Awuku, A., Cocker, D. R. (2013). NO3 radical, OH radical and O-3-initiated secondary aerosol formation from aliphatic amines. Atmospheric Environment 72:105-112.

United States. Laws, s. e. (1977). The Clean air act as amended August 1977. U.S. Govt. Print. Off., Washington.

van Pinxteren, M., Fomba, K. W., van Pinxteren, D., Triesch, N., Hoffmann, E. H., Cree, C. H. L., Fitzsimons, M. F., von Tumpling, W., Herrmann, H. (2019). Aliphatic amines at the Cape Verde Atmospheric Observatory: Abundance, origins and sea-air fluxes. Atmospheric Environment 203:183-195.

WHO (2016). WHO Releases Country Estimates on Air Pollution Exposure and Health Impacts.

Yin, F., Grosjean, D., Flagan, R. C., Seinfeld, J. H. (1990 I). Photooxidation of dimethyl sulfide and dimethyl disulfide. II: Mechanism evaluation. Journal of Atmospheric Chemistry, Dordrecht, The Netherlands 11:365-399.

Yin, F., Grosjean, D., Seinfeld, J. H. (1990 II). Photooxidation of dimethyl sulfide and dimethyl disulfide. I: Mechanism development. Journal of Atmospheric Chemistry, Dordrecht, The Netherlands 11:309-364.

Chapter 2: Experimental Methodology to Successfully Run Amine and Reduced Sulfur Oxidation Experiments in an Environmental Chamber

This chapter will cover the methods used to run experiments and process data for this thesis research. Additionally, this chapter will discuss issues involved in running amine and reduced sulfur experiments and how to overcome these issues.

2.1 Environmental Chambers and Experimental Background

Environmental chambers are an ideal method of studying aerosol formation under controlled, atmospherically relevant conditions. Chambers have been used to study gas-phase chemistry as well as secondary aerosol formation for several decades (Atkinson et al., 1980, Odum et al., 1996, Carter et al., 2005). Knowledge gained from chamber studies, in particular aerosol yields (the ratio of organic aerosol formed to the amount of precursor consumed), is often used in atmospheric models.

In order to investigate the secondary aerosol forming potential and oxidation products of amines and reduced sulfur compounds, a 37.5 cubic meter Teflon environmental chamber equipped with black lights will be utilized as described in Price et al., 2014 and Tang et al., 2013. Prior to experiments, the environmental chamber was filled with clean air, either dry or humid, using an Aadco 737 air purification system to ensure the fill air NO_x, hydrocarbon, and particle concentrations are below detection limits. The chamber is coupled to a suite of real-time gas- and particle-phase instrumentation. A list of all instruments used, both gas- and particle-phase, along with a brief description and

a source describing how the instrument works or was used can be found on Table 2-1 and Table 2-2.

Two types of experiments were run during this study: 1) traditional, single-precursor experiments where 100 ppb of an amine or a reduced sulfur compound was injected into the chamber along with an oxidant; 2) multiple precursor interaction experiments, where 100 ppb of an amine and 100 ppb of a reduced sulfur were injected along with an oxidant. Physical and chemical characteristics of the aerosol formed during the single precursor experiments was compared to that formed during interacting experiments to determine 1) if an interaction between reduced sulfur oxidation products and amine products was occurring, and 2) the nature of the interaction. A list of chemicals used can be seen on Table 2-3. A full list of the experiments run for this thesis can be seen on Table 2-4 along with the initial conditions for each experiment.

2.2 Methodology Development: Amine and Reduced Sulfur Oxidation Chamber Experiments

Running oxidation experiments on reduced sulfur compounds in the same chamber as amines proved to be very difficult. There were two major issues that occurred while running reduced sulfur compounds, which form acidic products, along with amines, which are slightly basic. The issues that will be discussed here essentially resulted in the necessity to run nearly all experiments listed on Table 2-4, two to five times prior to obtaining a repeatable, contaminant-free results. While the bulk of Chapters 3-5 focus on data from approximately 40 chamber experiments, completion of this thesis research required a total

of more than 200 chamber or pillow bag experiments. Because of the frustration and wasted time that these issues caused, this section will cover the major issues as well as the solutions to these issues in great detail.

The first issue would occur during a reduced sulfur oxidation experiment after running any number of amine oxidation experiments. The reduced sulfur would be injected into the chamber along with an oxidant. Gas-phase instrumentation would measure the precursor at or near the expected value with trace background levels of other compounds. However, as oxidation commenced and particle formation occurred, the HR-ToF-AMS would measure substantial concentrations of fragments belonging to amine aerosol, as can be seen on Figure 2-1. The amine aerosol fragments, which did not include any oxidized fragments, at times added up to over 50% of the total organic mass measured by the AMS.

A first attempt to fix this issue was to simply continue running reduced sulfur oxidation experiments until the amine no longer played a role in aerosol formation. While this was successful, it took at least five experiments that formed high mass concentrations of aerosol to minimize the amine fragments on the AMS to an acceptable level. Running six experiments to obtain a single set of good data is not logical nor does it get to the root of the issue. In order to determine if the amine contamination was coming from the chamber walls or the AMS sample line, the sample line was cleaned using methanol in the middle of an amine-contaminated reduced sulfur oxidation experiment. Cleaning the sample line resulted in a drop in the organic-to-sulfate mass ratio from 2:1 to 1:1; this can be seen on Figure 2-2. Based on reduced sulfur oxidation experiments run in a brand new, clean chamber, an organic-to-sulfate mass ratio of approximately 1:1 is the expected

outcome. This indicates that the amine contamination was occurring in the sample lines. Likely, during amine oxidation experiments, the amines, which are notoriously sticky and difficult to sample, were getting stuck to the copper particulate sample lines. During reduced sulfur oxidation experiments, these amines would off-gas and react with the acidic aerosol. This process was especially prominent in the AMS sample line because of the low sample flow rate. Gas-wall partitioning has been identified in the past, even in Teflon sampling lines (Pagonis et al., 2017). However, off-gassing at such levels that result in a major impact on the bulk composition of the aerosol, as was seen here, have not been recorded.

To solve this issue, all particulate lines were converted from copper to stainless steel. A single sample line was connected to the AMS, APM, and VTDMA in order to increase the flow to the AMS inlet, thereby reducing vapor and particle losses to the sample line walls. Furthermore, after each set of amine or reduced sulfur oxidation experiment the stainless steel lines were flushed with water and methanol and dried with clean, compressed air over night. For interaction experiments, sample lines were cleaned prior to switching to a new amine precursor. A typical set of experiments would commence in the following order: Individual reduced sulfur oxidation experiments, clean lines, individual amine oxidation experiments, clean lines, interaction experiments, clean lines. The six-inch AMS inlet along with the AMS orifice, which still pulled a very low flow, was cleaned between each experiment.

Beyond contaminating lines, gas-phase amines can also degraded analyzers. It was determined that gas-phase amines were to blame for dirty photodetectors in NO_x analyzers,

resulting in incorrect concentration readings. To avoid this, frequent calibration checks are necessary. If the calibration check does not match the expected value, instrument cleaning may be necessary.

The second major issue would occur during an amine oxidation experiment after running a set of reduced sulfur oxidation experiments. In these cases, after injecting an amine it would take several hours for the compound to show up on gas-phase instrumentation. In some cases, the amine would not show up at all. After running reduced sulfur oxidation experiments, the chamber walls, gas-phase Teflon sample line, and Teflon filters upstream of the gas-phase instrumentation are coated with acidic particulate. Apparently an extreme case of vapor wall loss is occurring; the basic amines are either being completely consumed by the acidic particulate on the walls, or they are interacting with the walls until an equilibrium is reached, at which time they will begin to show up on the gas phase samplers. This wall interaction was especially strong after multiple DMDS experiments, as one molecule of DMDS can potentially form 2 molecules of acidic aerosol with one or two available amine bonding sites.

The first attempt to solve this problem was by treating the chamber walls with ammonia. Several ppm of ammonia was injected into the chamber with the goal of neutralizing all of the acidic particulate on the walls. Not only did this fail to work, but the following three-weeks of experiments were contaminated due to ammonia off gassing from the walls and interacting with the acidic particulate, rendering the data largely useless. The ammonia off gassing was likely due to amine replacement reactions with the ammonium-acid salts, as described by (Dawson et al., 2014). After injecting excess ammonia, the walls

became coated with ammonium salts. Upon injecting an amine, all of which are more basic than ammonia in this study, the amine replaces the ammonium in the salt, resulting in depletion of the gas-phase amine and the presence of gas-phase ammonia. It is possible that, by using a stronger base to neutralize the walls, this method of treating the chamber walls may work. However, this option was not explored any further. Instead, a novel chamber-cleaning procedure was implemented.

Traditionally, after each experiment an environmental chamber is cleaned by flushing with clean, dry air until all particles and unwanted gas-phase compounds are no longer present. Occasionally, hydroxyl radical, ozone, or nitrate radical is injected into the chamber without any precursor in order to react any background contamination away for a deeper clean. In this case, neither of these methods of chamber-cleaning were sufficient. Instead, it was necessary to manually spray-clean the chamber walls with water. A step-by-step procedure of preparing and performing a chamber wall water scrub is as follows:

1. In preparation for the very first chamber water scrub it is necessary to cut several slits in the chamber. These slits will allow arm access inside the chamber for spraying the walls. The slits should be approximately 1.5 feet in length at a comfortable height off the ground when the chamber is approximately 30% filled with air. The number and spacing of the slits will be determined by the size of the chamber. They must be spaced properly in order to ensure the ability for the water sprayer to reach the entire chamber wall. Three slits evenly spaced out was sufficient for the 20 foot long, 37.5 cubic meter chamber used here To cut these slits, first vertically place a 2

foot length of green Teflon tape in the desired slit locations. Use a clean razor to slice the 1.5 foot slit. Finally, place a second piece of tape over the slit. This piece of tape should have a tab folded on the top to allow easy opening and closing of the slit. The second piece of tape will need to be replace occasionally as it wears out.

2. All tubing connected to instrument from the sample manifold lines should be disconnected to avoid any water from getting into an instrument. All open lines connected to the sample manifold should be capped to avoid any dripping of water in the lab. The only lines that do not have to be disconnected from the manifold and capped are the fill-air line and the line connected to the dump-pump.
3. Lift both ends of the chamber off the ground and place them on a platform. Lift the sample manifold and place several bricks underneath to hold it off the ground. The lines connected to the sample manifold should allow for lifting the base of the chamber approximately 1 foot off the ground. The purpose of this step is to prevent water from pooling around the chamber seams where leaks are most likely to be present.
4. After the base of the chamber is off the ground, locate a good location to cut a hole for a drain. The drain should be located at the lowest possible elevation where all the water sprayed in to the chamber can be funneled to. Here, the drain was located on the ground, half a foot out and one foot below the lifted sample manifold. To cut the hole, first place a piece of green

Teflon tape, several inches in length, where the drain is to be located. Slice a slit large enough to fit a Teflon washer and a nut that can fit on a ½ inch Swagelok union. Push the washer and nut through the slit. Attach a second washer to the Swagelok union and press the union through the slit with the second washer on the outside of the chamber. Maneuver the washer and nut onto union and hand-tighten the nut while avoiding any damage to the chamber walls. For the time being, cap the drain.

5. After the drain union is attached, a method to funnel the water from the drain to a waste bucket will need to be developed. This will largely depend on the chamber design. Here, the chamber enclosure is located on a mezzanine level and is therefore elevated off the ground floor. A hole was drilled into the mezzanine floor. The drain union was placed through the hole and a 5 foot plastic line was connected from the drain union to a 5 gallon bucket located on the ground floor.
6. If there is a possibility that water may make contact with any instrumentation during the cleaning process, cover instrumentation with plastic.
7. Fill a clean pump sprayer that has not been used for any other applications with purified laboratory water. Ensure the chamber is filled to approximately 30% with air. If desired, fill air can be left on very low to avoid all air from leaking out of the chamber while cleaning.

8. Open the first chamber slit and begin spraying the chamber walls. The walls should be sprayed until they drip with water. After the first section of chamber is cleaned, close the slit with tape and continue on to the remaining slits until the entire chamber has been sprayed with water. In the case of the 37.5 cubic meter chamber here, this task consumed up to ten liters of water.
9. After chamber has been scrubbed and all slits have been closed, vigorously shake the chamber walls in order to pool as much of the water on the floor as possible.
10. Funnel all water to the chamber drain. It is important to remove as much of the water as possible because if water is allowed to dry in the chamber, the acidic particulate will also remain in the chamber, providing a sink for the amine precursor.
11. After all water has been funneled through the drain and into a waste bucket, dispose of the waste, disconnect the drain line from the drain union, and cap the drain union. Remove the bricks and platforms and place the base of the chamber as well as the sample manifold back on the floor. Protective plastic can be removed from the instruments.
12. Turn the fill-air on to a flow rate that matches the dump-pump and allow the chamber to flush overnight in order to completely dry the chamber.

13. The following day, verify that the chamber has been completely dried. At this time, any instruments can be reconnected to the sample manifold and cleaning is complete.

It is also important to be sure to flush any Teflon sample line that is connected to a gas-phase instrument with water. Furthermore, frequently changing Teflon filters upstream of the gas-phase instrumentation is also important. Prior to the development of this cleaning procedure, repeatability in mass formation was a major issue. This issue was resolved by implementation of this procedure (Figure 2-3). Additionally, reduced sulfur mass spectra no longer show at *m/z* 30 and 58, which are indicative of the presence of amines (Figure 2-4).

This procedure should ideally be completed prior to any experiment involving an amine after any experiment involving a reduced sulfur was run. However, this is not always feasible due to time constraints. To avoid performing this procedure every other day, it is very important to plan experiments properly. For example, for this study, all reduced sulfur experiments were conducted in a brand-new chamber. After completing all the necessary reduced sulfur experiments, the chamber was scrubbed with water. The following experiment was an individual precursor amine oxidation experiment, followed by the interaction experiments involving the same amine. After a set of amine experiments were completed for one amine, the chamber was scrubbed with water again and the next amine was tested. It is important to note that in some cases, even after a chamber scrub, the amine would take up to an hour to show up on any instrumentation. In these cases, patience is very important. Often times the amine would eventually show up at or slightly

below the expected injection concentration. However, injecting 200 ppb of the amine the night before an experiment while flushing the chamber with clean air appeared to minimize the time between amine injection and amine measurement the following day.

2.3 Methodology Development: HR-ToF-AMS Data Work-up

Many oxidation product fragments of reduced sulfur compounds as well as amines are not part of the traditional AMS fragment library and need to be added manually. It is paramount that high resolution peaks are thoroughly scanned and fit properly by the user. Because the AMS fragment library does not contain many of the amine and reduced sulfur fragments, there are several fragment table updates that need to be made when oxidation products of amines or reduced sulfurs are expected to be sampled through the AMS.

Both amines and reduced sulfurs form products with aerosol fragments with a mass-to-charge ratio of 46. The fragment table assumes that all mass at *m/z 46* can be attributed to nitrate aerosol. The *m/z 46* is also used to calculate nitrate mass fragments at *m/z 30* and *m/z 14*. Therefore, if care is not taken to update the fragmentation table, amine and reduced sulfur oxidation products can result in artificially high nitrate mass signals. In the case of the experiments presented in this study, no nitrate aerosol formed. Thus, updates to the fragmentation table were simple: assigning all of *m/z 46* to organic rather than nitrate and setting the organic fraction of *m/z 30* to total minus the air fragment. However, in many cases when oxidation products from reduced sulfurs and amines are sampled, nitrate aerosol will also be present. In this case it will be necessary to update the fragmentation table more carefully. For reduced sulfur compounds, it is the CH_2S fragment that interferes

with the nitrate signal. If nitrate is also present at *m/z 46,* a unique fragment that has a constant ratio when compared to CH_2S will have to be found. As CH_2S is a fragment of methanesulfonic acid, it is likely that this fragment will scale nicely with more unique methanesulfonic acid fragments at *m/z 79* (CH_3SO_2) and *m/z 96* (CH_4SO_3). Using mass-to charge of 96, assuming the entire fragment consists of this single peak, the following fragmentation table updates can be made to

$$frag\_Organic[46] = frag_{Organic[96]} \times Average\ ratio\ of\ \frac{CH_2S}{CH_4SO_3}$$

$$frag\_Nitrate[46] = 46 - frag\_Organic[46]$$

This calculation will only work if the ratio of CH_2S to CH_4SO_3 is constant.

A similar procedure can be utilized and changes can be made if an amine fragment is present at *m/z 46.* In some cases, especially for the amine oxidation products, fragment interference will also occur at *m/z 30.* If this is the case, it is often necessary to first update the organic calculation at *m/z 30* based on a constant ratio, similar to the calculation above, and then set the nitrate fragmentation calculation to the following:

$$frag\_Nitrate[30] = 30 - frag\_Air[30] - frag\_Organic[30]$$

Finally, reduced sulfur oxidation products will occasionally result in fragments of HS, H_2S, and H_3S (*m/z 33, 34,* and *35)*. These fragments will result in mass that will falsely be applied to chloride aerosol. Similar updates as those described previously will need to be made in order to correct the fragmentation table.

2.4 Summary of Major Lessons Learned

- Injection line should be heated Teflon and/or quartz. Whenever possible, injection line should be no more than two feet in length.
- Gas-phase amines and ammonia will stick to metal lines. For gas-phase instrumentation, sample lines should be heated Teflon and kept as short as possible. Sample lines for particle-phase instrumentation should be flushed regularly with water and methanol to prevent amine off gassing.
- Sampling lines for particle-phase instruments should be stainless steel. Instruments pulling a low flow-rate should have an external pump pulling flow through the sample line to prevent particle wall loss in the lines. Particulate lines should also be kept as short as possible.
- Sampling amines through an NO_x analyzer will result in eventual failure of the analyzer. Regular maintenance and cleaning of the analyzer is necessary in order to avoid instrument drift or failure.
- For best, most repeatable results, the environmental chamber should be spray cleaned with water, "treated" with whichever amine is to be tested next, and flushed for 24 hours after each high aerosol forming (>100 $\mu g/m^3$) reduced sulfur or amine-reduced sulfur oxidation experiment. At a minimum, the chamber should be "treated" with an amine and flushed overnight after high aerosol forming experiments.
- Even after cleaning the chamber and lines, amines may take more than one hour to be detected by analyzers. If an amine takes more than an hour and a half to be

detected, a second injection is recommended. Additionally, the chamber and sample lines should be spray-cleaned/flushed at the earliest convenience.

- Because of the difficulty in detection of amines, the presence of two analyzers that can detect amines is recommended.
- Running a reduced sulfur oxidation experiment (especially DMDS) can provide insight into the level of amine contamination in the chamber or sample lines. The presence of mass-to-charge of 58 indicates amine contamination. If present, the chamber should be spray-cleaned with water and the sample lines should be flushed with water and methanol.
- Great attention must be paid to data processing of HR-ToF-AMS data. Amines and reduced sulfurs form oxidation products with fragments that are not in the AMS fragment library and must be added manually.

2.5 References

Atkinson, R., Carter, W. P. L., Darnall, K. R., Winer, A. M., Pitts, J. N. (1980). A Smog Chamber and Modeling Study of the Gas-Phase NOx-Air Photo-Oxidation of Toluene and the Cresols. International Journal of Chemical Kinetics 12:779-836.

ASTM D7493-14 (2018), Standard Test Method for Online Measurement of Sulfur Compounds in Natural Gas and Gaseous Fuels by Gas Chromatograph and Electrochemical Detection, ASTM International, West Conshohocken, PA, 2018, www.astm.org

Carter, W. P. L., Cocker Iii, D. R., Fitz, D. R., Malkina, I. L., Bumiller, K., Sauer, C. G., Pisano, J. T., Bufalino, C., Song, C. (2005). A new environmental chamber for evaluation of gas-phase chemical mechanisms and secondary aerosol formation. Atmospheric Environment 39:7768-7788.

Cocker, D. R., Flagan, R. C., Seinfeld, J. H. (2001a). State-of-the-art chamber facility for studying atmospheric aerosol chemistry. Environmental Science & Technology 35:2594-2601.

Cocker, D. R., Whitlock, N. E., Flagan, R. C., Seinfeld, J. H. (2001b). Hygroscopic properties of Pasadena, California aerosol. Aerosol Science and Technology 35:637-647.

Collins, D. R., Flagan, R. C., Seinfeld, J. H. (2002). Improved inversion of scanning DMA data. Aerosol Science and Technology 36:1-9.

Dawson, M. L., Varner, M. E., Perraud, V., Ezell, M. J., Wilson, J., Zelenyuk, A., Gerber, R. B., Finlayson-Pitts, B. J. (2014). Amine-Amine Exchange in Aminium-Methanesulfonate Aerosols. Journal of Physical Chemistry C 118:29431-29440.

DeCarlo, P. F., Kimmel, J. R., Trimborn, A., Northway, M. J., Jayne, J. T., Aiken, A. C., Gonin, M., Fuhrer, K., Horvath, T., Docherty, K. S., Worsnop, D. R., Jimenez, J. L. (2006). Field-deployable, high-resolution, time-of-flight aerosol mass spectrometer. Analytical Chemistry 78:8281-8289.

Jayne, J. T., Leard, D. C., Zhang, X. F., Davidovits, P., Smith, K. A., Kolb, C. E., Worsnop, D. R. (2000). Development of an aerosol mass spectrometer for size and composition analysis of submicron particles. Aerosol Science and Technology 33:49-70.

Jimenez, J. L., Jayne, J. T., Shi, Q., Kolb, C. E., Worsnop, D. R., Yourshaw, I., Seinfeld, J. H., Flagan, R. C., Zhang, X. F., Smith, K. A., Morris, J. W., Davidovits, P.

(2003). Ambient aerosol sampling using the Aerodyne Aerosol Mass Spectrometer. Journal of Geophysical Research-Atmospheres 108:13.

Malloy, Q. G. J., Nakao, S., Qi, L., Austin, R., Stothers, C., Hagino, H., Cocker, D. R. (2009). Real-Time Aerosol Density Determination Utilizing a Modified Scanning Mobility Particle SizerAerosol Particle Mass Analyzer System. Aerosol Science and Technology 43:673-678.

Markovic, M. Z., VandenBoer, T. C., Murphy, J. G. (2012). Characterization and optimization of an online system for the simultaneous measurement of atmospheric water-soluble constituents in the gas and particle phases. Journal of Environmental Monitoring 14:1872-1884.

McMurry, P. H., Wang, X., Park, K., Ehara, K. (2002). The relationship between mass and mobility for atmospheric particles: A new technique for measuring particle density. Aerosol Science and Technology 36:227-238.

Odum, J. R., Hoffmann, T., Bowman, F., Collins, D., Flagan, R. C., Seinfeld, J. H. (1996). Gas/particle partitioning and secondary organic aerosol yields. Environmental Science & Technology 30:2580-2585.

Pagonis, D., Krechmer, J. E., de Gouw, J., Jimenez, J. L., Ziemann, P. J. (2017). Effects of gas-wall partitioning in Teflon tubing and instrumentation on time-resolved measurements of gas-phase organic compounds. Atmospheric Measurement Techniques 10:4687-4696.

Price, D. J., Clark, C. H., Tang, X., Cocker, D. R., Purvis-Roberts, K. L., Silva, P. J. (2014). Proposed chemical mechanisms leading to secondary organic aerosol in the reactions of aliphatic amines with hydroxyl and nitrate radicals. Atmospheric Environment 96:135-144.

Prince, B. J., Milligan, D. B., McEwan, M. J. (2010). Application of selected ion flow tube mass spectrometry to real-time atmospheric monitoring. Rapid Communications in Mass Spectrometry 24:1763-1769.

Tang, X. C., Price, D., Praske, E., Lee, S. A., Shattuck, M. A., Purvis-Roberts, K., Silva, P. J., Asa-Awuku, A., Cocker, D. R. (2013). NO3 radical, OH radical and O-3-initiated secondary aerosol formation from aliphatic amines. Atmospheric Environment 72:105-112.

Tritscher, T., Dommen, J., DeCarlo, P. F., Gysel, M., Barmet, P. B., Praplan, A. P., Weingartner, E., Prevot, A. S. H., Riipinen, I., Donahue, N. M., Baltensperger, U. (2011). Volatility and hygroscopicity of aging secondary organic aerosol in a smog chamber. Atmospheric Chemistry and Physics 11:11477-11496.

2.6 Tables

Instrument	Description	Manufacturer/Model	Source
Scanning Mobility Particle Sizer (SMPS)	Measures particle diameter distribution, number and volume concentration.	Home built using a TSI® Model 308100 Differential Mobility Analyzer (DMA) and a TSI® model 3760A Condensation Particle Counter (CPC).	Cocker et al., 2001a, Collins et al., 2002
Aerosol Particle Mass Analyzer – SMPS (APM)	Selects particle mass and measured particle diameter in order to calculate particle density.	Kanomax Aerosol Particle Mass Analyzer attached to a home built SMPS.	Malloy et al., 2009 McMurry et al., 2002
Volatility Tandem DMA (VTDMA)	Measures particle volatility at 100 degrees Celsius.	Home built using a TSI® Model 308100 DMA, a TSI® model 3760A CPC, and a Dekati® Thermodenuder model TD3.	Tritscher et al., 2011
Hygroscopicity Tandem DMA (HTDMA)	Measures the ability of a particle to uptake water at ~85% RH.	Home built using a TSI® Model 308100 DMA and a TSI® model 3760A CPC.	Cocker et al., 2001a, Cocker et al., 2001b
High Resolution - Time of Flight - Aerosol Mass Spectrometer (HR-ToF-AMS)	Measures mass to charge ratio of non-refractory particle fragments to allow for determination of bulk aerosol composition.	Aerodyne Research Inc.	Jimenez et al., 2003 Jayne et al., 2000 Decarlo et al., 2006
Ambient Ion Monitor (AIM)	Measures gaseous and particulate anions and cations. Adapted specifically for amine measurements.	URG® Model 9000D	Markovic et al., 2012

Table 2-1: Particle-phase instrumentation used during this study.

Instrument	Description	Manufacturer/Model	Source
Selected Ion Flow Tube Mass Spectrometer (SIFT-MS)	Measures mass spectra of gas-phase compounds. Obtains concentration time series of calibrated gasses.	Syft™ Technologies model v200	Prince et al., 2010 Price et al., 2014
NO_x Analyzer	Measures NO and NO_2 concentrations.	Thermo Environmental Instruments Inc. model 42C	
Nitrogenous Gas Analyzer	Measures all gas-phase nitrogen compounds.	NO_x Analyzer with Thermal Oxidizer (CDNOVA model CDN-101) attached to inlet.	
CO_2 and H_2O Analyzer	Measures humidity.	LI-COR® model LI-840.	
Sulfur Gas Chromatograph (GC)	Measures gas-phase reduced sulfur precursors and some oxidation products.	Medor GC from Chromatotec.	ASTM, 2018
Ambient Ion Monitor (AIM)	Measures gaseous and particulate anions and cations. Adapted specifically for amine measurements.	URG® Model 9000D	Markovic et al., 2012

Table 2-2: Gas-phase instrumentation used during this study.

Compound	Formula	Structure
Hydrogen peroxide as a source of hydroxyl radical	H_2O_2	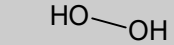
Dinitrogen pentoxide as a source of nitrate radical	N_2O_5	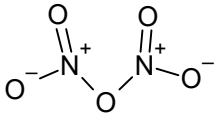
Nitrogen Dioxide as a source of $O(^3P)$	NO_2	
Dimethylsulfide (DMS)	C_2H_6S	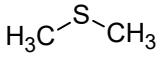
Dimethyldisulfide (DMDS)	$C_2H_6S_2$	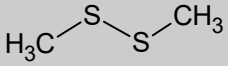
Dimethylsulfoxide (DMSO)	C_2H_6SO	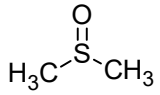
Dimethylsulfone (DMSO2)	$C_2H_6SO_2$	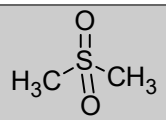
Methanesulfonic Acid (MSA)	CH_4SO_3	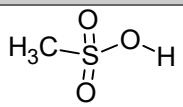
Ammonia	NH_3	
Trimethylamine (TMA)	C_3H_9N	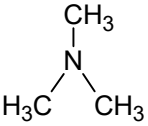
Diethylamine (DEA)	$C_4H_{11}N$	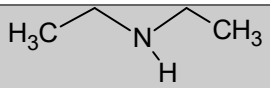
Butylamine (BA)	$C_4H_{11}N$	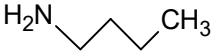

Table 2-3: List of compounds injected into the chamber or through an instrument.

Experiment	[Amine]* ppb	[Sulfur Compound] ppb	$[H_2O_2]$, $[N_2O_5]$, or $[NO_2]$ ppb
DMS+OH (dry) 022619	-	100	1000
DMS+$O(^3P)$+NO_x (dry) 022719	-	100	100
DMS+NO_3+NO_2 (dry) 061518	-	100	300
DMDS+OH (dry) 030119	-	100	1000
DMDS+ $O(^3P)$+NO_x (dry) 022819	-	100	100
DMDS+NO_3+NO_2 (dry) 061818	-	100	300
DMSO+OH (dry) 041219	-	200	1000
DMS+OH (40%RH) 110918	-	100	1000
DMS+$O(^3P)$+NO_x (40%RH) 030519	-	100	100
DMS+NO_3+NO_2 (40%RH) 062018	-	100	300
DMDS+OH (2%RH) 102918	-	100	1000
DMDS+OH (35%RH) 030419	-	100	1000
DMDS+ $O(^3P)$+NO_x (35%RH) 030619	-	100	100
DMDS+NO_3+NO_2 (55%RH) 061918	-	100	300
DMSO+OH (20%RH) 041419	-	100	1000
TMA+OH (dry) 060118	125	-	1000
TMA+OH (dry) 032019	100	-	1000
TMA+OH (35%RH) 032119	100	-	1000
TMA+DMS+OH (27%RH) 032219	100	100	-
TMA+DMDS+UV On (dry) 032319	100	100	1000
TMA+DMDS+OH (dry) 032519	100	100	1000
TMA+DMDS+OH (30%RH) 032419	100	100	1000
TMA+MSA (dry) 091818	100	100	-
DEA+OH (dry) 052318	200	-	1000
DEA+OH (dry) 031419	100	-	1000
DEA+OH (30%RH) 031519	100	-	1000
DEA+DMS+OH (30%RH) 031619	100	100	1000
DEA+DMDS+OH (dry) 031719	100	100	1000
DEA+DMDS (30%RH) 031819	100	100	1000
BA+OH (dry) 052918	400	-	1000
BA+OH (30%RH) 040219	100	-	1000
BA+DMS+OH (30%RH) 040319	100	100	1000
BA+DMDS+OH (dry) 040519	100	100	1000
BA+DMDS+OH (30%RH) 040419	100	100	1000
NH_3+DMS+OH (45%RH) 031319	200	100	1000
NH_3+DMDS+OH (dry) 031219	200	100	1000
NH_3+DMDS+OH (35%RH) 031119	200	100	1000

Table 2-4: Complete list of experiments used in Chapters 3-5 of this thesis along with initial conditions.

*these are maximum concentrations calculated based on the volume injected. The exact concentration is unknown due to losses to chamber wall as well as sample lines.

2.7 Figures

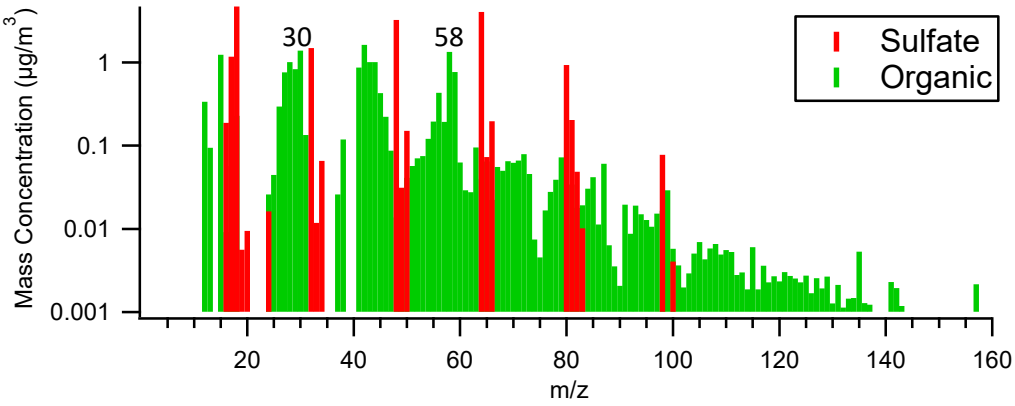

Figure 2-1: An example of amine contamination in a DMDS-only oxidation experiment. Peaks at *m/z* 30 and 58 are fit to fragments CH_4N and C_3H_8N and are indicative of the presence of amines.

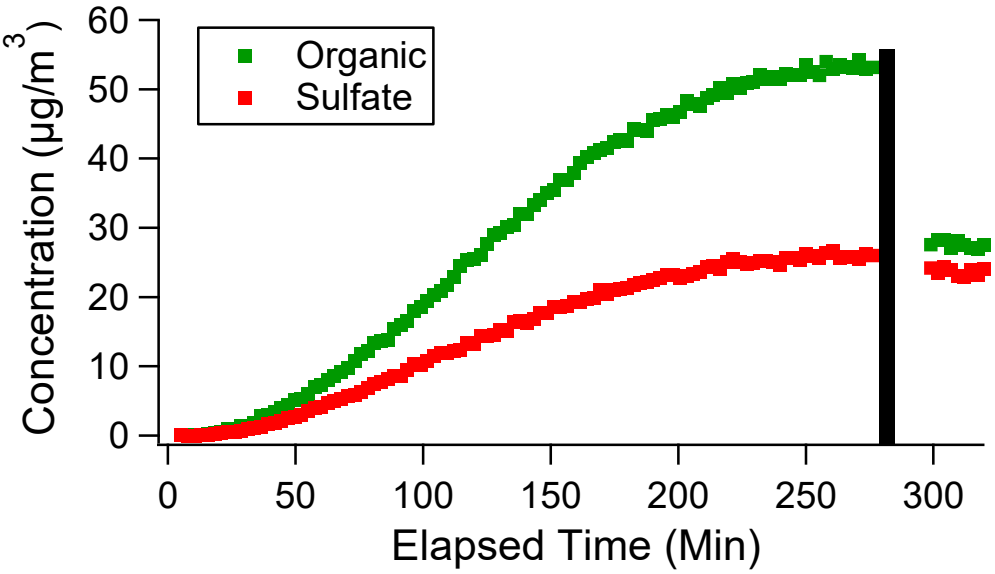

Figure 2-2: Evidence of amine contamination in a DMDS-only oxidation experiment. The black line indicates the time at which the sample line was disconnected and cleaned. The drop in organic signal is due to flushing amines off the sample line.

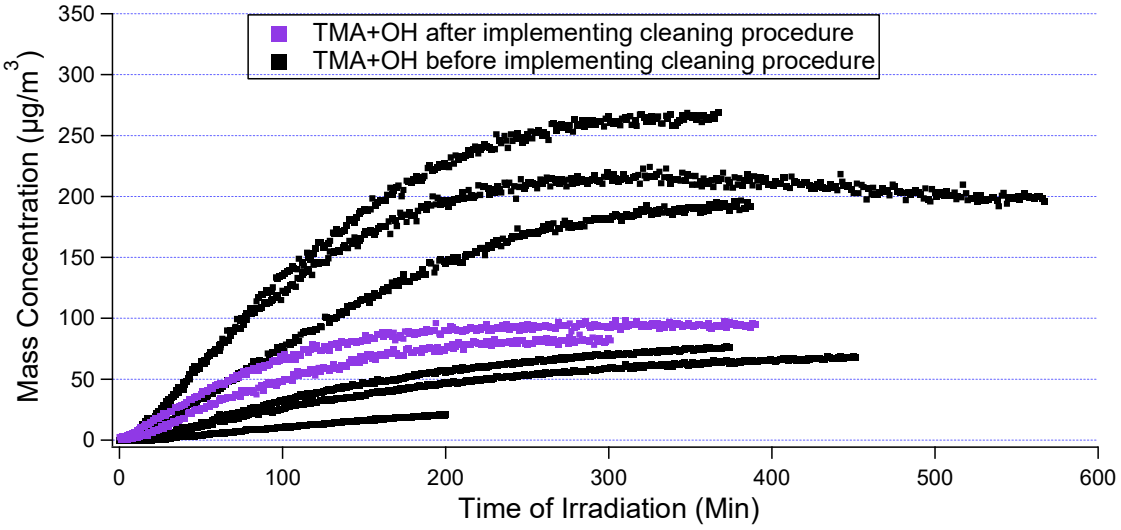

Figure 2-3: Mass concentration of eight identical TMA-OH oxidation experiments. Six were performed prior to the improved experimental methodology, two were completed after implementation of the new methodology. Note the successful repeatable after implementing the new cleaning procedures.

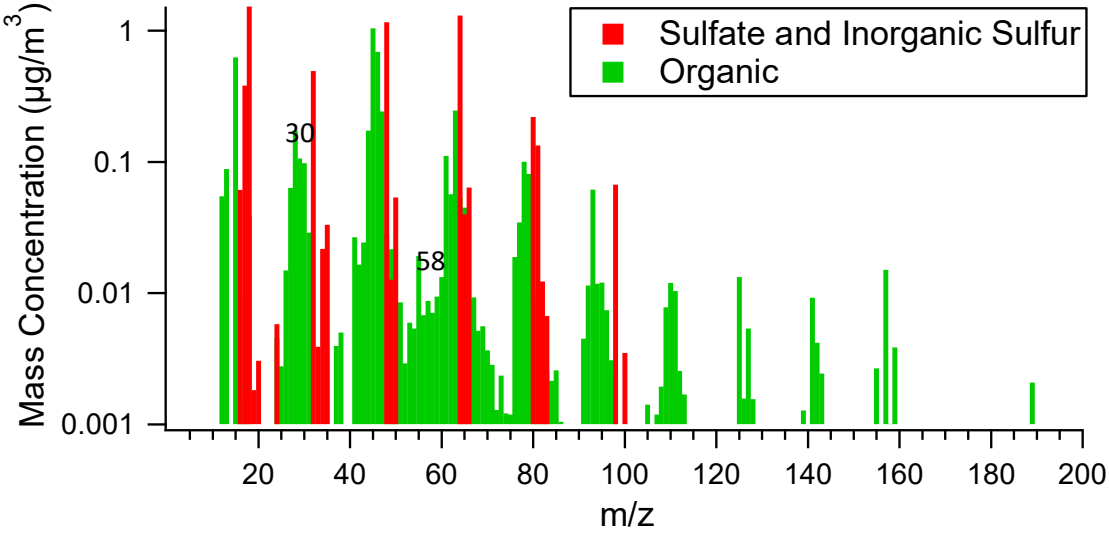

Figure 2-4: An example of the bulk aerosol composition from a DMDS-only oxidation experiment run after the new methodology was implemented. Note that peaks at *m/z* 30 and 58 no longer present, indicating amine contamination has been minimized.

Chapter 3: Oxidation of Reduced Sulfur Compound Under Extreme Dry Conditions

This chapter will discuss results and implications from chamber experiments focused on the oxidation of reduced sulfur compounds, dimethylsulfide (DMS) and dimethyldisulfide (DMDS), under extreme dry conditions.

3.1 Dimethylsulfide OH Oxidation

After 600 minutes of hydroxyl radical oxidation, DMS forms a steadily increasing aerosol mass concentration of 7.5 $^{\mu g}/_{m^3}$, as can be seen on Figure 3-1. The steady increase of aerosol formation can be explained by incomplete consumption of the DMS precursor due to a relatively slow initial reaction rate of 0.44 $x10^{-11}$ $^{cm^3}/_{molecule \cdot s}$ (Atkinson et al., 1992). The decay of DMS during a typical hydroxyl radical oxidation experiment as measured by the SIFT-MS, which can be seen on Figure 3-2, is in good agreement with the decay measured by the sulfur GC, which can be seen on Figure 3-3. Under typical experimental temperatures, 297 K, it is estimated that the addition/abstraction branching ratio is ¼ (Hynes et al., 1986, Williams et al., 2001, Albu et al., 2006). Major oxidation products should include DMSO, $DMSO_2$, MSIA, via the addition pathway, and MSA, SO_2, and sulfuric acid via the abstraction pathway (Yin et al., 1990 (I), Barnes et al., 1988, 2006).

In agreement with the mechanism and previous studies, SO_2 was formed and measured by the sulfur GC (Figure 3-4). The SO_2 concentration continues to increase throughout the experiment, consistent with the continuous and incomplete consumption of DMS and subsequent reactions that lead to SO_2 formation. Evidence of low concentrations

of DMSO, $DMSO_2$, and MSIA was measured by the SIFT-MS and can be seen on Figure 3-5. DMSO has an initial increase followed by a leveling in concentration as it oxidizes to form $DMSO_2$ and MSIA.

Sulfuric acid and MSA are expected to make up a majority, if not all, of the sulfur-containing aerosol formed. In ambient, DMSO and DMSO2 has been measured in the aerosol phase (Watts et al., 1987), but are generally not considered to be a major contributor to particulate formation or growth. Aerosol mass spectra of DMS+OH products (Figure 3-6A) contains both organic and sulfate peaks. Based on high resolution data collected using the HR-ToF-AMS, approximately 30% of the aerosol fragments are sulfur-containing organics, another 30% is sulfur-containing inorganic, and the remainder is an assortment of reduced and oxidized organic fragments (Figure 3-7). Fragments included in these fragment families can be seen in Table 3-1.

The breakdown of all sulfur-containing organic fragments can be seen in figure 3-8A. Here, 83% of the sulfur-containing organic fragments are made up of reduced fragments, while only 17% are oxidized fragments. By contrast, atomization of MSA into the AMS resulted in 69% of sulfur-containing organic aerosol fragments that are oxidized, and only 31% that are reduced (figure 3-9). CH_4SO_3, at *m/z* 96, and CH_3SO_2, at *m/z* 79, are considered to be unique indicators of the presence of MSA (Zorn et al., 2008). The absence of these peaks suggests that MSA, an expected gas- and particle-phase product of DMS oxidation, is not forming under these experimental conditions. This lack of MSA formation is in contrast to the accepted mechanism, but in agreement with NO_x-free DMS oxidation studies (Yin et al., 1990 (II), Barnes et al., 1988).

While particulate MSA is clearly not forming, it is evident that some unexpected sulfur-containing organic particulate compound is forming. Interesting and unique peaks including C_2H_6S (*m/z* 62), CH_3SO (m*/z* 63), and C_2H_6SO (*m/z* 78) suggest that particulate containing a sulfur attached to two carbons and an oxygen is forming. While there are known DMS products with such a structure, such as DMSO and DMSO2, these are not expected in the particle-phase. To verify this assumption, a DMSO+OH oxidation experiment was performed under dry conditions. This experiment resulted in less than $1\,{}^{\mu g}/_{m^3}$ of aerosol and no evidence of C_2H_6S or C_2H_6SO fragments. Furthermore, DMSO2 was atomized into the AMS, but no particulate was measured. An alternative mechanism for OH oxidation of DMS that leads to these sulfur-containing organic fragment via build-up of sulfur-containing radicals is purposed in Figure 3-16.

A breakdown of major sulfur-containing inorganic fragments can be seen on Figure 3-10A. It is likely that some of the less oxidized sulfur-containing inorganics (SO and SO_2) are, in fact, fragments of organics. The more oxidized sulfur-containing inorganics (H_2SO_4 and SO_3) indicate the presence of sulfuric acid particulate and are not abundantly present in MSA particulate (Figure 3-11). A particle density of approximately 1.64 ${}^{g}/_{cm^3}$ (Table 3-2) is high compared to the density of traditional SOA at 1.2-1.5 ${}^{g}/_{cm^3}$ (Nakao et al., 2013). This indicates the formation of sulfuric acid, which has a density of 1.83 ${}^{g}/_{cm^3}$ (CRC Handbook, 2014), along with some other aerosol products. Sulfuric acid is known to be highly volatile at high temperatures (Orsini et al., 1999). Particle volatility, measured

at 100 ºC (Figure 3-12) increases as the particles grow, suggesting sulfuric acid is present and becoming a larger fraction of total particulate over time.

3.2 Dimethylsulfide $O(^3P)$ Oxidation in the presence of NO_x

$O(^3P)$ is expected to react with DMS by first adding an oxygen to the sulfur and then degrading into radicals $\cdot CH_3$ and $\cdot SOCH_3$. This reaction is not expected to form DMSO, DMSO2, or MSIA. Beyond this one difference, DMS is expected to form many of the same radicals during $O(^3P)$ oxidation as it does during OH oxidation (Figure 3-16). The presence of NO_x should speed up subsequent reactions. Additionally, Patroescu et al. (1999) suggest that the presence of NO_x, particularly NO_2, is necessary for MSA formation.

With a high initial NO_2 concentration of 100 ppb, the concentration of $O(^3P)$ increases an order of magnitude higher than what is expected in the atmosphere, at approximately $4 \times 10^4\ molecules/cm^3$. The accepted initial reaction rate of DMS with $O(^3P)$, at $5\,x10^{-11}\ {cm^3}/{molecule \cdot s}$ (Atkinson et al., 1989), was high enough to completely consume DMS, as can be seen in Figure 3-3. Given the oxidant concentrations and initial reaction rates, the decay rate of DMS with $O(^3P)$ and hydroxyl radical are expected to be similar. However, $O(^3P)$ oxidation resulted in a substantially swifter decay of DMS. Yin et al. (1990 (I)) argue that the reason for the increased decay rate of DMS in the presence of NO_x is due to an increased formation rate of CH_3SO_3 radical, which can react with DMS to form methanesulfonic acid. However, as will be discussed shortly, this experiment results in no evidence of methanesulfonic acid formation, indicating that

CH_3SO_3 radical is not playing a major role in the decay rate of DMS. There are two alternate possible explanations for this increase in reaction rate: 1) even in the absence of an H_2O_2 injection to boost hydroxyl radical concentration, there was enough hydroxyl radical present to speed up the overall decay rate; 2) the accepted initial reaction rate of DMS with $O(^3P)$ is low. Regardless of the reason, it is clear that even at NO_2 concentrations of 100 ppb, which is relatively low compared to other chamber and flow tube studies, $O(^3P)$ can play a major role in oxidation of DMS.

Aerosol mass concentration (Figure 3-1) steadily increases until minute 300, when the DMS precursor is almost completely consumed. After minute 300, aerosol mass concentration continues to slowly grow to over of 100 $\mu g/m^3$. Concentration of SO_2 follows a similar trend, peaking at just after 300 minutes followed by a slow decay. This suggests that SO_2 is slowly oxidizing further to sulfuric acid, resulting in a slow increase in aerosol mass after minute 300. Aerosol mass formed during $O(^3P)$ oxidation of DMS is over 10 times greater than that formed during OH oxidation, while consuming only 2 times more of the precursor. There are two likely explanations for this large increase in mass concentration during $O(^3P)$ oxidation: 1) after the initial reaction, the presence of NO_x speeds up subsequent reactions allowing DMS+ $O(^3P)$ to quickly form aerosol while DMS+OH needs additional time; and 2) approximately ¼ of the DMS goes down the addition pathway to form gas phase products during OH oxidation, this does not occur during $O(^3P)$ oxidation.

As expected, no evidence of DMSO, DMSO2, or MSIA was measured in the gas phase. Similar to DMS+OH oxidation, despite high NO_x concentrations, no evidence of

gas-phase MSA was detected. Aerosol mass spectra (Figure 3-5) reveals that many of the same major organic and sulfate peaks that were present in the DMS+OH oxidation experiment are also present, suggesting a similar bulk composition. Two minor peaks stick out as unique: *m/z* 141 and *m/z* 170. The *m/z* 141 may be CH_3SNO_5, a fragment of methanesulfonyl peroxynitrate, which can form in the presence of NO_x. No known previous studies have recorded this in the particle phase. The *m/z* 170 peak is currently unknown.

The aerosol formed through $O(^3P)$ oxidation of DMS is approximately 45% sulfur-containing inorganic and 25% sulfur-containing organic, with the remainder being reduced or oxidized organic fragments. The majority of the sulfur-containing organic fraction of aerosol resembles that of DMS+OH. Major peaks (Figure 3-6B) include CHS (*m/z* 45), CH_2S (m/*z* 46), CH_3S (m/*z* 47), C_2H_5S (*m/z* 61), C_2H_6S (m/*z* 62), CH_3SO (m/*z* 63), and C_2H_6SO (*m/z* 78). Minor peaks are likely due to higher aerosol concentration, more complete oxidation of the precursor, and minor products due to the presence of NO_x. The steps leading to the formation of these unexplained sulfur-containing organic fragments is likely identical to that of OH oxidation. Still, there is no evidence of MSA in the particle phase. This is in contrast with previous studies on DMS oxidation in the presence of NO_x (Yin et al., 1990 (II), Patroescu et al., 1999, Chen et al., 2012). This results suggests that high NO_x alone is not responsible for MSA formation.

The breakdown of sulfur-containing inorganic fragments present during the $O(^3P)$ oxidation experiment are almost identical to those present during OH oxidation. Again, the highly oxidized inorganic sulfur containing fragments are indicators of the formation

of sulfuric acid. The aerosol density ranges from 1.80 to 1.55 $^{g}/_{cm^3}$ (Table 3-2), consistent with the higher density of sulfuric acid. Volatility of the particulate levels out to be higher than that of DMS+OH particulate. This is likely due to a higher fraction of sulfur-containing inorganic fragments (Figure 3-7), indicating the presence of more sulfuric acid particulate, which is highly volatile at 100 ºC. The higher fraction of sulfur-containing inorganic can be the explained by the complete consumption of the precursor and the multiple pathways leading to the formation of SO_3. The $O(^3P)$ oxidation mechanism of DMS in the presence of NO_x can be seen on Figure 3-16.

3.3 Dimethylsulfide NO_3 Oxidation in the presence of NO_x

Nitrate radical is expected to react with DMS via hydrogen abstraction, following the same pathways as hydroxyl radical hydrogen abstraction. This reaction is expected to form the same sulfur containing organic radicals that form under OH and $O(^3P)$ oxidation. Similar to $O(^3P)$ oxidation, the presence of NO_x should speed up secondary reactions.

High initial concentration of nitrate radical resulted in nearly immediate consumption of the DMS precursor (Figure 3-2). This reaction resulted in approximately 20 $^{\mu g}/_{m^3}$ of aerosol (Figure 3-1); this is five times lower than the mass concentration formed during $O(^3P)$ oxidation, which also saw complete consumption of the DMS precursor. This can be partially explained by the difficulty to form sulfuric acid in the dark and in the absence of $O(^3P)$ or OH as an oxidant for SO_2. In this case, the primary pathway for SO_3 formation will be the degradation of CH_3SO_3 into $\cdot CH_3$ and SO_3. Additionally,

there are reversible reactions involving NO_x and UV radiation (Figure 3-16). For example, Yin et al. (1990) suggest that $\cdot SCH_3$ can react with NO to form CH_3SNO. In the absence of UV, as is the case during nitrate radical oxidation, this reaction acts as a gas-phase sink. In the presence of UV, as is the case during $O(^3P)$ oxidation, CH_3SNO can photodecompose back into, $\cdot SCH_3$ and NO, allowing the sulfur-containing organic radical to continue to oxidize and eventually form more particulate. Gas-phase mass spectra show formation of peaks consistent with CH_3SNO_2 formation. Unfortunately, gas-phase instrumentation that could potentially measure elevated SO_2 was not available for this experiment.

The average mass spectra of the particulate products formed through nitrate radical oxidation of DMS can be seen on Figure 3-6C. The same major organic and sulfate peaks that were previously seen in OH and $O(^3P)$ are also present here, suggesting a similar formation mechanism. However, the overall sulfur-containing organic to sulfur-containing inorganic ratio is higher during nitrate radical oxidation, at approximately 1:1, compared to that during OH and $O(^3P)$, at 0.8:1 and 0.85:1, respectively. OH and $O(^3P)$ react with DMS to form higher fractions of inorganic sulfur-containing fragments, which are indicative of the presence of sulfuric acid. This is consistent with lack of available oxidant to react with SO_2 and form sulfuric acid during nitrate radical experiments.

Major sulfur-containing organic fragments that formed during this experiment (Figure 3-8c) are identical to the other two oxidants tested. While it is apparent that a smaller fraction of sulfuric acid formed during nitrate radical oxidation, the high sulfur-

containing inorganic mass-to-charge ratio peaks along with the high volatility of the aerosol again indicate the presence of sulfuric acid.

3.4 Dimethylsulfide Summary of Major Findings

Based on the nearly identical aerosol compositions that formed during these three reactions, it is clear that, under the experimental conditions tested here, the DMS-OH addition pathway is not important to aerosol formation. Furthermore, these results indicate that, under dry conditions and in the absence of any other organic compound, DMS will not oxidize to form gas- or particle-phase MSA. This is in contrast with what has been suggested in the currently accepted DMS and DMDS mechanisms as well as several laboratory studies (Yin et al., 1990 (II), Patroescu et al., 1999, Chen et al., 2012). However, many previous lab studies have been run at high NO_x and under humid conditions. Yin et al. (1991) and Barnes et al. (1988) recorded results similar to these, with MSA yields close to zero for DMS experiments run under NO_x-free conditions. Patroescu et al. (1999) presented data indicating that gas-phase MSA concentration increases with increasing NO_x. Here, however, it has been established that high NO_x alone is not responsible for MSA formation and that there may be something missing from this mechanism.

As mentioned previously, MSA is the only major sulfur-containing organic compound that is expected to form through DMS oxidation. However, under the extreme dry conditions tested here, sulfur-containing aerosol that is clearly not MSA is being

formed through DMS oxidation. The formation mechanism of this aerosol may include radical chemistry. A possible mechanism for this formation can be seen on Figure 3-16.

This study has established that, while $O(^3P)$ may not be an important oxidant of DMS in the atmosphere, it is important to consider in the laboratory. Historically, $O(^3P)$ oxidation of DMS has been ignored. The results from this study indicate that even at initial NO_x concentrations of 100 ppb, which is considerably lower than previous DMS chamber studies run at 180 ppb (Chen et al., 2012) and more than 300 ppb (Yin et al., 1990 (II)), $O(^3P)$ dominates DMS oxidation. This implies that, to date, there have been no true $DMS + OH + NO_x$ chamber studies where $O(^3P)$ does not play a major role in oxidation. While it appears that $O(^3P)$ oxidation yields the same aerosol products that OH oxidation does, the presence of high concentrations of NO_x, and thus, $O(^3P)$, results in a bypass of several important gas-phase products of DMS+OH oxidation (DMSO, DMSO2, and MSIA). Therefore, the presence of high NO_x concentrations may artificially increase DMS+OH aerosol yield, MSA yield, and sulfuric acid yield.

3.5 Dimethyldisulfide OH oxidation

The initial reaction rate for DMDS and OH is 50 times faster than that of DMS, at $21\,x10^{-1}\ \ {}^{cm^3}/_{molecule \cdot s}$ (Atkinson et al., 1989). This faster initial reaction rate allows for complete consumption of the DMDS precursor around minute 200 (Figure 3-2). However, despite complete consumption, the mass concentration, as seen in Figure 3-1,

continues to increase past minute 300, indicating the importance of slower secondary reactions to overall aerosol formation.

DMDS is expected to react with OH radical by addition, swiftly followed by decomposition into $\cdot SCH_3$ radical and methanesulfenic acid (CH_3SOH) (Yin et al., 1990 (I)). Further reactions with methanesulfenic acid have been purposed to form $\cdot SOCH_3$ radicals, potentially through losing a hydrogen to the CH_3SO_3 radical to form MSA. Under UV radiation, DMDS is also known to photodecompose into two $\cdot SCH_3$ radicals. DMDS forms two times more of the same sulfur-containing organic radicals that DMS oxidation produces; therefore, the DMDS+OH oxidation products are expected to be of identical composition, but in higher concentrations. Similar to DMS+OH, previous studies suggest that particulate products include sulfuric acid and MSA. SO_2 is expected to form more abundantly, given the higher concentration or sulfur-containing organic radicals, while gas phase DMS products like DMSO, DMSO2, and MSIA are not expected to form.

Measurements made by the SIFT-MS verify the lack of DMSO, DMSO2, and MSIA formation during OH oxidation of DMDS. SO_2 data was not gathered for this experiment. Aerosol formed through this reaction is composed of a higher fraction of sulfur-containing inorganic fragments, at 45% of the total mass, as compared to DMS oxidation (Figure 3-7). Average mass spectra of the DMDS+OH aerosol products can be seen in Figure 3-13A. While DMDS+OH is still forming aerosol with the same sulfate fragments and lower mass-to-charge ratio organic fragments (CHS (*m/z* 45), CH_2S (*m/z* 46), and CH_3S (*m/z* 47)) that were measured during DMS oxidation (Figure 3-6), DMDS+OH is forming several unique, prominent peaks. These peaks include *m/z* 78, 93,

110, 125, 141, and 157. Mass-to-charge of 141 was previously mentioned as CH_3SNO_5, a potential fragment of methanesulfonyl peroxynitrate, that formed during $DMS + O(^3P) + NO_x$ oxidation. However, in this case there is not enough NO_x present to make formation of this compound feasible; instead, *m/z* 141 can be attributed to $C_2H_5S_2O_3$. Mass-to-charge of 78 was also detected during DMS experiments, however, in this case the high-resolution data shows a shift in mass that aligns with a CH_2S_2 fragment. The remaining peaks of interest all contain sulfur-sulfur bonds and these fragment compositions can be seen on Table 3-1.

These odd particulate fragments containing a sulfur-sulfur have not been mentioned in previous DMDS+OH chamber oxidation experiments. To verify the formation of these compounds, multiple identical experiments were conducted. The peaks formed throughout all DMDS+OH experiments run under dry conditions. Interestingly, during longer oxidation experiments these sulfur-containing organic fragments would grow in early and then begin to decay away due to particle wall loss, or possible further reactions. This growth and decay of the sulfur-containing organic fragments is evident in Figure 3-14. After minute 300, the growth of sulfur-containing organics stops while the sulfur-containing inorganic continues to form. This, along with the continuous increase in volatility over time (Figure 3-12), is indicative of the continuous growth of sulfuric acid.

While the organic disulfide compounds that are forming during DMDS oxidation have not been measured previously, there is an explanation for their formation. As mentioned previously, one of the major differences between DMS and DMDS oxidation is that DMDS will quickly form methanesulfenic acid, while DMS will form little, if any.

Yin et al. (1990 (I)) suggested that methanesulfenic acid primarily undergoes hydrogen abstraction as a reaction pathway, a proposal based on results from liquid-phase chemistry (Gilbert et al., 1975, Block et al., 1978). However, sulfenic acids are also known to condense on themselves to form thiosulfinates (Gupta et al., 2014). A particulate forming mechanism involving condensation of methanesulfenic acid can be seen on Figure 3-16.

This reaction can explain some of the major sulfur-containing organic fragment differences that can be seen when comparing DMS oxidation with DMDS+OH oxidation (Figure 3-15). While DMS oxidation results in aerosol that contains two carbon for one sulfur, presumably due to radical chemistry mentioned previously, this is minimal in DMDS oxidation. Instead, DMDS+OH oxidation results in aerosol with a large fraction CH_xS fragments, which would be consistent with the presence of sulfur-sulfur bonds. Additionaly, 15% of the total sulfur-containing organic mass is consists of "Other" fragments; "Other" is made up of the high *m/z* compounds with two sulfurs that would result from methanesulfenic acid condensation. It is important to note that the C_2H_5S (*m/z* 61) and C_2H_6S (m/*z* 62) fragments that formed during DMS oxidation are still present in this DMDS oxidation experiment. However, because of formation of thiosulfinates via methanesulfenic acid, they account for a smaller fraction of the total sulfur-containing organic aerosol.

3.6 Dimethyldisulfide photodecomposition followed by $O(^3P)$ oxidation in the presence of NO_x

Prior to reacting DMDS with $O(^3P)$, UV lights were turned on to allow for photodecomposition of the precursor into two $CH_3S\cdot$ radicals to determine the importance of decomposition to aerosol formation. Photodecomposition of DMDS is well documented and considered to be an important initial step to oxidation (Sheraton et al., 1981, Yin et al. 1990 (I)). Here, it was established that photodecomposition of DMDS is an important consumer of DMDS, with 40% consumption after 200 minutes (Figure 3-3). It is also important to SO_2 formation, as is evident by the steady increase in signal seen in Figure 3-4. Despite the presence and oxidation of radicals, no particulate formed during photodecomposition of DMDS. This is in contrast with all other experiments that formed the same radicals.

The only major difference here is the lack of an oxidant, which is traditionally necessary to form sulfuric acid. This implies that these sulfur-containing organic radicals are not an important source of secondary aerosol nucleation. Instead, sulfuric acid needs to be present at sufficient concentrations in order to nucleate particles, after which the radicals are able to play a role in particle growth. It is important to note that the reaction rates to oxidize SO_2 to sulfuric acid with $O(^3P)$ or OH are very slow. Some sulfuric acid can form through degradation of the CH_3SO_3 radical, but apparently, during this experiment the concentration of sulfuric acid that formed through this pathway was not great enough to result in particle nucleation and sufficient growth to be measured by the SMPS. Crigee intermediates are thought to contribute to oxidation of SO_2 (Kurten et al.,

2011), however it is unlikely these are forming during reduced sulfur experiments. Kurten et al. (2011) performed a computational study on the reaction of peroxyradicals with SO_2 and determined this reaction is too slow to form SO_3 under atmospherically relevant conditions.

Further evidence of the importance of an oxidant to traditional sulfuric acid formation, and thus particulate formation, comes after minute 200 in this experiment when NO_2 is added to the chamber. As soon as this addition is made, the remainder of the DMDS precursor is consumed (Figure 3-3), and particulate is immediately formed. The SO_2 signal also immediately increases to approximately two times higher than what formed during complete consumption of DMS, which makes sense considering DMDS will form two times more sulfur-containing radicals. SO_2 signal goes on to steadily decay while it reacts to form more sulfuric acid, which explains the steady increase in mass concentration. The initial reaction between DMDS and $O(^3P)$ will form $CH_3S\cdot$ radical and $CH_3SO\cdot$ radical. These two radicals will also be present during the DMDS UV-decomposition experiment. The only major differences are: 1) now an oxidant is present to react with SO_2 and push sulfuric acid growth; 2) NO_x is present to push more formation of CH_3SO_3 radical, which may further increase sulfuric acid concentrations and lead to particle nucleation.

The particulate that formed during $O(^3P)$ oxidation of DMDS is approximately 55% sulfur-containing inorganic fragments and 25% "Other" fragments consisting of H_2O and OH fragments (Figure 3-7). All of these fragments, along with the consistently high volatility (Figure 3-12) and high density of 1.6 g/cm^3, are indicators of sulfuric acid formation. This elevated fraction of sulfuric acid, as compared to hydroxyl radical

oxidation of DMDS (Figure 3-7), is likely due to the absence of abundant CH_3SOH formation. Because $O(^3P)$ oxidation of DMDS does not form any methanesulfenic acid, thiosulfinate particulate will not form. Instead, DMDS will oxidize to form a higher concentration of sulfur-containing organic radicals, which can go on to form higher concentrations of SO_2 and sulfuric acid. Additionally, this experiment was allowed to continue for 300 minutes after DMDS was consumed. As previously established by Figure 3-14, due to the slow reaction rate of sulfuric acid formation, the sulfate signal will become a larger fraction of total aerosol as more time passes.

While the fraction of sulfur-containing organic is small, at approximately 7% of total mass, the mass of these fragments is still important, at over 10 $\mu g/m^3$. The mass spectra (Figure 3-13B) shows organic peaks that are very similar to $O(^3P)$ oxidation of DMS, including the high mass-to-charge ratios associated with the formation of methanesulfonyl peroxynitrate, at 141 and 157, as well as the unknown fragment peak at 171. A breakdown of all the major sulfur-containing organic fragments (Figure 3-15) reveals a bulk composition very similar to all the DMS oxidation experiments. Similar to DMDS+OH oxidation, the concentration, and thus over all fraction, of C_2H_5S (*m/z* 61), C_2H_6S (m/*z* 62), and C_2H_6SO (*m/z* 78) fragments are lower that of DMS oxidation. The presence of these fragments, albeit at lower concentrations, is consistent with the formation of identical sulfur-containing radicals throughout all DMS and DMDS experiments. Hydroxyl radical oxidation of DMDS uniquely forms methanesulfenic acid, which condenses with itself and goes on to form sulfur-containing particulate with a different bulk composition than what is seen here.

3.7 Dimethyldisulfide NO_3 Oxidation in the presence of NO_x

Few studies have focused on nitrate radical oxidation of DMDS. Compared to DMS, DMDS is less prevalent in the atmosphere and is therefore considered to be less atmospherically relevant. Older studies that have looked at DMDS nitrate radical oxidation suggest nitrate addition to a sulfur followed by decomposition into $CH_3SO\cdot$ and $CH_3S\cdot$ radicals (Yin et al., 1990 (I), Jensen et al., 1992). More recently, Jee et al. (2006) performed a theoretical study on the initial nitrate oxidation step with DMDS and found that hydrogen abstraction is actually the more probably oxidation pathway. The hydrogen abstraction mechanism has not been purposed nor has it been studied.

Given the high initial concentration of nitrate radical, DMDS was quickly and completely consumed (Figure 3-2). However, despite complete consumption of the precursor, less than 2 $\mu g/m^3$ of aerosol formed after 500 minutes of oxidation. The aerosol formation occurs within the first 200 minutes and levels. This is 10 times lower than that formed during DMS-nitrate radical oxidation, which steadily formed aerosol over the course of 400 minutes before beginning to level off. Under the nitrate addition followed by decomposition pathway, it is expected that the same radicals as those present in the DMS+NO_3 and DMDS+$O(^3P)$ oxidation experiments would also quickly form here. If this were the case, DMDS should form approximately two times more sulfuric acid than DMS. The minimal sulfuric acid particulate indicate nitrate addition is not the first step in DMDS oxidation and that the current accepted mechanism is incorrect. Unfortunately,

knowledge of gas-phase products of nitrate-radical oxidation of DMDS are not sufficient to present a new mechanism with confidence.

3.8 Dimethyldisulfide Summary of Major Findings

Major finding in DMDS oxidation are largely the same as DMS oxidation. Similar to DMS oxidation under dry conditions, DMDS will not oxidize to form gas- or particle-phase MSA, even in the presence of high NO_x. This suggests that a major step is missing from the MSA formation mechanism. DMDS oxidation results in unique particulate organic products that are not currently included in any mechanism. However, as is evident by the photodecomposition of DMDS, sulfuric acid is necessary in order to allow these organic compounds to nucleate. Both $O(^3P)$ and OH oxidation of DMDS resulted in high mass concentrations of aerosol, while nitrate radical did not. The reason for this lack of aerosol is unclear and requires further investigation. As is the case for DMS oxidation, at high NO_x, DMDS oxidation is initiated by $O(^3P)$ rather than OH. Again, while this may not be atmospherically relevant, it is relevant in the laboratory. While $O(^3P)$ oxidation of DMDS will form the same sulfur-containing organic radicals, it will not form methanesulfenic acid, an intermediate species that is important to aerosol formation under extreme dry conditions.

3.9 Implications

The extreme dry conditions tested here are not considered atmospherically relevant. Some of the particulate compounds formed have never been measured in the lab or in the

field, indicating they are not likely to form under typical atmospheric conditions. This provides important insight into how chamber experiments are currently run. Often times chamber experiments are initially run under extreme dry conditions in order to keep the chemistry as simple as possible. These results suggest that running chambers under these atmospherically irrelevant conditions may result in the formation of compounds that are irrelevant to the atmosphere. Furthermore, while most previous chamber experiments have been run under humid conditions and thus cannot provide an adequate comparison to the experiments presented here, flow tube experiments have been run under dry conditions in the past. The dry flow tube experiments do not record the same compound that were measured here. Additionally, methanesulfonic acid was formed during dry flow tube experiments, especially in the presence of NO_x; no methanesulfonic acid was measured during dry oxidation of reduced sulfur compounds in these chamber experiments. The differences in products between these two methods imply that the chemistry involved in oxidation in a chamber is different than the chemistry in a flow tube. This is likely due to the unreasonably high oxidant, precursor, and radical concentrations that are present in a flow tube.

By oxidizing reduced sulfurs in the absence of water vapor, this study has also provided useful insight into the mechanism by which these reduced sulfurs form aerosol. By rerunning these same experiments under humid conditions (Chapter 4 of this thesis), the importance of water vapor to the aerosol mass concentration and composition can be established.

3.10 References

Albu, M., Barnes, I., Becker, K. H., Patroescu-Klotz, I., Mocanu, R., Benter, T. (2006). Rate coefficients for the gas-phase reaction of OH radicals with dimethyl sulfide: temperature and O-2 partial pressure dependence. Physical Chemistry Chemical Physics 8:728-736.

Atkinson, R., Baulch, D. L., Cox, R. A., Hampson, R. F., Kerr, J. A., Troe, J. (1989). Evaluated Kinetic and Photochemical Data for Atmospheric Chemistry Supplement III IV – IUPAC subcommittee on Gas Kinetic Data Evaluation for Atmospheric Chemistry. Journal of Physical and Chemical Reference Data 18:881-1097.

Atkinson, R., Baulch, D. L., Cox, R. A., Hampson, R. F., Kerr, J. A., Troe, J. (1992). Evaluated Kinetic and Photochemical Data for Atmospheric Chemistry Supplement IV – IUPAC subcommittee on Gas Kinetic Data Evaluation for Atmospheric Chemistry. Journal of Physical and Chemical Reference Data 21:1125-1568.

Barnes, I., Bastian, V., Becker, K. H. (1988). Kinetics and Mechanisms of the Reaction of OH Radicals with Dimethyl Sulfide. International Journal of Chemical Kinetics 20:415-431.

Barnes, I., Hjorth, J., Mihalopoulos, N. (2006). Dimethyl sulfide and dimethyl sulfoxide and their oxidation in the atmosphere. Chemical Reviews 106:940-975.

Block, E. (1978). Reactions of organosulfur compounds. Academic Press, New York.

Chen, T. Y. and Jang, M. (2012). Secondary organic aerosol formation from photooxidation of a mixture of dimethyl sulfide and isoprene. Atmospheric Environment 46:271-278.

CRC handbook of chemistry and physics. (1977). CRC handbook of chemistry and physics.

Daubert, T. E. (1989). Physical and thermodynamic properties of pure chemicals : data compilation. Hemisphere Pub. Corp., New York.

Gilbert, B. C., Norman, R. O. C., Sealy, R. C. (1975). Electron-Spin Resonance Studies: Formation of Alkyl-Sulfonyl Radicals by Oxidation of Aliphatic Sulfoxides with Hydroxyl Radical and by Reaction of Alkyl Radicals with Sulfur Dioxide. Journal of the Chemical Society-Perkin Transactions 2:308-312.

Gupta, V. and Carroll, K. S. (2014). Sulfenic acid chemistry, detection and cellular lifetime. Biochimica Et Biophysica Acta-General Subjects 1840:847-875.

Hynes, A. J., Wine, P. H., Semmes, D. H. (1986). Kinetics and Mechanism of OH reactions with Organic Sulfides. Journal of Physical Chemistry 90:4148-4156.

Jee, J. and Tao, F. M. (2006). Reaction mechanisms and kinetics for the oxidations of dimethyl sulfide, dimethyl disulfide, and methyl mercaptan by the nitrate radical. Journal of Physical Chemistry A 110:7682-7689.

Jensen, N. R., Hjorth, J., Lohse, C., Skov, H., Restelli, G. (1992). Products and Mechanisms of the Gas-phase Reactions of NO3 with CH3SCH3, CD3SCD3, CH3SH, and CH3SSCH3. Journal of Atmospheric Chemistry 14:95-108.

Kurten, T., Lane, J. R., Jorgensen, S., Kjaergaard, H. G. (2011). A Computational Study of the Oxidation of SO2 to SO3 by Gas-Phase Organic Oxidants. Journal of Physical Chemistry A 115:8669-8681.

Nakao, S., Tang, P., Tang, X. C., Clark, C. H., Qi, L., Seo, E., Asa-Awuku, A., Cocker, D. (2013). Density and elemental ratios of secondary organic aerosol: Application of a density prediction method. Atmospheric Environment 68:273-277.

Orsini, D. A., Wiedensohler, A., Stratmann, F., Covert, D. S. (1999). A new volatility tandem differential mobility analyzer to measure the volatile sulfuric acid aerosol fraction. Journal of Atmospheric and Oceanic Technology 16:760-772.

Patroescu, I. V., Barnes, I., Becker, K. H., Mihalopoulos, N. (1999). FT-IR product study of the OH-initiated oxidation of DMS in the presence of NOx. Atmospheric Environment 33:25-35.

Sheraton, D. F. and Murray, F. E. (1981). Quantum Yields in the Photolytic Oxidation of somme Sulfur Compounds. Canadian Journal of Chemistry-Revue Canadienne De Chimie 59:2750-2754.

Watts, S. F., Watson, A., Brimblecombe, P. (1987). Measurements of the Aerosol Concentrations of Methanesulfonic Acid, Dimethylsulfoxide and Dimethylsulfone in the Marine Atmosphere of the British-Isles. Atmospheric Environment 21:2667-2672.

Williams, M. B., Campuzano-Jost, P., Bauer, D., Hynes, A. J. (2001). Kinetic and mechanistic studies of the OH-initiated oxidation of dimethylsulfide at low temperature - A reevaluation of the rate coefficient and branching ratio. Chemical Physics Letters 344:61-67.

Yin, F., Grosjean, D., Flagan, R. C., Seinfeld, J. H. (1990a). Photooxidation of dimethyl sulfide and dimethyl disulfide. II: Mechanism evaluation. Journal of Atmospheric Chemistry, Dordrecht, The Netherlands 11:365-399.

Yin, F., Grosjean, D., Seinfeld, J. H. (1990b). Photooxidation of dimethyl sulfide and dimethyl disulfide. I: Mechanism development. Journal of Atmospheric Chemistry, Dordrecht, The Netherlands 11:309-364.

Zorn, S. R., Drewnick, F., Schott, M., Hoffmann, T., Borrmann, S. (2008). Characterization of the South Atlantic marine boundary layer aerosol using an aerodyne aerosol mass spectrometer. Atmospheric Chemistry and Physics 8:4711-4728.

3.11 Tables

Compound Fragment Family	Possible Fragments Present
Reduced Organic	All fragments with the formula C_xH_y, with $x \geq 1$ and $y \geq 0$
Oxidized Organic	All fragments with the formula $C_xH_yO_z$, with $x, z \geq 1$ and $y \geq 0$
S-Containing Organic	$CHS, CH_2S, CH_3S, C_2H_3S, CSO, CHSO, CH_2SO, CH_3SO, CS_2,$ $CH_2SO_2, CH_3SO_2, C_2HSO_2, C_2H_2SO_2, CH_4SO_3, C_2H_5S, C_2H_6S$ $C_2H_5S, C_2H_6SO, C_2H_5S_2O_2, C_2H_5S_2O_3, C_2H_5S_2O_4$
S-Containing Inorganic	$S, HS, H_2S, H_3S, HSO, SO_2, HSO_2, SO_3, HSO_3, H_2SO_3, HSO_4, H_2SO_4$
Other	OH, H_2O

Table 3-1: Shown here is a list defining the typical composition of aerosol fragments in each compound family. This should not be taken as a complete list. Missing from this list are compound fragments that contain both nitrogen and sulfur (which made up less than 0.1% of total mass when they were present).

Experiment	Elapsed Time (min)	Precursor Consumed ΔHC (ppb)	Mass Formed ΔM_o $(\mu g/m^3)$	Density (g/cm^3)	Volume Fraction Remaining	Aerosol Yield $\Delta M_o/\Delta HC$ (%)
DMS+OH 022619	560	50	7.5+	1.64	0.70-0.40	6.1*
DMS+$O(^3P)$+NO_x 022719	380	100	100+	1.80-1.55	0.30	40.8*
DMS+NO_3+NO_2 061518	440	93	19	1.97	0.33	8.3
DMDS+OH 030119	320	100	50+	1.57	0.80-0.50	13.5*
DMDS+ $O(^3P)$+NO_x 022819	440	100	170+	1.60	0.30	45.8*
DMDS+NO_3+NO_2 061818	540	94	<2	x	x	<0.6

Table 3-2: Aerosol properties measured during reduced sulfur oxidation experiments. In some cases, properties changed over the course of the experiment, this is indicated by a range of values (start-end). Mass concentration was calculated by applying the density measurement to the volume concentration as measured by the SMPS. In most cases, aerosol continues to form throughout the experiment at does not level out (indicated by "+"). Because of this, a true aerosol yield could not be calculated. Most of the aerosol yields recorded here are low estimations based on the available data (indicated by the "*").

3.12 Figures

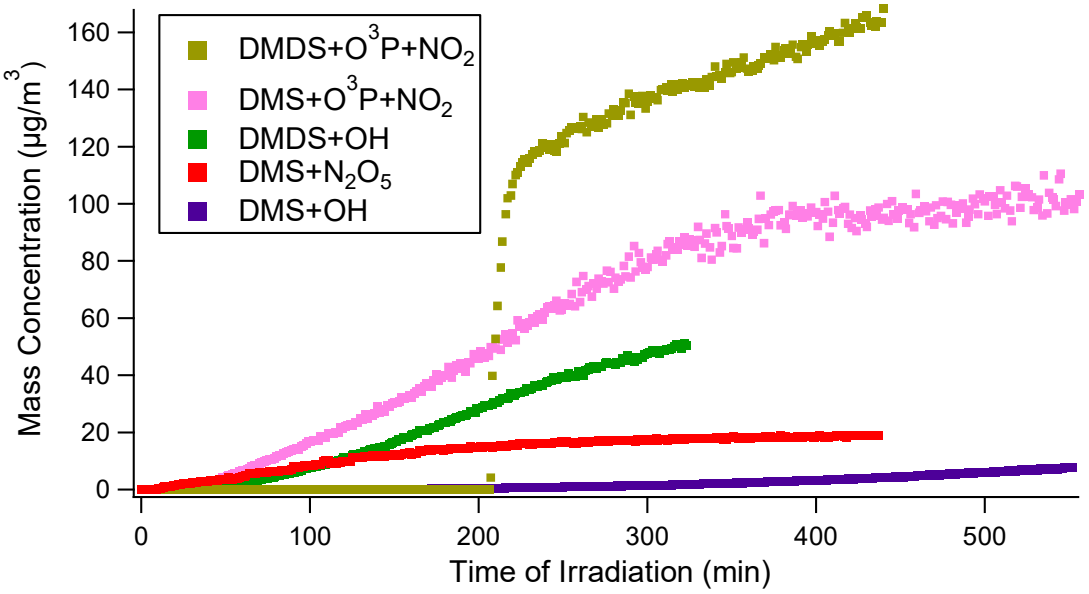

Figure 3-1: Mass concentration time series for all particle-forming reduced sulfur oxidation experiments under dry chamber conditions. Mass concentration was calculated by applying the particle density, as measured by the APM-SMPS, to the volume concentration measured by the SMPS.

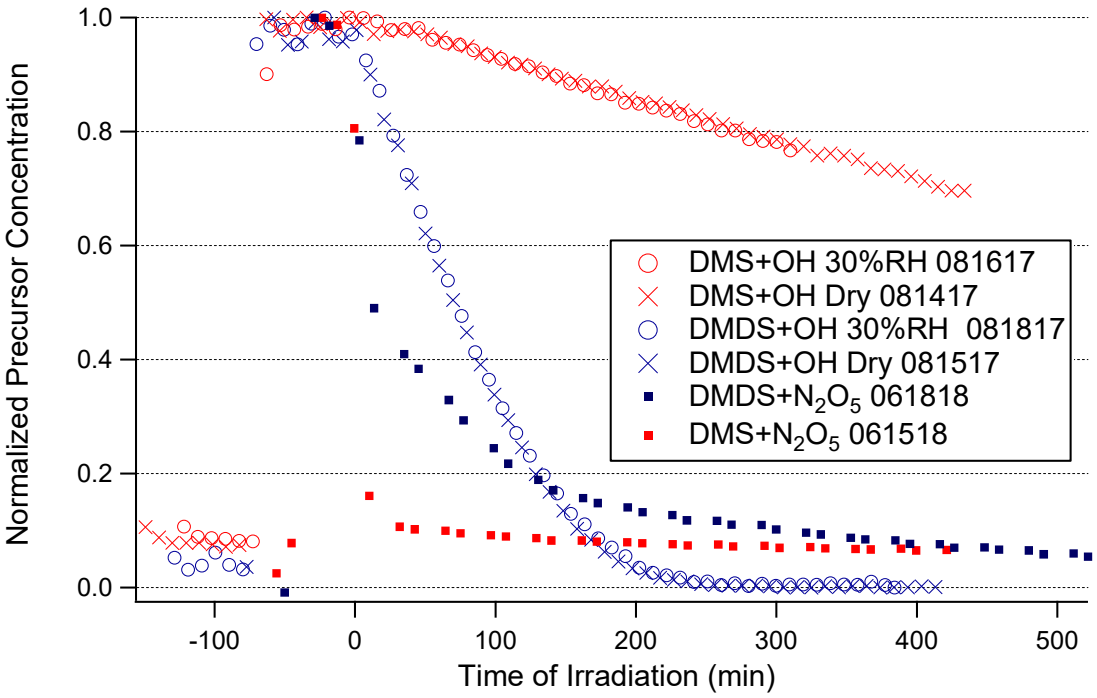

Figure 3-2: Decay of the reduced sulfur precursors from various oxidants under dry and humid conditions as measured by the SIFT-MS. Several experiments included in this plot are duplicates of experiments that are discussed in this thesis but do not have gas-phase SIFT-MS data. The decay rates of these duplicate experiments can be applied to the identical experiment discussed in this thesis.

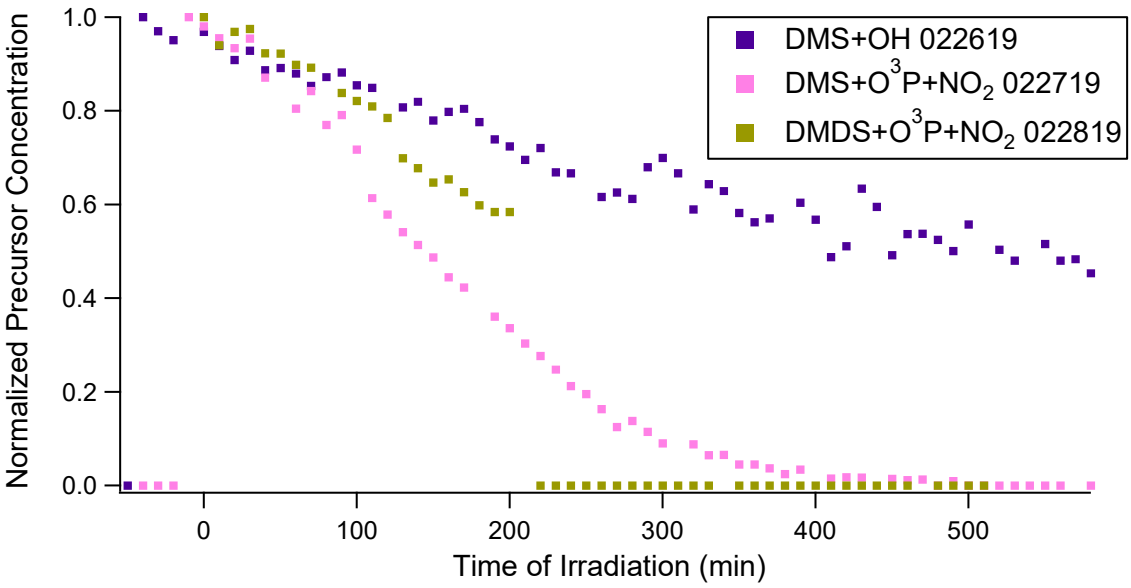

Figure 3-3: Precursor decays of several reduced sulfur oxidation experiments as measured by the Sulfur GC. Concentrations were measured as 10-15 minute averages.

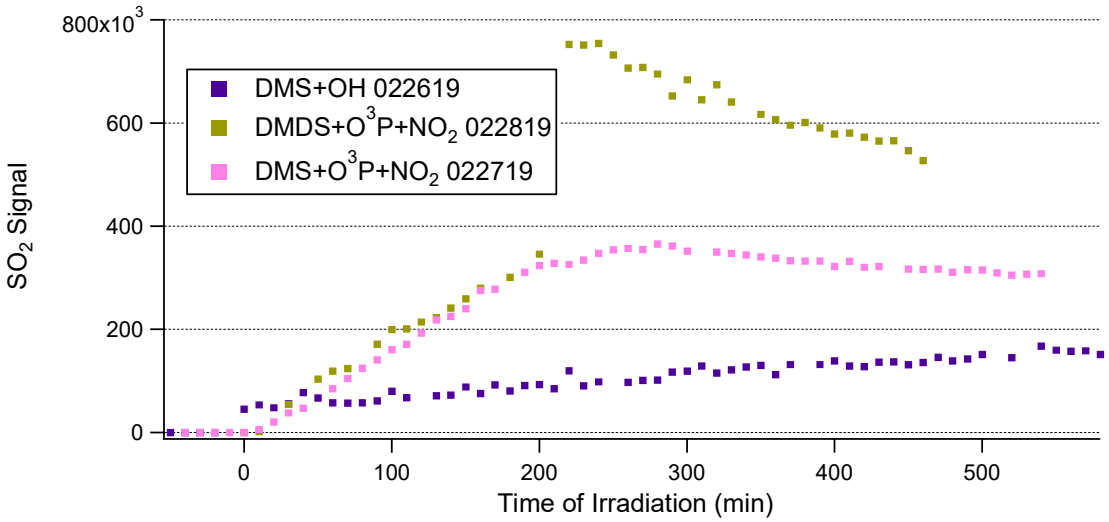

Figure 3-4: Growth of sulfur dioxide for select reduced sulfur oxidation experiments. The first 200 minutes of the DMDS oxidation experiment contains the growth of sulfur dioxide from DMDS photodegradation. The subsequent growth and decay is due to the addition of $O(^3P)$ and NO_2.

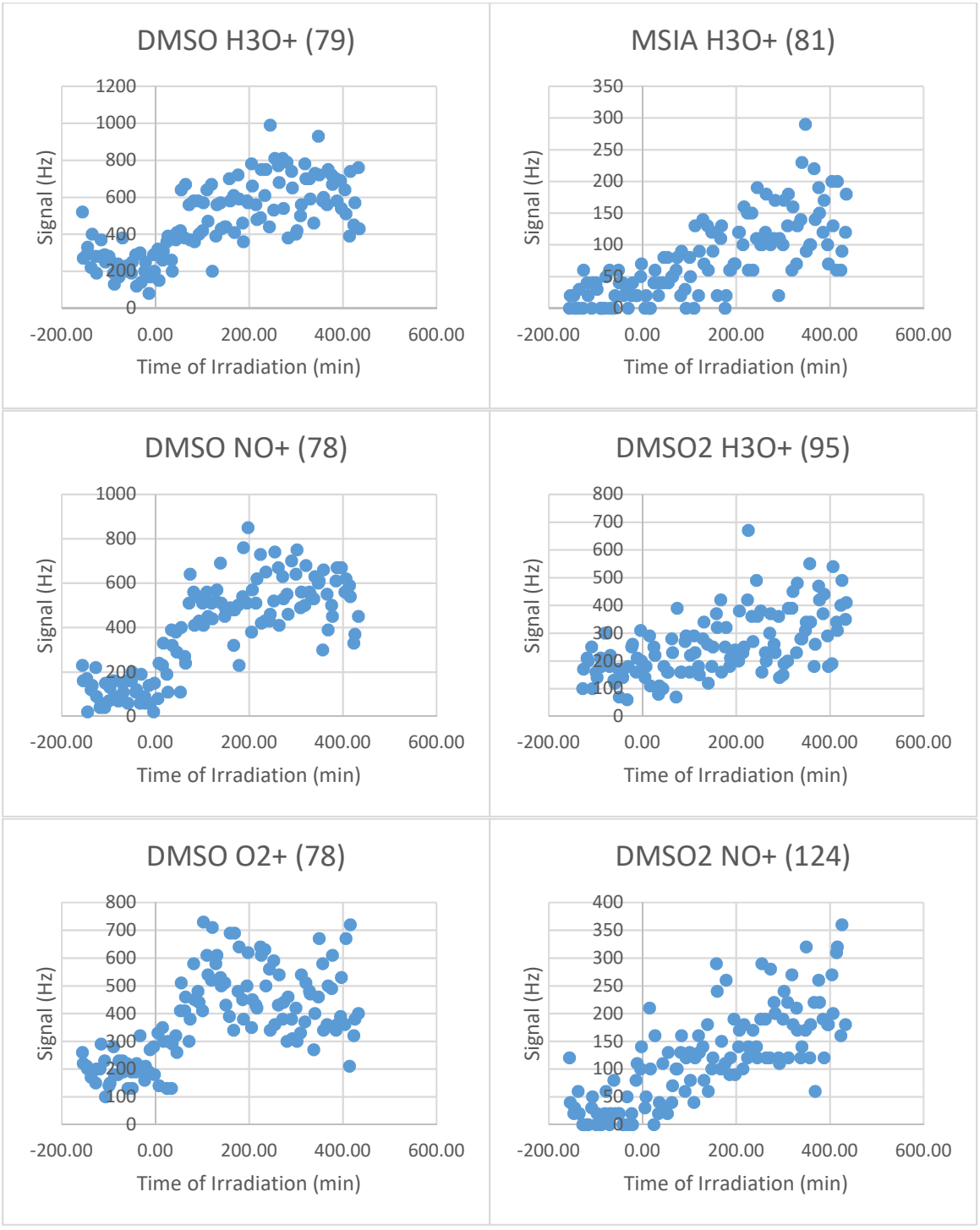

Figure 3-5: Evidence of the growth of several known DMS-OH oxidation products including dimethylsulfoxide (DMSO), dimethylsulfone (DMSO2), and methanesulfinic acid (MSIA). These compounds were measured by the SIFT-MS during a DMS-OH duplicate experiment (081417). H_3O^+ reacts with the analyte via hydrogen addition, O_2^+ reacts via electron transfer, and NO^+ reacts via electron transfer or NO^+ association.

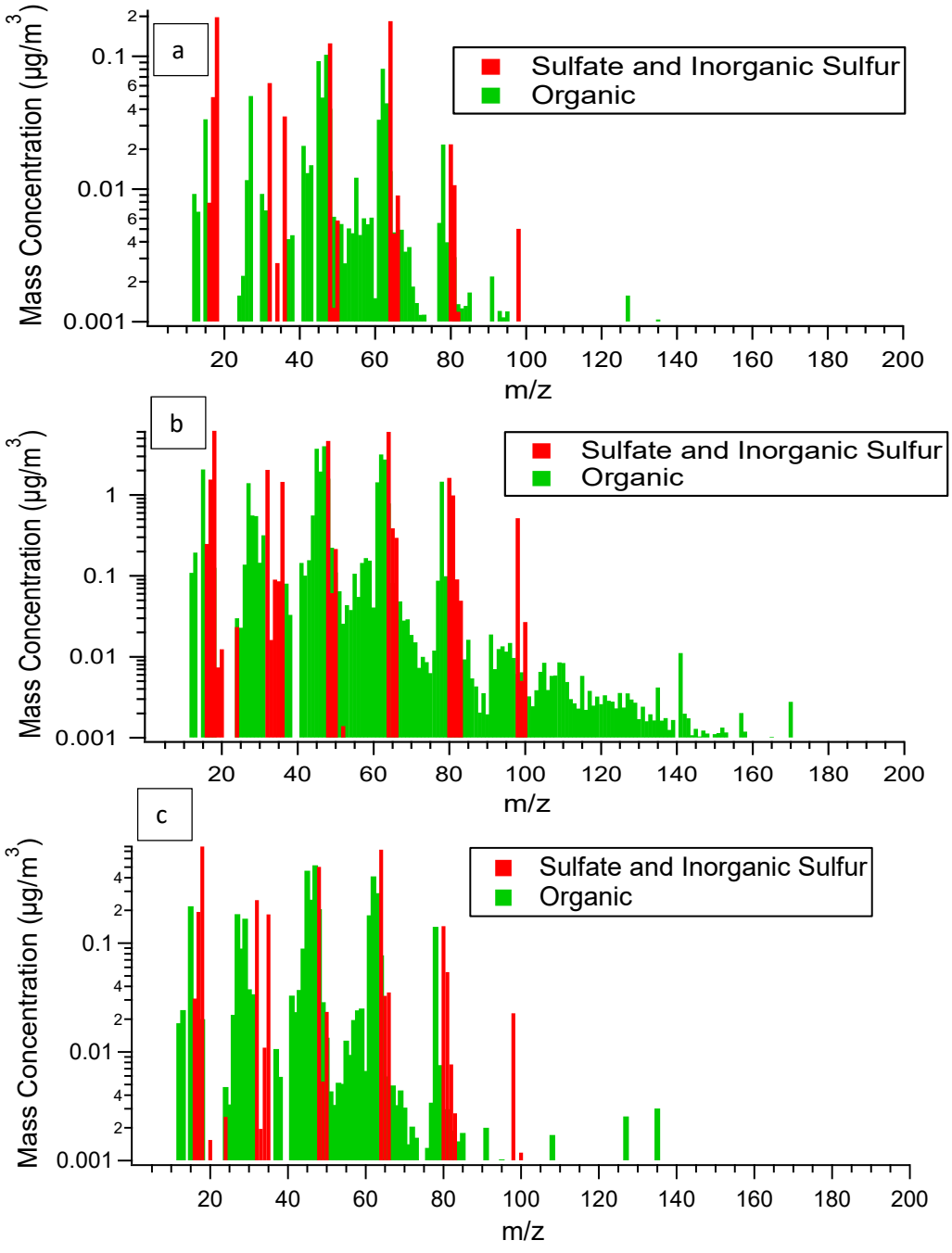

Figure 3-6: Average aerosol mass spectra (as measured by the HR-ToF-AMS) from the following reduced sulfur oxidation experiments: a) $DMS + OH$ 022619, b) $DMS + O(^3P) + NO_x$ 022719, and c) $DMS + NO_3$ 061518.

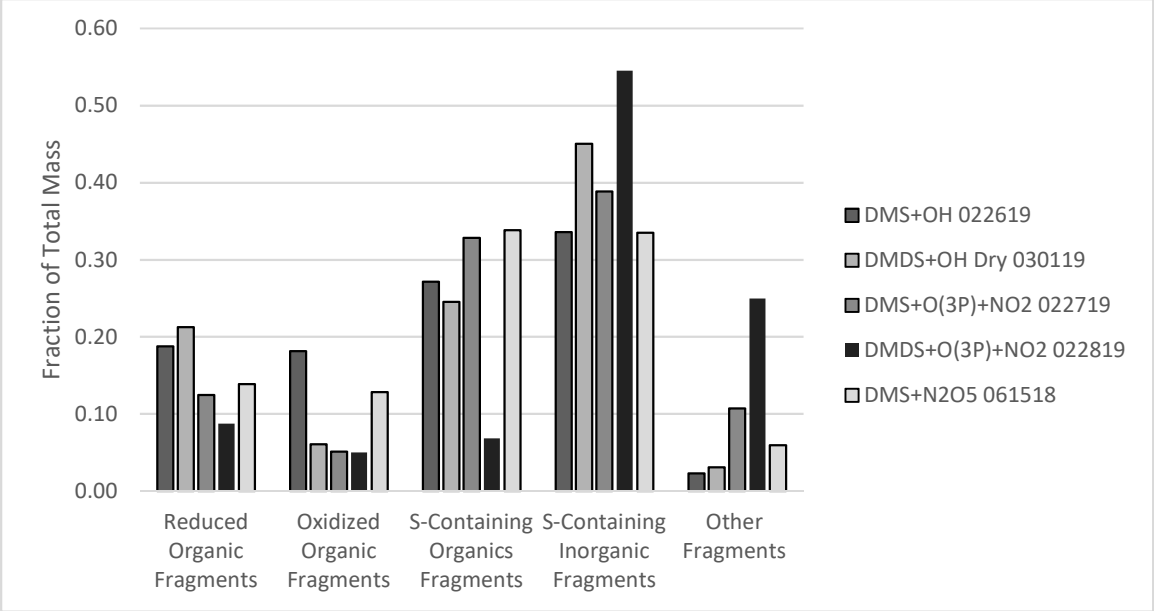

Figure 3-7: Bulk composition of the aerosol (as measured by the HR-ToF-AMS) formed during each reduced sulfur oxidation experiment broken down by fragment compound families. Examples of compound fragments present in each family can be seen on Table 3-1. The fractions of each compound family are averages over the course of the last 100 minutes of oxidation. These fractions were relatively constant during this time period.

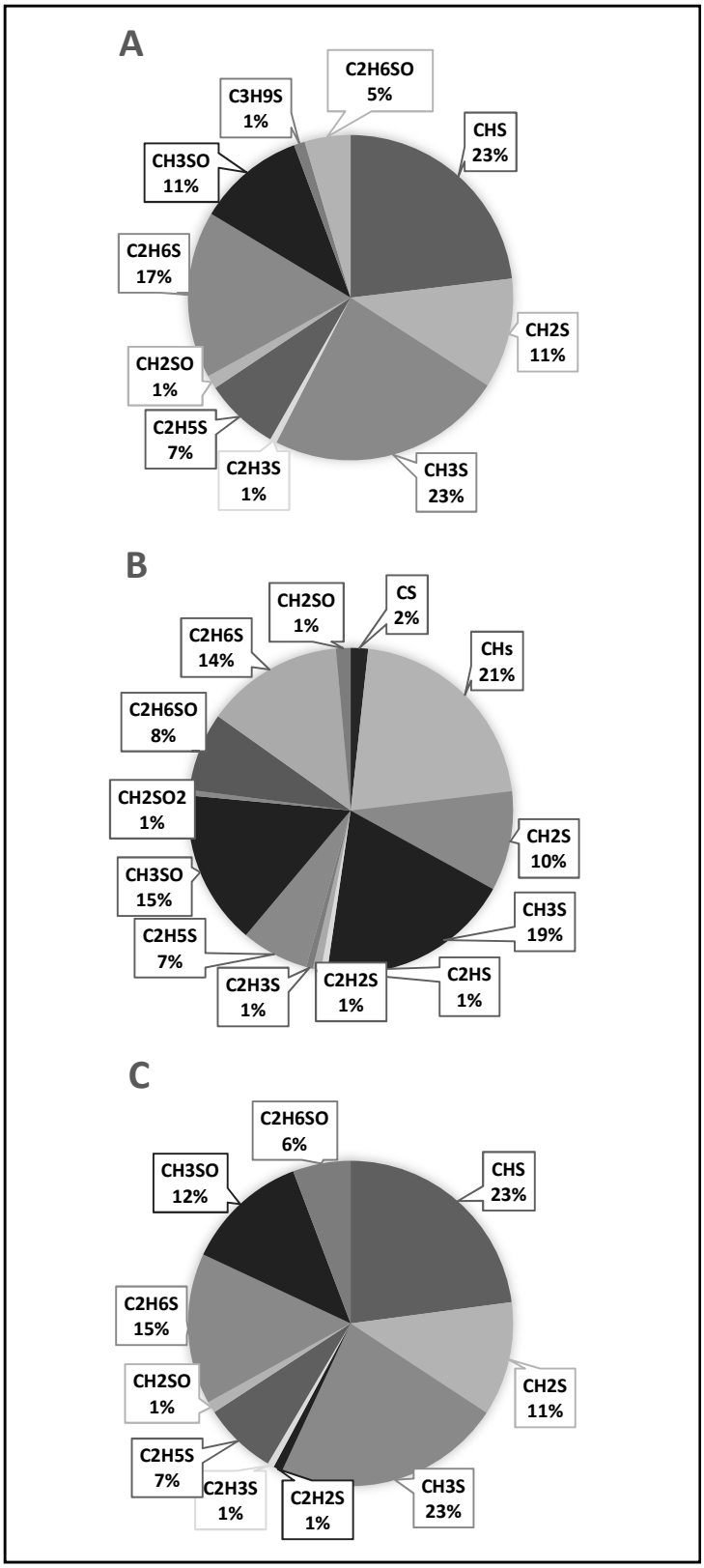

Figure 3-8: Composition of the sulfur-containing organic fragments (both reduced and oxidized) for the following reduced sulfur oxidation experiments:

a) $DMS + OH$ 022619

b) $DMS + O(^3P) + NO_x$ 022719

c) $DMS + NO_3$ 061518

This figure (and others like it) was made using high resolution data gathered by the AMS during oxidation experiment. The fraction of each fragment was averaged over the last 100 minutes of each experiment. These fractions were constant during this time period.

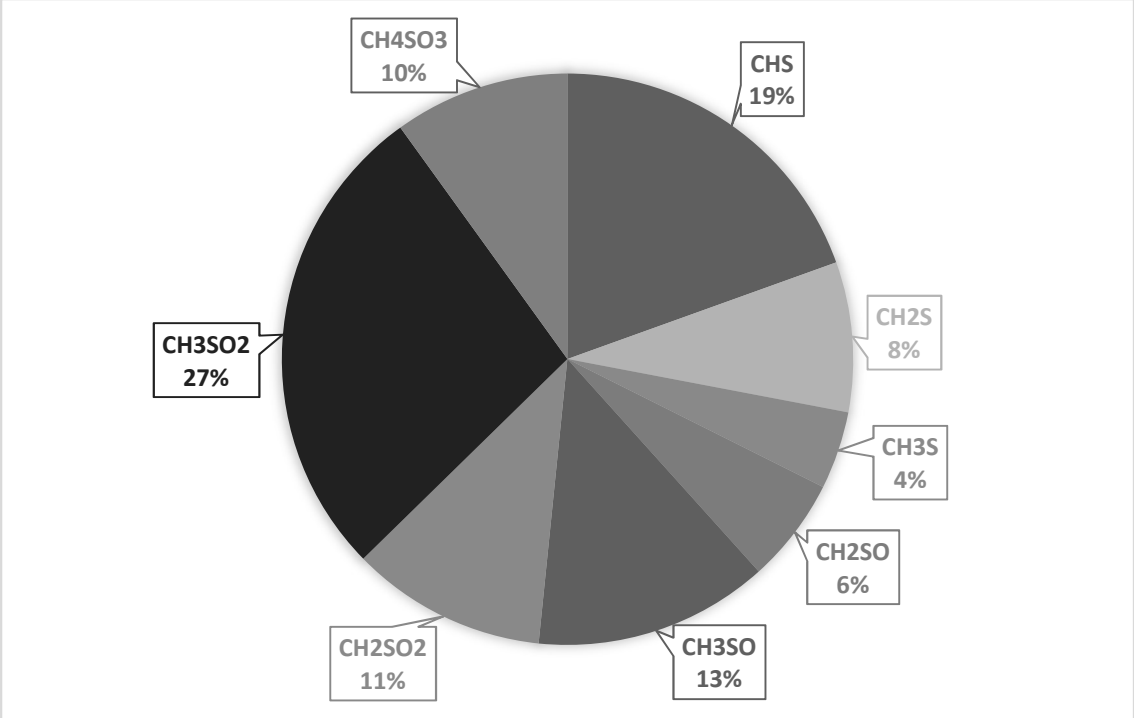

Figure 3-9: Breakdown of sulfur-containing organic fragments present in methanesulfonic acid. To obtain this plot, methanesulfonic acid was atomized through the AMS. Data was averaged over the course of the entire period of atomization. Ratios held constant throughout.

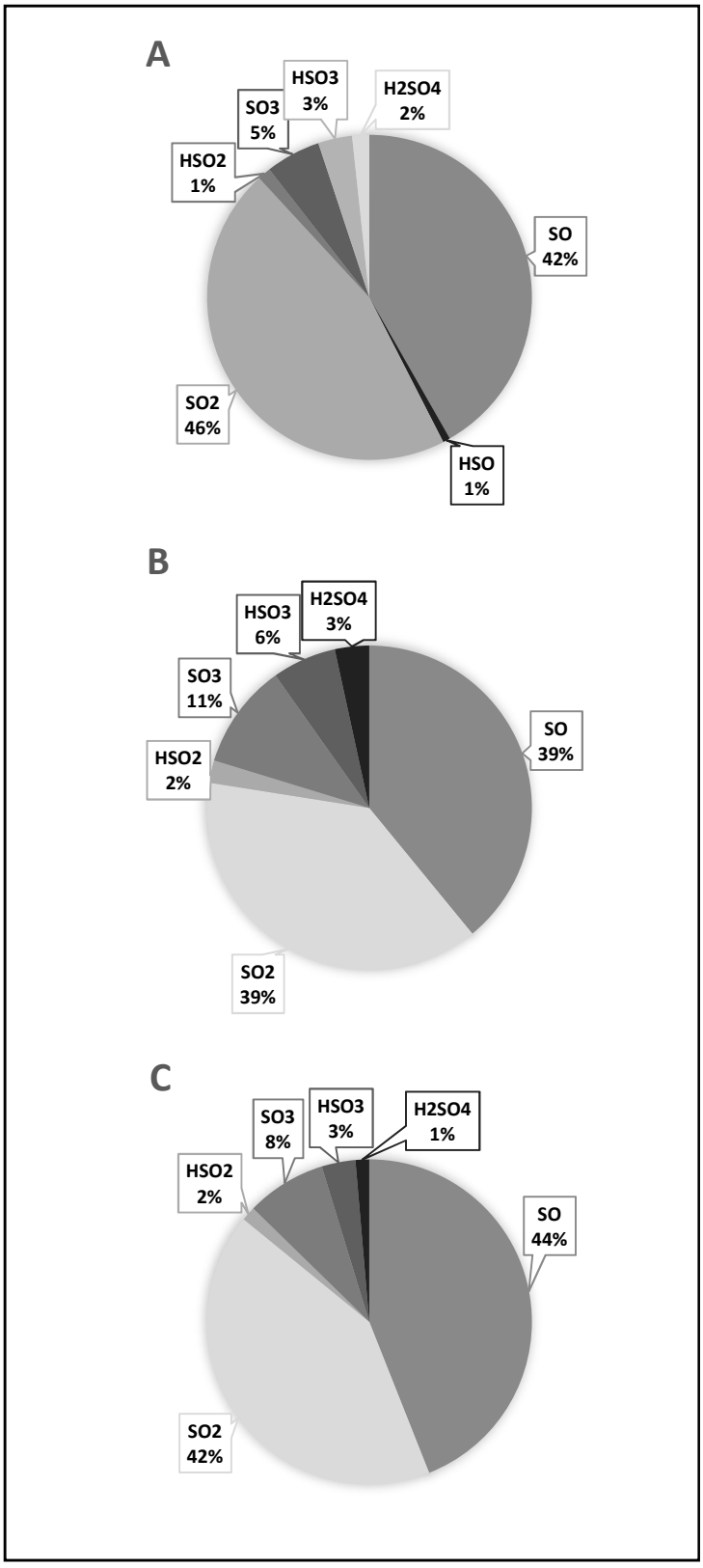

Figure 3-10: Composition of the sulfur-containing inorganic fragments for the following reduced sulfur oxidation experiments:

a) $DMS + OH$ 022619

b) $DMS + O(^3P) + NO_x$ 022719

c) $DMS + NO_3$ 061518

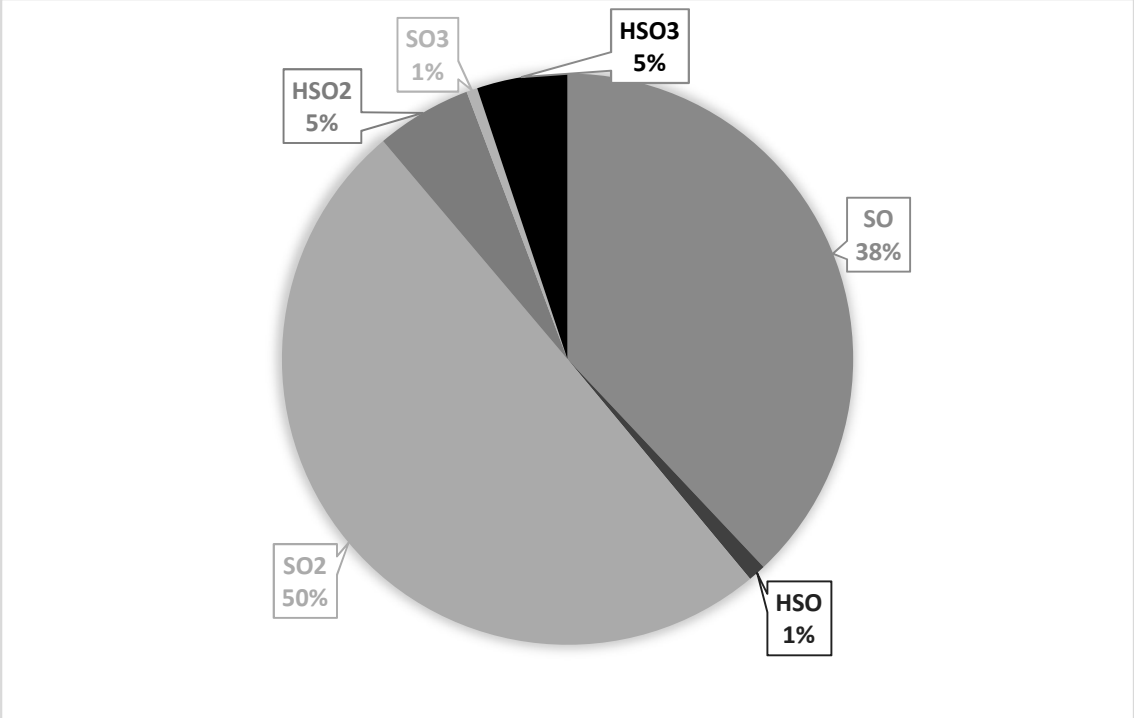

Figure 3-11: Breakdown of sulfur-containing inorganic fragments present in methanesulfonic acid. To obtain this plot, methanesulfonic acid was atomized through the AMS. Data was averaged over the course of the entire period of atomization. Ratios held constant throughout.

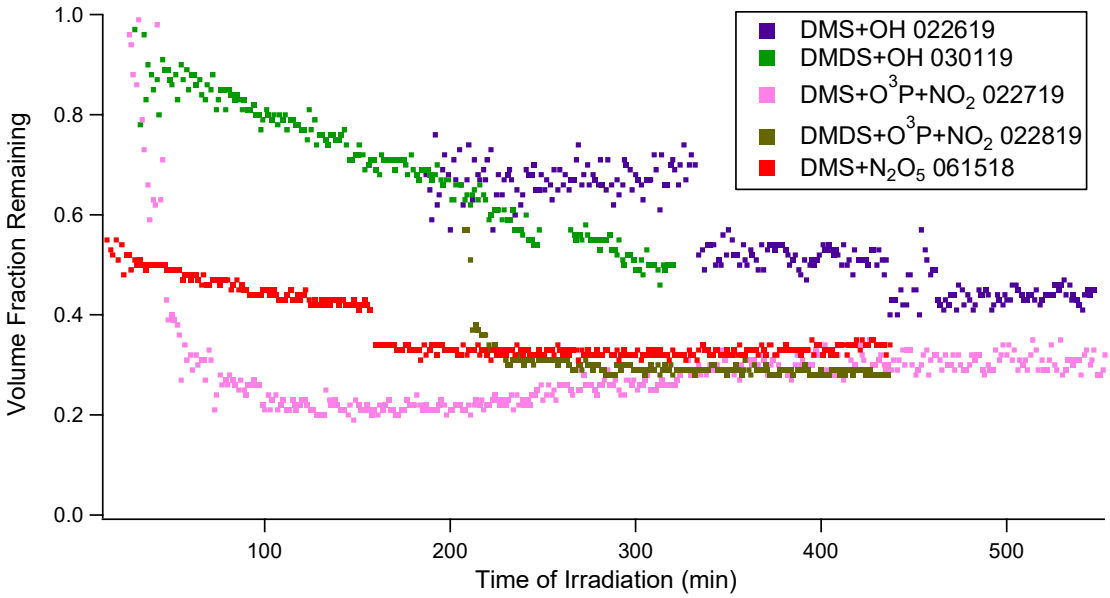

Figure 3-12: Time series of volume fraction remaining, as measured by the VTDMA, for select reduced sulfur oxidation experiments.

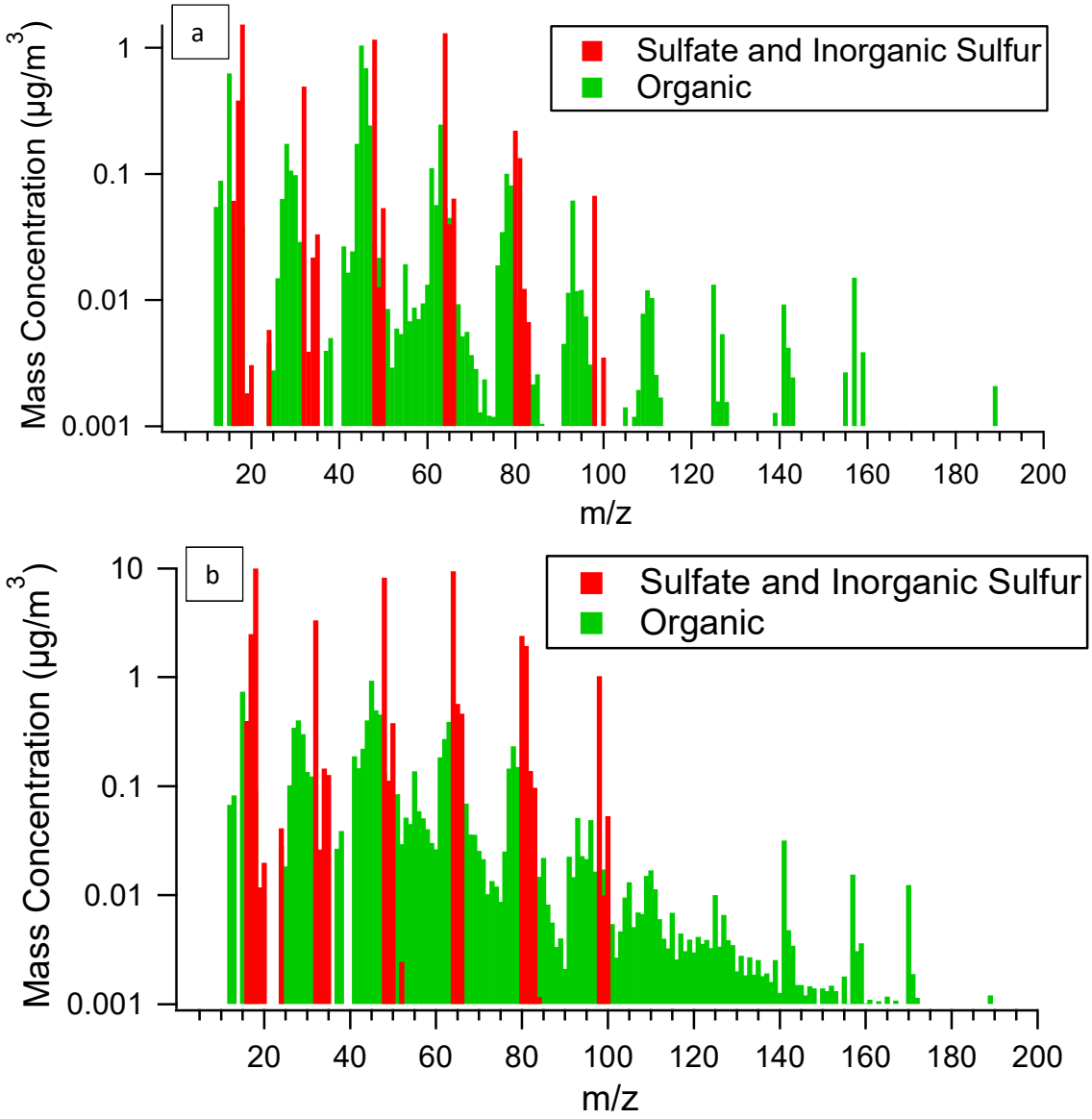

Figure 3-13: Average aerosol mass spectra (as measured by the HR-ToF-AMS) from the following reduced sulfur oxidation experiments: a) $DMDS + OH$ 022619 and b) $DMDS + O(^3P) + NO_x$ 022719. $DMDS + NO_3$ did not form an aerosol concentration that was high enough to adequately measure and record the bulk composition using the AMS.

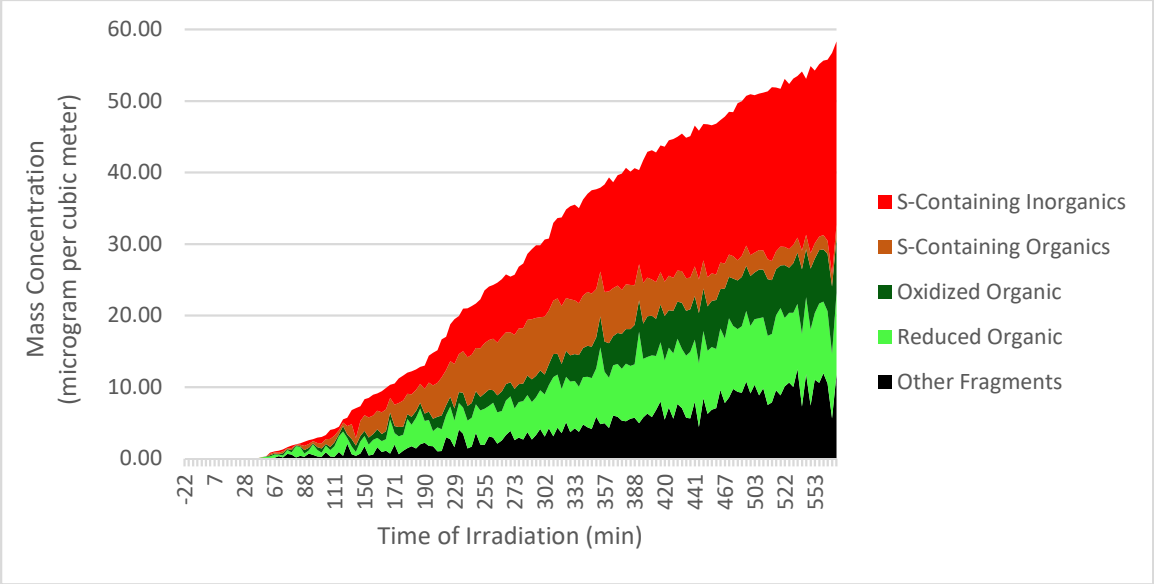

Figure 3-14: Evolution over time of each compound family's contribution to total mass for a DMDS+OH duplicate experiment. This was made by applying the fraction of each compound family, as measured by the AMS, to the corrected mass concentration, as measured by the SMPS along with the APM.

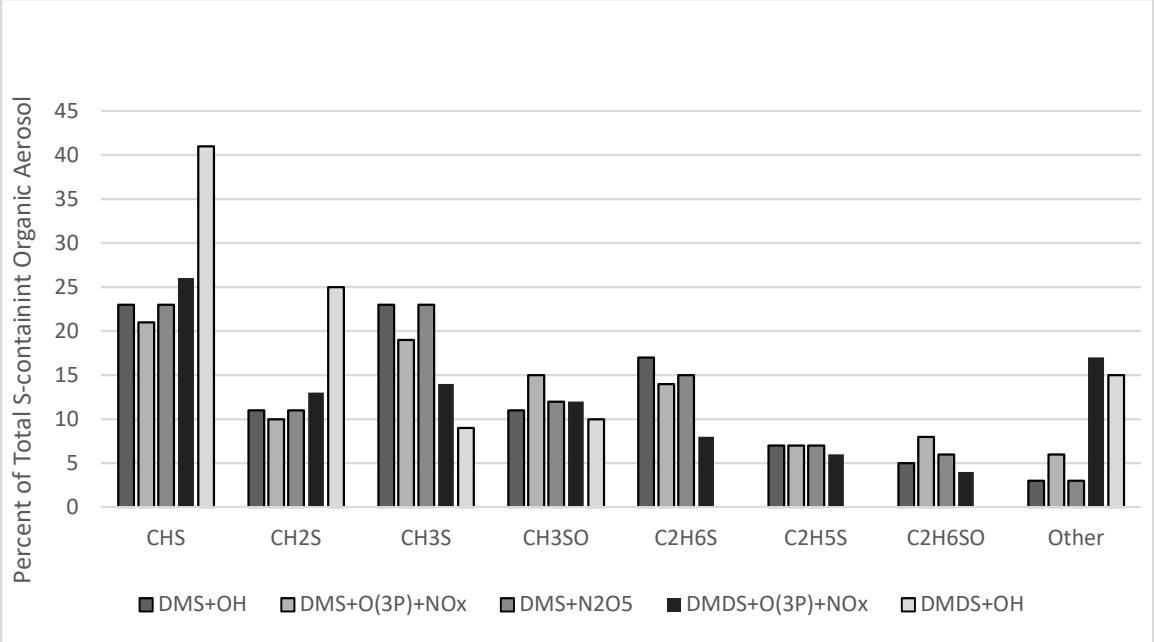

Figure 3-15: A comparison of the major sulfur-containing organic fragments that formed during each oxidation experiment. The bulk of the "Other" fragments that formed during oxidation of DMDS contain two sulfurs.

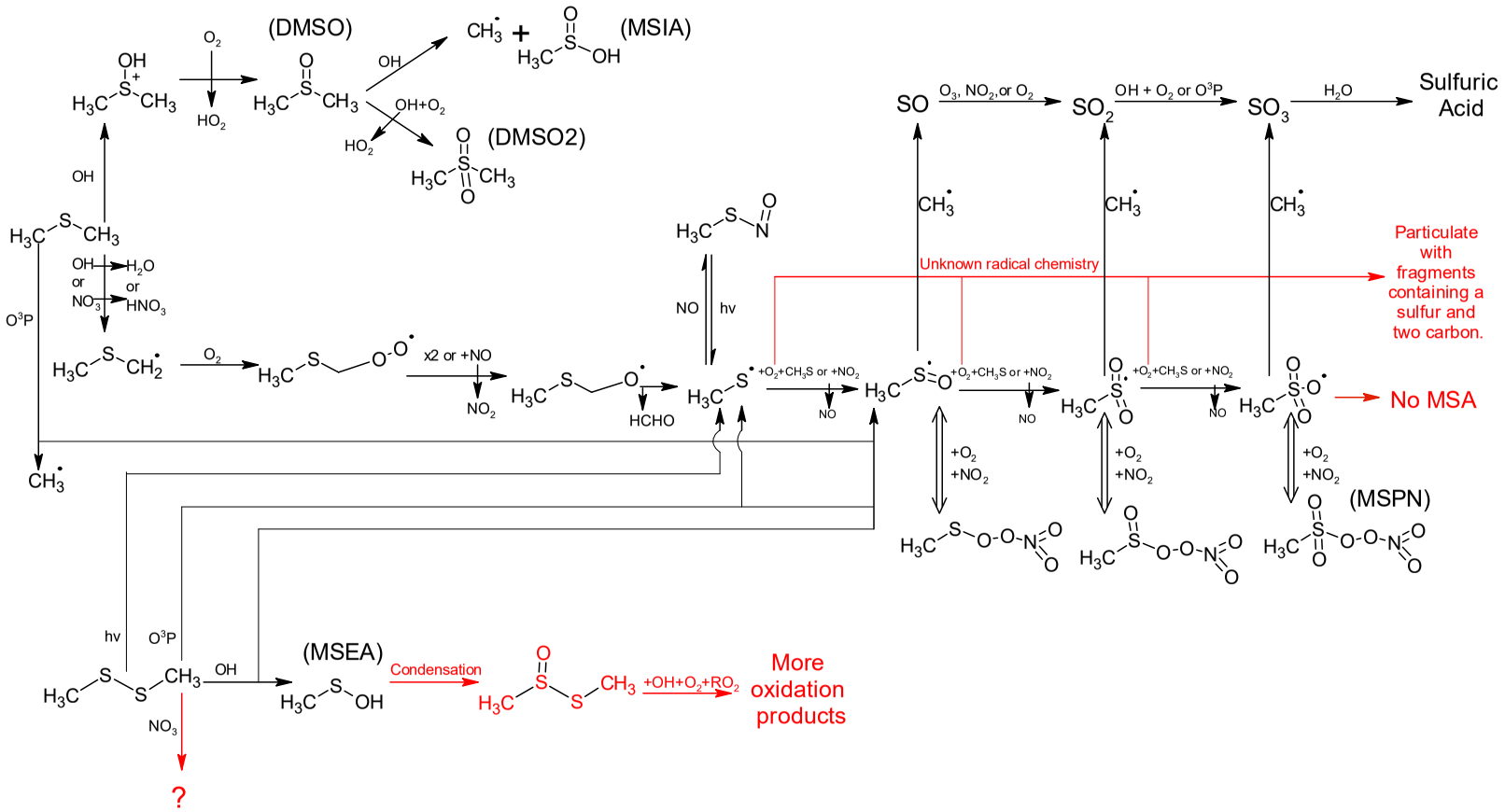

Figure 3-16: A purposed mechanism by which aerosol forms through $OH, O(^3P)$, and NO_3 oxidation of DMS and DMDS under extreme dry conditions. Black represents pathways that have been previously purposed and are supported by this research. Red represents changes to the previously purposed mechanisms that have been determined by this research.

Chapter 4: Oxidation of Reduced Sulfur Compounds Under Humid Conditions

This chapter will cover results from chamber experiments involving oxidation of dimethylsulfide (DMS) and dimethyldisulfide (DMDS) in the presence of humidity as well as the atmospheric implications of these results. The experiments discussed in this chapter were conducted at the most atmospherically relevant conditions of any reduced sulfur oxidation study to date.

4.1 OH Oxidation of DMS and DMDS in the Presence of Humidity

Under humid conditions, both DMS and DMDS oxidize to form similar mass concentrations as they do under dry conditions (Figure 4-1). Precursor decay of DMDS with OH under humid conditions is identical to that under dry conditions (Figure 4-2, Figure 3-2) and the maximum SO_2 signal that is reached matches the dry DMDS +$O(^3P)$ oxidation experiment (Figure 3-3). This indicates that: 1) the presence of humidity does not impact the OH reaction rate, as expected; and 2) given similar oxidation mechanisms, neither humidity nor initial oxidant play a major role in maximum SO_2 formation. Under similar experimental temperatures and precursor concentrations, branching ratio between decomposition to form SO_2 and further oxidation of CH_3SO and CH_3SO_2 radicals appears to be consistent. Concentrations of 100 ppb of NO_2 are not substantial enough to force this branching ratio in the direction of further oxidation. This is in agreement with (Yin et al., 1990(I)) who pointed out that NO_2 concentrations greater than 100 ppb are necessary to make this an important oxidation step for CH_3SO_x and shift the branching ratio away from SO_2 formation. The effects of temperature on maximum SO_2 formation are currently

unknown, but likely to play a role. The SO_2 concentration data is not available for the humid DMDS+OH oxidation experiment, but based on other DMDS oxidation results, it is expected that the trends will be similar to those measured during the dry experiment. Gas-phase DMSO, $DMSO_2$, and MSIA were measured during dry and humid OH oxidation of DMS but nowhere else.

While mass concentration and gas-phase products of DMS and DMDS oxidation were similar under dry and humid conditions (Table 3-1, Table 4-1), mass spectra of the particle-phase indicate some major differences (Figure 4-3). Sulfate fragments are still elevated, however, for DMS oxidation several prominent sulfur-containing organic fragments (*m/z 78* and *m/z 62*) that formed during dry oxidation experiments presumably via radical-chemistry, are no longer forming. In fact, less than 1% of the aerosol fragments are sulfur-containing organics, suggesting that the presence of water inhibits this radical chemistry, and instead follows a more traditional oxidation pathway as can be seen in the purposed mechanism (Figure 4-11). Exactly how the water is playing a role in this chemistry is unknown. It is possible that a higher concentration of water vapor speeds up the overall oxidation mechanism, thereby reducing the buildup of radicals that, under dry conditions, form the unknown particulate discussed in Chapter 3. A high fraction of sulfate fragments, about one-third of total aerosol mass, indicate the formation of sulfuric acid.

Similarly, humidity is no longer allowing the formation of *m/z 78, 93* and the higher mass-to-charge ratio fragments that occurred during dry DMDS oxidation via methanesulfenic acid condensation. Under dry conditions, 25% of the aerosol mass was made up of sulfur-containing organic fragments (Figure 4-4). At a relative humidity of

35%, nearly half the aerosol mass is sulfur-containing inorganics and another third is "other" fragments, which consist of OH and H_2O, common fragments of sulfuric acid. Only 4% of the aerosol mass consists of sulfur-containing organic fragments. Even at 2% relative humidity, only 8% of the mass is sulfur-containing organics. However, in contrast with DMS oxidation under humid conditions, DMDS oxidation presents several new fragments at *m/z 79* (CH_3SO_2) and *m/z 96* (CH_4SO_3). These fragments are considered to be unique to MSA formation (Zorn et al., 2008). Previous mechanisms suggest that MSA can form via reaction of CH_3SO_3 and methanesulfenic acid. However, no methanesulfonic acid formed under dry conditions. This may be due to the consumption of methanesulfenic acid via condensation onto itself (Figure 3-16) as well as reactions with hydroxyl radical. The formation of methanesulfonic acid, and absence of the sulfur-containing organic fragments, indicate that water as well as methanesulfenic acid play an important role in the formation of methanesulfonic acid, possibly by way of heterogeneous processes.

Methanesulfonic acid was atomized through the HR-ToF-AMS in order to obtain a fragmentation pattern (Figure 3-9, 3-11). Using this data, ratios of a unique methanesulfonic acid peak (*m/z 79* or *96*) to total sulfur-containing organic were calculated as follows:

$$\frac{sulfur-containing\ organic}{CH_3SO_2} = 3.59 \pm 0.22, \quad \frac{sulfur-containing\ organic}{CH_4SO_3} = 9.58 \pm 0.99$$

These fragmentation ratios can be applied to experiments that are believed to form methanesulfonic acid in order to determine the amount of total sulfur-containing organic fragments that can be explained by methanesulfonic acid. Furthermore, the total mass fraction of methansulfonic acid can be estimated with the knowledge that sulfur-containing

organic fragments make up approximately $12 \pm 2\%$ of the total non-water mass. This total mass can then be distributed between the various compound families (reduced organic, oxidized organic, sulfur-containing organic, sulfur-containing inorganic, and other) using the bulk fragmentation of methanesulfonic acid into these families (Table 4-2). Because the fragmentation pattern of methanesulfonic acid depends on the instrument heater temperature (Zorn et al., 2008) there may be some discrepancies when applying the ratios recorded here, which were collected using a heater temperature 570 degrees Celsius, to other experiments, which were typically run with a heater temperature between 530 and 610 degrees Celsius. Nonetheless, applying these ratios will give a rough estimate of the percentage of total non-water mass concentration that can be explained by methanesulfonic acid formation at the end of each experiment.

Applying these ratios to the humid DMDS+OH oxidation products (Figure 4-5), it can be determined that 80-100% of the mass of sulfur-containing organic fragments. This means that 13-19% of the total mass can be explained by methanesulfonic acid formation. The range of values is based on calculations using both ratios above; an example calculation can be seen on (Equation 4-1). Table 4-2 shows the fraction of each compound family that can be explained by methanesulfonic acid formation. A majority of the remaining sulfur-containing inorganic aerosol as well as the "other" compound family, which consists primarily of OH and H_2O fragments, can likely be explained by sulfuric acid formation, leaving only about 10% of organic mass that is unexplained.

4.2 $O(^3P)$ Oxidation of DMS and DMDS in the Presence of NO_x and Humidity

The addition of humidity to $O(^3P)$ oxidation results in mass concentrations 2.5 and 40 times higher than for DMS and DMDS, respectively (Figure 4-6). If it is assumed that the mass formed through $O(^3P)$ oxidation of DMDS levels off at $2000\frac{\mu g}{m^3}$, which is not the case as is evident by the continuous growth in aerosol mass, a DMDS aerosol yield is calculated to be 540%. If DMDS were to completely oxidize to the expected particulate products (sulfuric acid and methanesulfonic acid), and nothing else, a yield of just over 200% is expected. Here, we are seeing a much higher yield and, based on the formation and availability of SO_2 (Figure 4-7), complete oxidation was not attained. There are two possible reasons for this massive aerosol formation and it is likely that both are playing a role: 1) greater mass is formed due to condensation of water onto existing acidic particles, which have been measured to be very hydrophilic, with a growth factor greater than 1.4; and 2) the organic radicals that form when CH_3SO_x radicals decompose are further oxidizing and playing a role in particle formation via condensation or possible reacting in the acidic compounds. The yield for DMS at the end of the experiment was around 100%. The maximum yield expected, if all DMS went on to form particulate sulfuric acid, is just over 150%. Again, based on the continuous mass formation of aerosol and the availability of SO_2, this reaction is not close to complete oxidation. Despite this, we are still seeing 100% yield, indicating that the same possible reasons mentioned for the massive DMDS aerosol yield are also true for DMS.

As mentioned previously, both oxidation experiments continue to form mass slowly; this also occurs during the identical dry experiments. The continuous growth is

likely due to the slow reaction that must occur to oxidize SO_2 to H_2SO_4. Similar results in the presence or absence of water indicate that water is not the limiting reactant here. Hydroxyl radical, which was injected at minute 270 of the $DMS + O(^3P)$ oxidation experiment, was found to have no impact on the decay rate of DMS, which matches well with the identical dry experiment, and did not substantially contribute to the rate of aerosol mass formation. However, it did result in a leveling of the SO_2 concentration (Figure 4-7). This suggests that the initial SO_2 oxidation step is not the rate limiting reaction to form sulfuric acid. Again, DMDS oxidized to form a SO_2 signal similar to that measured during the NO_x-free oxidation experiment, further indicating that 100 ppb of NO_x will not substantially impact the branching ratio of CH_3SO or CH_3SO_2 radicals.

The presence of humidity allows both DMS and DMDS to more abundantly form particulate methanesulfonic acid, as the magnitude fragments of *m/z 79* and *m/z 96* imply (Figure 4-8). This is the first evidence of DMS oxidizing to form methanesulfonic acid. DMDS oxidized to form methanesulfonic acid during OH oxidation under humid conditions, however, here the peaks associated with methanesulfonic acid are more prominent. This agrees with previous studies that have pointed out the importance of NO_x to methanesulfonic acid formation (Patroescu et al., 1999). However, based on the lack of formation during identical dry experiments, it can be concluded that both humidity and NO_x are paramount in the formation of methanesulfonic acid. Furthermore, the primary pathway to methanesulfonic acid, in the presence of humidity and NO_x and absence of other compound with an available hydrogen, may be a multiple step reaction including CH_3SO_3 radical, water, and NO_x (Figure 4-11). A NO_x sensitivity study must be performed

to determine the importance of this reaction at more atmospherically relevant conditions; it is likely that this reaction may be more important during laboratory experiments, which are typically run at NO_x concentrations much higher than those seen in the atmosphere. This may result in an artificially high methanesulfonic acid yield and, therefore, artificially low sulfuric acid yield.

DMDS mass spectra also shows elevated peaks at *m/z 141* and *m/z 157*. These peaks fragments were also present during $O(^3P)$ oxidation in the presence of NO_x under dry conditions and are thought to be evidence of methanesulfonyl peroxynitrate (MSPN) formation (Figure 4-11). As is the case for the dry $DMDS + O(^3P)$ oxidation experiment, an unknown peak forms at *m/z 170.* Two new unknown fragments at *m/z 103* and *m/z 118* also appear. These unknown fragments are likely due to reactions involving radicals and NO_x, however, they cannot be adequately explained by any known product of reduced sulfur oxidation. These same higher mass-to-charge peaks are also present, but less prominent, in the humid $DMS + O(^3P)$ oxidation experiment.

Particulate $DMS + O(^3P)$ oxidation products for humid conditions have a bulk composition of 43% by mass sulfur-containing inorganic fragments and 3% sulfur-containing organics (Table 4-2). Particulate mass formed during the similar DMDS experiment consist of 38% sulfur-containing inorganic fragments and 8% sulfur-containing organic fragments. The fragmentation pattern for these two experiments can be seen on Figure 4-8. Both experiments present identical sulfur-containing organic fragments with variable contributions to the total (Figure 4-9). Again, using the ratio of *m/z 79* and *m/z 96*

to total sulfur-containing organic, an estimate of methanesulfonic acid's contribution to total aerosol formation can be estimated for both of these experiments (Table 4-2).

In both the DMDS and DMS humid $O(^3P)$ oxidation experiments, methanesulfonic acid formation can explain most, if not all, of the sulfur-containing organic mass. Methanesulfonic acid formation cannot explain a combined 10% of the mass belonging to reduced and oxidized organic fragment families, and a combined 65% of the mass belonging to the sulfur-containing inorganic and "other" fragment families. The unexplained 65% is likely due to sulfuric acid formation, leaving only 10% of total mass that is unexplained. An increase in density from 1.2 to 1.8 $\frac{g}{cm^3}$ over the course of the experiment provides further evidence of initial methanesulfonic acid formation, with a density of 1.48 $\frac{g}{cm^3}$, followed by the growth of sulfuric acid, which has a density of 1.84 $\frac{g}{cm^3}$. The lower than expected density is due to water condensing on to the particulate.

In contrast with the DMS experiment, methanesulfonic acid formation can explain all of the organic mass formed during the DMDS experiment and all but 25% of the total mass that can be attributed to sulfur-containing inorganic and other fragments, which can be explained by sulfuric acid formation. An increase in density from 1.20 to 1.55 $\frac{g}{cm^3}$ indicates an initial growth of methanesulfonic acid followed by a less substantial growth of sulfuric acid compared to DMS oxidation, in agreement the aforementioned results based on aerosol composition. It is important to recall that an estimated yield, based on the incorrect assumption that mass concentration would level at $2000\frac{\mu g}{m^3}$, was calculated to be at 540%. Based on AMS data, the aerosol formed consists of 75% methanesulfonic

acid and 25% sulfuric acid. If we assume that all DMDS oxidizes to particulate methanesulfonic acid and sulfuric acid, which is an incorrect assumption based on the presence of SO_2, a calculated yield should come out to be around 200%; a mass concentration of about $750\,\frac{\mu g}{m^3}$. To calculate the impact of water on the particle growth, a growth factor of 1.4 can be applied; this growth factor is based on a humid DMDS+OH oxidation experiment, because of the higher concentration of acidic particulate in the humid $O(^3P)$ oxidation of DMDS in the presence of NO_x it is expected that 1.4 is a low estimate of the hygroscopic growth factor. Nonetheless, applying this growth factor yields a total mass of $2050\frac{\mu g}{m^3}$, proving that condensation of water makes it feasible to obtain this 540% aerosol yield. This condensed water will not show up as a fragment on the HR-ToF-AMS.

4.3 NO_3 Oxidation of DMS and DMDS in the Presence of NO_2 and Humidity

During nitrate radical oxidation of reduced sulfur compound in the presence of humidity, nitrate radical preferably reacted with water, forming nitric acid, over the reduced sulfur compound. Nitrate radical was consumed prior to complete oxidation of the reduced sulfur precursor. Only 20% of DMDS was consumed and 60% of DMS was consumed (Figure 4-10). Despite the lack of complete precursor oxidation, DMS formed a mass concentration 6 times higher compared to the dry experiment, which had complete consumption of DMS. Similarly, DMDS formed a mass concentration 30 times greater than the dry duplicate that allowed complete consumption of the precursor. This again points towards the importance of water vapor as well as NO_2 to particle formation.

Mass spectra for these humid nitrate radical experiments are similar to those taken during $O(^3P)$ oxidation. However, these mass spectra no longer show the prominent higher mass-to-charge ratio peaks that were present in the $O(^3P)$ oxidation experiments. Additionally, a major methanesulfonic acid indicator, *m/z 96,* now has a higher magnitude than that of *m/z 98,* a sulfuric acid indicator. In fact, according to the aforementioned ratio calculations, methanesulfonic acid can explain nearly 100% of the aerosol that formed during nitrate radical formation of DMDS as well as DMS. It is important to note that *m/z 98* is not a major fragment of methanesulfonic acid. The mere presence of this fragment suggests that sulfuric acid does form, though in small quantities, during these experiments.

Because N_2O_5 swiftly decomposes to nitrate radical and NO_2, initial concentrations of NO_2 are three time greater than those injected during $O(^3P)$ oxidation experiments. This higher NO_2 concentration resulted in very little, if any, sulfuric acid formation. The lack of sulfuric acid formation at these high NO_2 conditions have one of two implications: 1) while NO_x does not appear to have a major impact on the branching ratios of CH_3SO_2 and CH_3SO radicals, in the presence of humidity, NO_x does have a major impact on the branching ratio of CH_3SO_3 radical thereby playing an important role in the ratio of methanesulfonic acid to sulfuric acid; or 2) CH_3SO_3 radical is not an important player in sulfuric acid formation, therefore, in the absence of an oxidant to react with SO_2, no sulfuric acid will form. This quandary further emphasizes the importance of a NO_x sensitivity chamber study; not only could a study of this nature help to uncover the importance of CH_3SO_3 decomposition to sulfuric acid formation, it would also provide a more

atmospherically relevant idea of the typical methanesulfonic acid to sulfuric acid formation ratios that occur during oxidation of reduced sulfur species.

4.4 Aerosol Yields

Table 4-1 shows aerosol yields, as well as other physical properties, for all three sets of humid experiments discussed here. Precursor concentrations were 100 ppb in all cases. Aerosol yields were calculated based on the amount of precursor consumed and mass formed, as measured by the SMPS-APM-SMPS, at the end of each experiment. The impact of condensation of water onto the particulate on the total mass concentration cannot be reasonably estimated based on the data gathered, therefore, product yields have not been calculated. Instead, aerosol mass fractions have been calculated based on the fragmentation of methanesulfonic acid in the HR-ToF-AMS. Calculations of these mass fractions were discussed previously and an example can be seen in Chapter 3 (Equation 3-1). Because these mass fractions are based on data gathered from the HR-ToF-AMS, they do not include water condensation. Therefore, these calculated mass fractions should not be applied to the total mass formed that was measured by the SMPS-APM-SMPS, which does include growth due to condensation of water, to calculate product yields. These non-water mass fractions that have been discussed throughout this chapter are also compiled in Table 4-2. As noted previously, continuous growth of aerosol, likely due to sulfuric acid formations, forms through the duration of most experiments. The continuous growth implies that 1) the calculated aerosol yields recorded here are low and 2) the calculated mass fraction of methanesulfonic acid is high.

4.5 Summary of Major Findings

By atomizing methanesulfonic acid through the HR-ToF-AMS and applying the unique fragmentation patterns to reduced sulfur oxidation experiment, the aerosol mass fraction of methanesulfonic acid that formed during each reduced sulfur oxidation experiment was estimated. Based on the estimated calculations of methanesulfonic acid mass fraction coupled with results from dry oxidation of these compounds, it has been determined that both NO_x and humidity play an important role in methanesulfonic acid formation. In the presence of humidity, hydroxyl radical oxidation of DMS results in no methanesulfonic formation, very little organic growth, evidence of sulfuric acid particle formation, and a similar mass concentration as compared to the dry conditions. DMDS-hydroxyl radical oxidation under humid conditions resulted in a small fraction, at 16% of total non-water aerosol mass, of methanesulfonic acid growth, very little other organic growth, evidence of sulfuric acid particle formation, and a similar mass concentration as compared to dry conditions. Oxidation by $O(^3P)$ of DMS and DMDS in the presence of NO_x resulted in substantially higher mass concentrations under humid conditions as compared to dry.

Methanesulfonic acid formation can explain approximately 24% and 90% of the aerosol mass formed in the DMS and DMDS oxidation experiment, respectively. Humid nitrate radical oxidation of these compounds resulted in higher mass concentrations of aerosol compared to dry conditions, which can be nearly 100% explained by the formation of methanesulfonic acid. In all experiments apart from the nitrate radical oxidation

experiments, mass concentration continues to increase due to slow reactions to form sulfuric acid. Because of the continuous sulfuric acid formation, it is not possible to adequately calculate true aerosol yields of these experiments. This implies that product yields calculated from previous chamber experiments, typically run for shorter time periods than what was done here, also do not adequate reflect end product yields.

The importance of NO_x is in agreement with previous flow tube DMS oxidation experiments that were run with NO_x concentrations ranging from 0 to 2000 ppb and found gas phase concentrations of methanesulfonic acid increased with increasing NO_2 from 4 to 17% of the total sulfur (Patroescu et al., 1999). Methanesulfonic acid was also measured during two previous chamber studies focused on DMS and/or DMDS oxidation. Yin et al. (1990 (II)) ran a series of outdoor environmental chamber experiments on both DMS and DMDS under various NO_x conditions and found that methanesulfonic acid yields were generally highest, at about 7%, under higher NO_x concentrations. In the absence of NO_x, methanesulfonic acid yields dropped below 0.5%.

More recently, Chen et al. (2012) performed humid DMS oxidation experiments with 200 ppb of NO_x present and calculated a methanesulfonic acid yield of 45%. While the importance of NO_x to methanesulfonic acid formation is well documented, the importance of humidity is less so. Chen et al. (2012) ran experiments at multiple levels of relative humidity, ranging from 10% to 80%, and found that methanesulfonic acid formation increased with humidity. It is noted that a possible reason for this increase is aqueous processing of methanesulfinic acid (MSIA) on the aerosol surface. Results presented here from NO_x-free hydroxyl radical oxidation of DMDS support a similar

particle-forming mechanism involving methanesulfenic acid (MSEA), however, both of these pathways are minor compared to the more important methanesulfonic acid pathway including NO_x, MSPN, and water vapor. This pathways is not prominently, if at all, featured in previous mechanisms (Barnes et al., 2008, Yin et al., 1990 (I), Barnes et al., 1988, Jensen et al., 1992) and has been added here (Figure 4-11).

It is important to note that while the trends of the Yin et al. study and the Chen et al. study are similar to the ones seen here, the quantitative results are much different. Highly variable quantitative results are also common in previous flow tube studies focused on oxidation of these compounds. The reason for the inconsistencies when comparing flow tube results to chamber results is likely due to the extreme high concentrations of radicals as well as precursors in the flow tube experiments is resulting in chemistry that may not be relevant to the atmosphere. Inconsistencies when comparing between chamber experiments is likely due to the sensitivity of these compounds to experimental conditions, like NO_x concentrations, type of oxidant, temperature, and humidity. For this reason, it is difficult to compare previous results to the results seen in this study. The results presented here are, to date, the most atmospherically relevant available

4.6 Atmospheric Implications

Sulfuric acid is known to be important to new particle formation (Doyle, 1961, Shaw, 1989, Kulmala et al., 2000, McMurry et al., 2005). Methanesulfonic acid is known to be more important to particle growth (Berresheim et al., 2002). New particle formation and growth in the atmosphere can cause direct climate effects, through absorbing or

scattering solar radiation (Charlson et al., 1992; Erlick et al., 2001), as well as indirect climate effects, through effecting cloud albedo (de Leeuw et al., 2011). The climate impacts of aerosol depend on the size, number, and composition of the particles (Bond et al., 2006). Particles up to 1 micrometer are most likely to be involved in the direct climate effect (Seinfeld and Pandis, 2006). Hydrophilic particles are more likely to act as cloud condensation nuclei (Petters et al., 2007). Based on the size and highly hydrophilic nature of the particles formed in this study, reduced sulfur oxidation products are important to both climate effects. A recent study by Hodshire et al. (2019) investigated the role of methanesulfonic acid in climate forcing. This study estimated the mass fraction of sulfuric acid and sulfate from DMS oxidation is 4-6 times higher than the mass fraction of methanesulfonic acid from DMS oxidation. With this assumption in place, it was determined that sulfate and sulfuric acid have a direct cooling effect that 5 to 10 times higher than methanesulfonic acid, at around -120 mW m^{-2}, and an indirect cooling effect that is similar to that of methanesulfonic acid, at around -40 mW m^{-2}. This implies that a unit mass of methanesulfonic acid is approximately 5 times more important than sulfuric acid to the indirect cooling effect and of similar importance to the direct cooling effect. Therefore, if the statement that DMS forms a larger mass of sulfuric acid than methanesulfonic acid no longer holds, methanesulfonic acid may actually be more important than sulfuric acid to climate and cloud effects.

While the assumption that DMS oxidation results in 4-6 times higher mass concentration of sulfuric acid and sulfate than methanesulfonic acid appears to be acceptable for day-time oxidation of the precursor (Table 4-1, Table 4-2), night-time

chemistry results in close to 100% of the aerosol mass explained by methanesulfonic acid formation. Similarly, DMDS oxidizes to form a non-water aerosol mass concentration that is between 16% and 91% methanesulfonic acid for day time chemistry, and close to 100% for night-time chemistry. This higher methanesulfonic acid to sulfuric acid mass ratio may result in a more substantial over all cooling effect.

4.7 References

Barnes, I., Bastian, V., Becker, K. H. (1988). Kinetics and Mechanisms of the Reaction of OH Radical with Dimethyl Sulfide. International Journal of Chemical Kinetics 20:415-431.

Barnes, I., Hjorth, J., Mihalopoulos, N. (2006). Dimethyl sulfide and dimethyl sulfoxide and their oxidation in the atmosphere. Chemical Reviews 106:940-975.

Berresheim, H., Elste, T., Tremmel, H. G., Allen, A. G., Hansson, H. C., Rosman, K., Dal Maso, M., Makela, J. M., Kulmala, M., O'Dowd, C. D. (2002). Gas-aerosol relationships of H2SO4, MSA, and OH: Observations in the coastal marine boundary layer at Mace Head, Ireland. Journal of Geophysical Research-Atmospheres 107:12.

Bond, T. C., Habib, G., Bergstrom, R. W. (2006). Limitations in the enhancement of visible light absorption due to mixing state. Journal of Geophysical Research-Atmospheres 111:13.

Charlson, R. J., Schwartz, S. E., Hales, J. M., Cess, R. D., Coakley, J. A., Hansen, J. E., Hofmann, D. J. (1992). Climate Forcing by Anthropogenic Aerosols. Science 255:423-430.

Chen, T. Y. and Jang, M. (2012). Secondary organic aerosol formation from photooxidation of a mixture of dimethyl sulfide and isoprene. Atmospheric Environment 46:271-278.

de Leeuw, G., Andreas, E. L., Anguelova, M. D., Fairall, C. W., Lewis, E. R., O'Dowd, C., Schulz, M., Schwartz, S. E. (2011). Production Flux of Sea Spray Aerosol. Reviews of Geophysics 49:1-39.

Doyle, G. J. (1961). Self-Nucleation in Sulfuric Acid-Water System. Journal of Chemical Physics 35:795-799.

Erlick, C., Russell, L. M., Ramaswamy, V. (2001). A microphysics-based investigation of the radiative effects of aerosol-cloud interactions for two MAST Experiment case studies. Journal of Geophysical Research-Atmospheres 106:1249-1269.

Hodshire, A. L., Campuzano-Jost, P., Kodros, J. K., Croft, B., Nault, B. A., Schroder, J. C., Jimenez, J. L., Pierce, J. R. (2019). The Potential Role of Methanesulfonic Acid (MSA) in Aerosol Formation and Growth and the Associated Radiative Forcings. Atmospheric Chemistry and Physics 19:3137-3160.

Jensen, N. R., Hjorth, J., Lohse, C., Skov, H., Restelli, G. (1992). Products and Mechanisms of the Ga-Phase Reactions of NO3 with CH3SCH3, CD3SCD3, CH3SH and CH3SSCH3. Journal of Atmospheric Chemistry 14:95-108.

Kulmala, M., Pirjola, U., Makela, J. M. (2000). Stable sulphate clusters as a source of new atmospheric particles. Nature 404:66-69.

McMurry, P. H., Fink, M., Sakurai, H., Stolzenburg, M. R., Mauldin, R. L., Smith, J., Eisele, F., Moore, K., Sjostedt, S., Tanner, D., Huey, L. G., Nowak, J. B., Edgerton, E., Voisin, D. (2005). A criterion for new particle formation in the sulfur-rich Atlanta atmosphere. Journal of Geophysical Research-Atmospheres 110:10.

Patroescu, I. V., Barnes, I., Becker, K. H., Mihalopoulos, N. (1999). FT-IR product study of the OH-initiated oxidation of DMS in the presence of NOx. Atmospheric Environment 33:25-35.

Petters, M. D. and Kreidenweis, S. M. (2007). A single parameter representation of hygroscopic growth and cloud condensation nucleus activity. Atmospheric Chemistry and Physics 7:1961-1971.

Seinfeld, J. H. (2006). Atmospheric chemistry and physics from air pollution to climate change. J. Wiley, Hoboken, N.J.

Shaw, G. E. (1989). Production of Condensation Nuclei in Clean-Air by Nucleation of H2SO4. Atmospheric Environment 23:2841-2846.

Yin, F., Grosjean, D., Flagan, R. C., Seinfeld, J. H. (1990a). Photooxidation of dimethyl sulfide and dimethyl disulfide. II: Mechanism evaluation. Journal of Atmospheric Chemistry, Dordrecht, The Netherlands 11:365-399.

Yin, F., Grosjean, D., Seinfeld, J. H. (1990b). Photooxidation of dimethyl sulfide and dimethyl disulfide. I: Mechanism development. Journal of Atmospheric Chemistry, Dordrecht, The Netherlands 11:309-364.

Zorn, S. R., Drewnick, F., Schott, M., Hoffmann, T., Borrmann, S. (2008). Characterization of the South Atlantic marine boundary layer aerosol using an aerodyne aerosol mass spectrometer. Atmospheric Chemistry and Physics 8:4711-4728.

4.8 Tables

Experiment	Elapsed Time (min)	Precursor Consumed ΔHC (ppb)	Mass Formed ΔM_o ($\mu g/m^3$)	Density (g/cm^3)	Volume Fraction Remaining	Aerosol Yield $\Delta M_o/\Delta HC$ (%)
DMS+OH (40%RH) 110918	420	30[a]	9.2+	1.60	0.6	12.5*
DMS+$O(^3P)$+NO_x (40%RH) 030519	410	100	247+	1.20-1.80	0.6	100.9*
DMS+NO_3+NO_2 (40%RH) 062018	420	75	120	1.20-1.50	0.6-0.3	65.4
DMDS+OH (2%RH) 102918	550	100	90+	1.46	0.6-0.3	24.2*
DMDS+OH (35%RH) 030419	520	100	95+	1.50	0.3	25.6*
DMDS+ $O(^3P)$+NO_x (35%RH) 030619	385	100	1990+	1.20-1.55	0.6	536.2*
DMDS+NO_3+NO_2 (55%RH) 061918	400	20	60	1.1	0.3-0.4	80.8

Table 4-1: Measured and calculated physical properties of the aerosol formed during each reduced sulfur oxidation experiment. In some cases, volatility and/or density substantially changed during an experiment, as indicated by a range of values. In most cases, aerosol mass continued to steadily increase for the duration of the experiment (indicated by "+"). For this reason, true aerosol yields could not be calculated. Instead a lower estimate of the aerosol yield is provided (indicated by "*") based on the data gathered during this study. Conversions of precursor concentration from ppb to $\mu g/m^3$ were calculated at 300K.

a: This values is an estimate based off of a duplicate experiment.

Experiment	Reduced Organic Fragments (Fraction explained by MSA)	Oxidized Organic Fragments (Fraction explained by MSA)	Sulfur-Containing Organic Fragments (Fraction explained by MSA)	Sulfur-Containing Inorganic Fragments (Fraction explained by MSA)	"Other" Fragments (Fraction explained by MSA)
DMS+OH (40%RH) 110918	0.33	0.32	0.01	0.33	0
DMS+$O(^3P)$+NO_x (40%RH) 030519	0.11 (0.06)	0.07 (0.03)	0.03 (0.03)	0.43 (0.08)	0.36 (0.05)
DMS+NO_3+NO_2 (40%RH) 062018	0.27 (0.27)	0.11 (0.11)	0.15 (0.14)	0.33 (0.33)	0.14 (0.14)
DMDS+OH (2%RH) 102918	0.12 (NA)	0.09 (NA)	0.04 (NA)	0.49 (NA)	0.26 (NA)
DMDS+OH (35%RH) 030419	0.08 (0.04)	0.08 (0.02)	0.02 (0.02)	0.47 (0.05)	0.35 (0.03)
DMDS+ $O(^3P)$+NO_x (35%RH) 030619	0.12 (0.12)	0.07 (0.07)	0.08 (0.08)	0.38 (0.29)	0.34 (0.18)
DMDS+NO_3+NO_2 (55%RH) 061918	0.24 (0.23)	0.13 (0.10)	0.11 (0.11)	0.32 (0.30)	0.20 (0.19)
Methanesulfonic Acid (Atomized)	0.25	0.11	0.12	0.32	0.21

Table 4-2: Mass fraction of aerosol formed belonging to each compound family, as measured by the HR-ToF-AMS. A description of each compound family can be found on Table 3-1. In parenthesis is the estimated mass fraction that can be explained by the formation of methanesulfonic acid, as described in Equation 4-1. These mass fractions are calculated using averages A sum of all values in the parenthesis will provide an estimate of total mass fraction that can be explained by methanesulfonic acid. These mass fractions are calculated using an average value from the final 100 minutes of each experiment. The fractions remained relatively constant for the duration the averages were calculated. These are rounded estimates and may add up to more (or less) than 1.00.

In some cases, the methanesulfonic acid was estimated to make up more than 100% of any given compound family. If this occurred, it was assumed that methanesulfonic acid could explain 100% of the compound family.

4.10 Equations

Equation 4-1: Example calculation estimating the total mass fraction of aerosol that can be explained by the formation of methanesulfonic acid.

Note: these calculations are only valid if $CH_4SO_3$and CH_3SO_2 fragments are assumed to be unique to the formation of methanesulfonic acid.

Methanesulfonic acid constants:

$$\frac{mass\ of\ sulfur-containing\ organic\ fragments}{mass\ of\ CH_3SO_2\ fragment} = \frac{CS}{79} = 3.59$$

$$\frac{mass\ of\ sulfur-containing\ organic\ fragments}{mass\ of\ CH_4SO_3\ fragment} = \frac{CS}{96} = 9.58$$

$$\frac{mass\ of\ sulfur-containing\ organic\ fragments}{total\ mass} = \frac{CS}{M} = 0.12$$

$$\frac{mass\ of\ reduced\ organic\ fragments}{total\ mass} = \frac{CH}{M} = 0.25$$

$$\frac{mass\ of\ oxidized\ organic\ fragments}{total\ mass} = \frac{CHO}{M} = 0.11$$

$$\frac{mass\ of\ sulfur-containing\ inorganic\ fragments}{total\ mass} = \frac{S}{M} = 0.32$$

$$\frac{mass\ of\ \text{"other"}\ fragments}{total\ mass} = \frac{OH}{M} = 0.20$$

Variable inputs determined by each individual experiment (example is based on DMDS+OH (35%RH) 030419):

$$\frac{79}{CS} = 0.22, \qquad \frac{96}{CS} = 0.12, \qquad \frac{CS}{M} = 0.02$$

Calculating the fraction of sulfur-containing organic fragments that can be explained by methanesulfonic acid formation (base on CH_3SO_2):

$$Total\ mass\ (based\ on\ SMPS-APM)\ of\ CH_3SO_2\ fragment = \frac{79}{CS}(variable) \times \frac{CS}{M}(variable) \times M_{smps} = M_{79}$$

All of M_{79} is assumed to be from methanesulfonic acid, therefore the constant methanesulfonic acid ratios can be applied.

$$Mass\ of\ sulfur-containing\ organic\ fragments\ explained\ by\ MSA = M_{79} \times \frac{CS}{79}(constant) = M_{CS\_MSA}$$

$$Mass\ fraction\ of\ sulfur-containing\ organic\ fragments\ explained\ by\ MSA = \frac{M_{CS_{MSA}}}{M_{CS_{Total}}}\ \ where\ M_{CS_{Total}} = M_{smps} \times \frac{CS}{M}(variable)$$

$$\frac{M_{CS_{MSA}}}{M_{CS_{Total}}} = \frac{\frac{79}{CS}(variable) \times \frac{\cancel{CS}}{\cancel{M}}\cancel{(variable) \times M_{smps}} \times \frac{CS}{79}(constant)}{\cancel{M_{smps}} \times \frac{\cancel{CS}}{\cancel{M}}\cancel{(variable)}}$$

$$\frac{CS}{79}(constant) \times \frac{79}{CS}(variable) = 3.59 \times 0.22 = 0.79$$

Calculating the fraction of total non-water aerosol mass that can be explained by methanesulfonic acid formation (based on CH_3SO_2):

It is now known that 79% of sulfur-containing organic fragments can be explained by MSA. Furthermore, it has been established that sulfur-containing organic fragments makes up 2% of the total aerosol, as defined by the $\frac{CS}{M}(variable)$.

$$fraction\ of\ total\ mass\ from\ sulfur\ containing\ organic\ fragments\ explained\ by\ MSA = \frac{M_{CS_{MSA}}}{M_{Total}} = \frac{M_{CS_{MSA}}}{M_{CS_{Total}}} \times \frac{CS}{M}(variable) = 0.79 * 0.02 = 0.0158$$

This means 1.58% of the total mass can be explained by the sulfur-containing fragments of methanesulfonic acid. It is also been previously determined that sulfur-containing organic fragments make up approximately 12% of the total methanesulfonic acid aerosol mass as defined by $\frac{CS}{M}(constant)$.

$$fraction\ of\ total\ mass\ explained\ by\ MSA = \frac{M_{CS_{MSA}}}{M_{Total}} \times \frac{M_{MSA}}{M_{CS_{MSA}}} = \frac{M_{CS_{MSA}}}{M_{Total}} \times \frac{1}{CS/_{M}\,(constant)} = 0.0158 \times \frac{1}{0.12} = 0.132$$

Based on the CH_3SO_2 particle fragment, 13.2% of the total aerosol can be explained by methanesulfonic acid formation. By applying the same procedure using ratios involving the CH_4SO_3 fragment, an estimated 19.2% of total aerosol can be explained by methanesulfonic acid formation.

This comes out to an average of $16.2\% \pm 20\%\ of\ the\ average$ ($\pm 3\%\ in\ this\ case$).

Calculating fractions of each compound family that can be explained by methanesulfonic acid:

$$\frac{CS}{M}, \frac{CH}{M}, \frac{CHO}{M}, \frac{S}{M}, or \frac{OH}{M}\ (constant) \times fraction\ of\ total\ mass\ explained\ by\ MSA$$

4.10 Figures

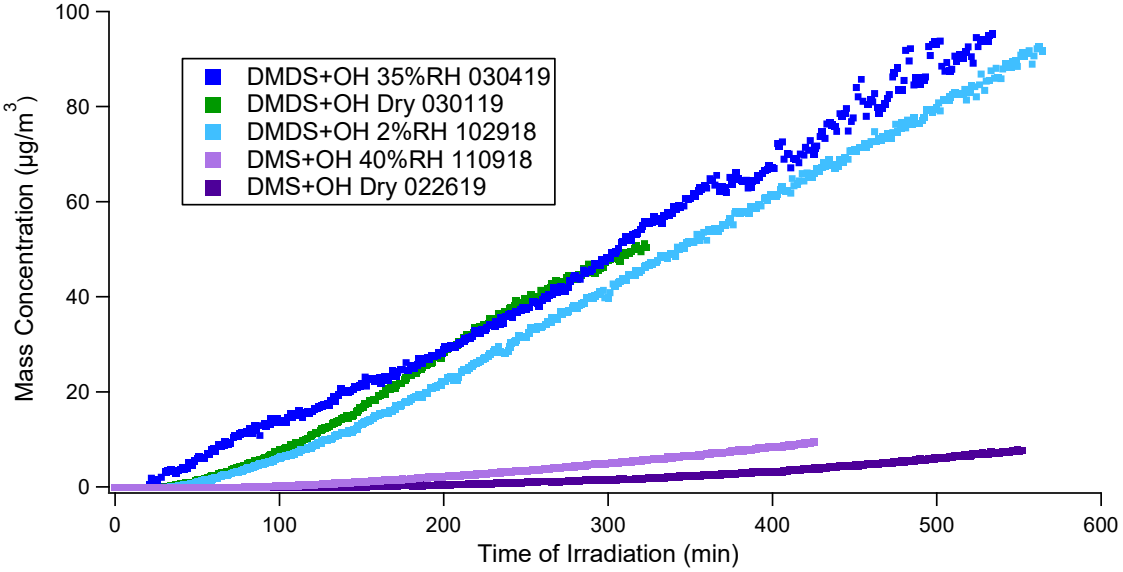

Figure 4-1: Wall loss-corrected aerosol mass concentration time series for reduced sulfur-hydroxyl radical oxidation experiments.

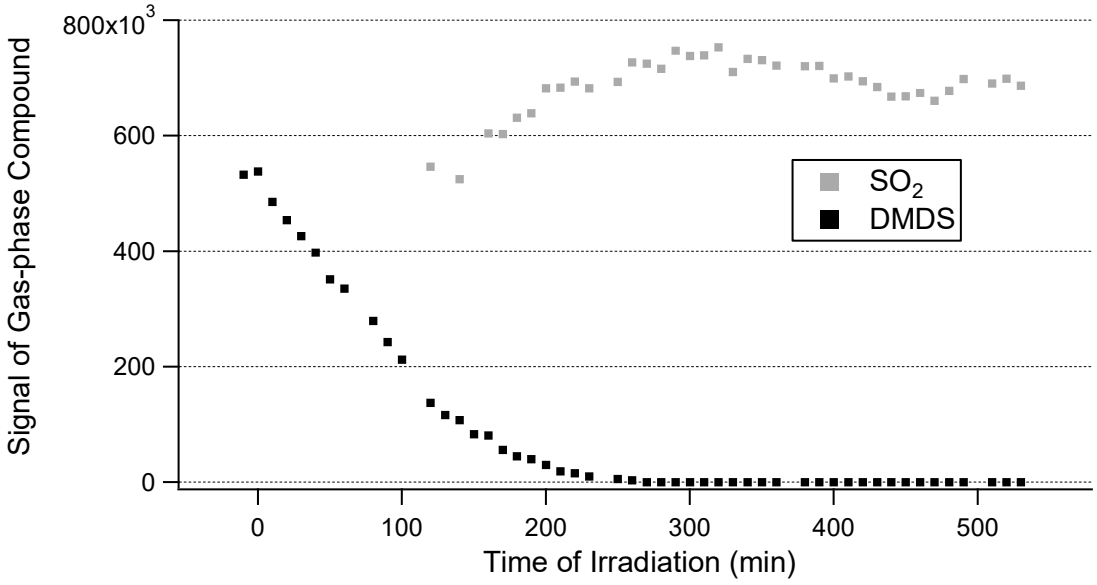

Figure 4-2: Precursor decay and sulfur dioxide formation during hydroxyl radical oxidation of DMDS (35%RH, 030519) as measured by the sulfur GC.

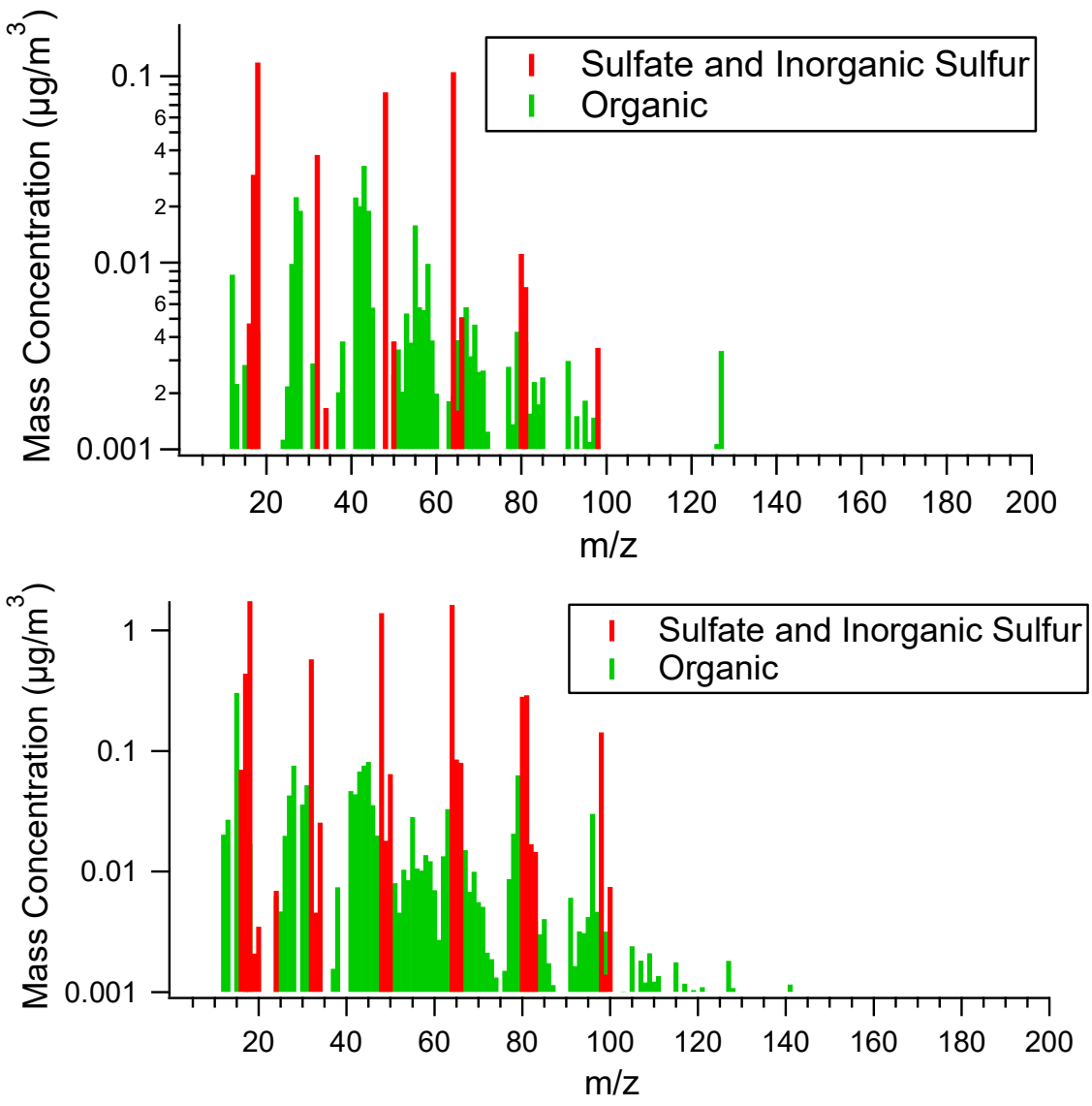

Figure 4-3: Average aerosol mass spectra from humid reduced sulfur-hydroxyl radical oxidation experiments: $DMS + OH + 40\%RH$ 110918 (Top), $DMDS + OH + 35\%RH$ 030419.

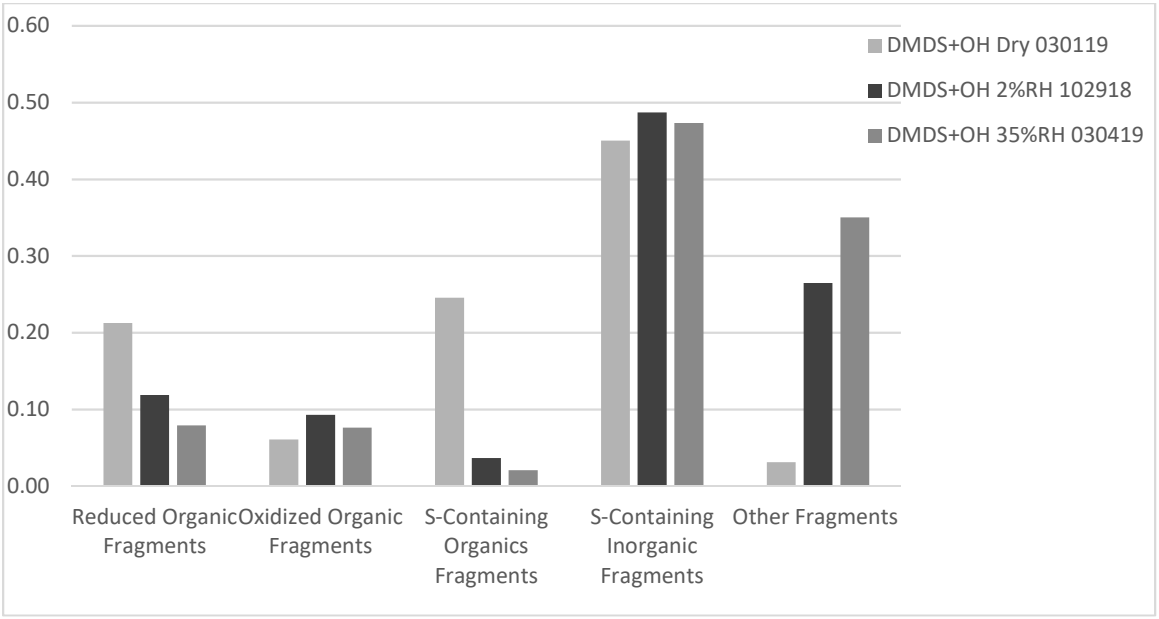

Figure 4-4: Mass fraction of particle fragments belonging to each compound family (Table 3-1), as measured by the AMS. Based on averages calculated during the last 100 minutes of each experiment.

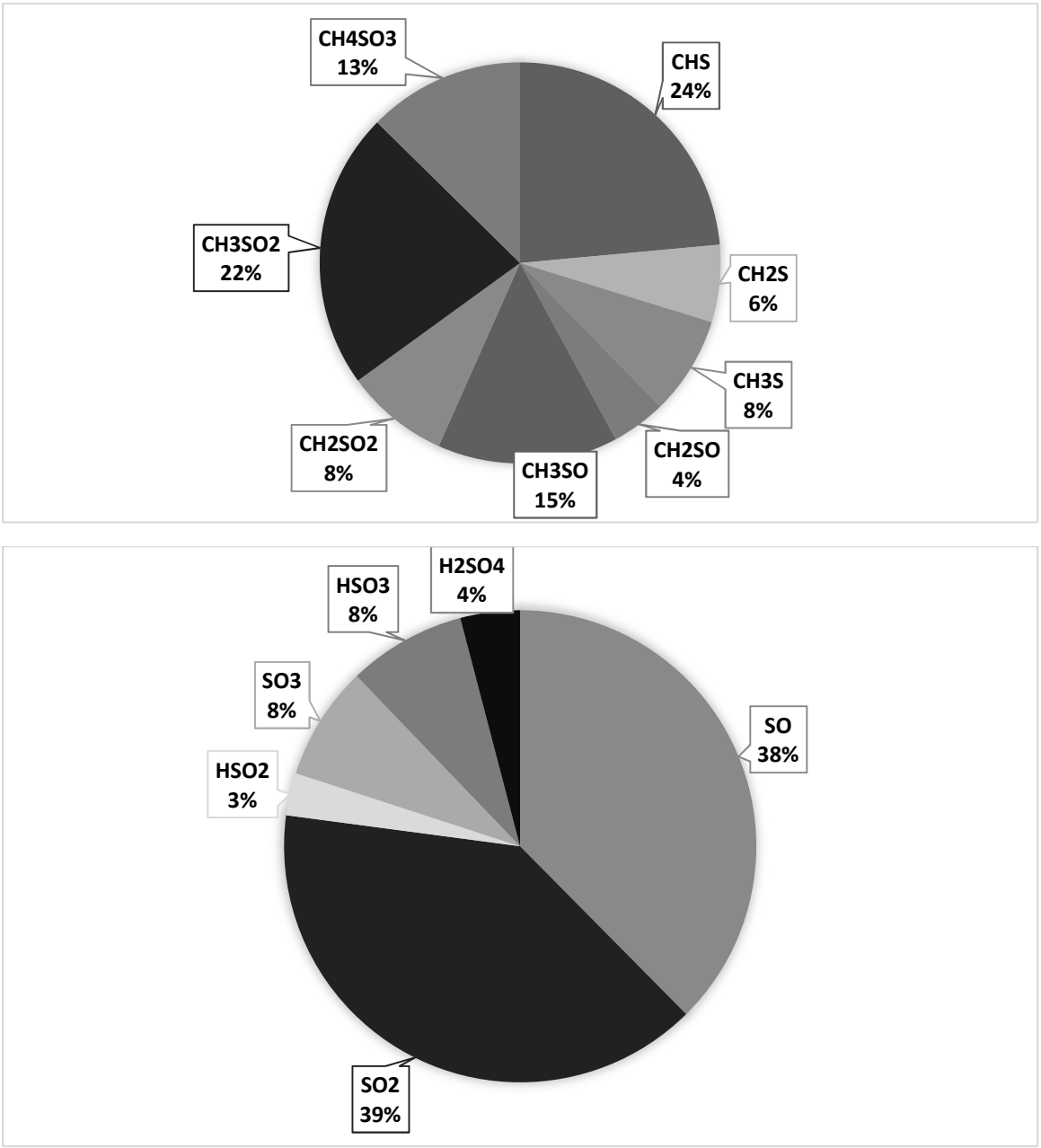

Figure 4-5: Fraction of each compound fragment that makes up the total sulfur-containing organic (top) and sulfur-containing inorganic (bottom) compound families measured during the $DMDS + OH + 35\%RH$ 030419 oxidation experiment.

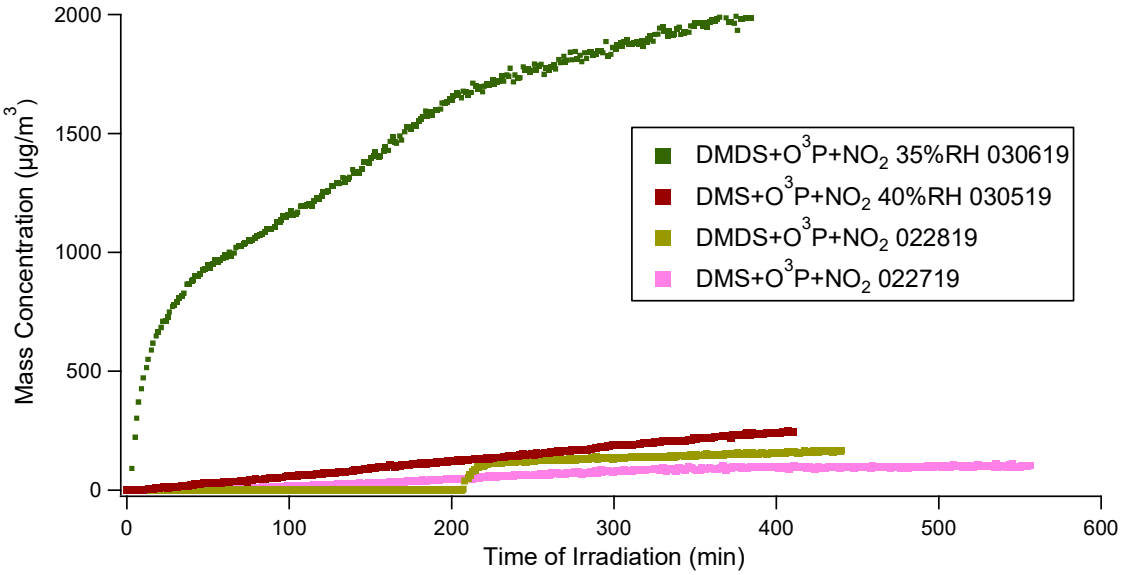

Figure 4-6: Wall loss corrected mass concentration time series for humid $O(^3P)$ oxidation experiments.

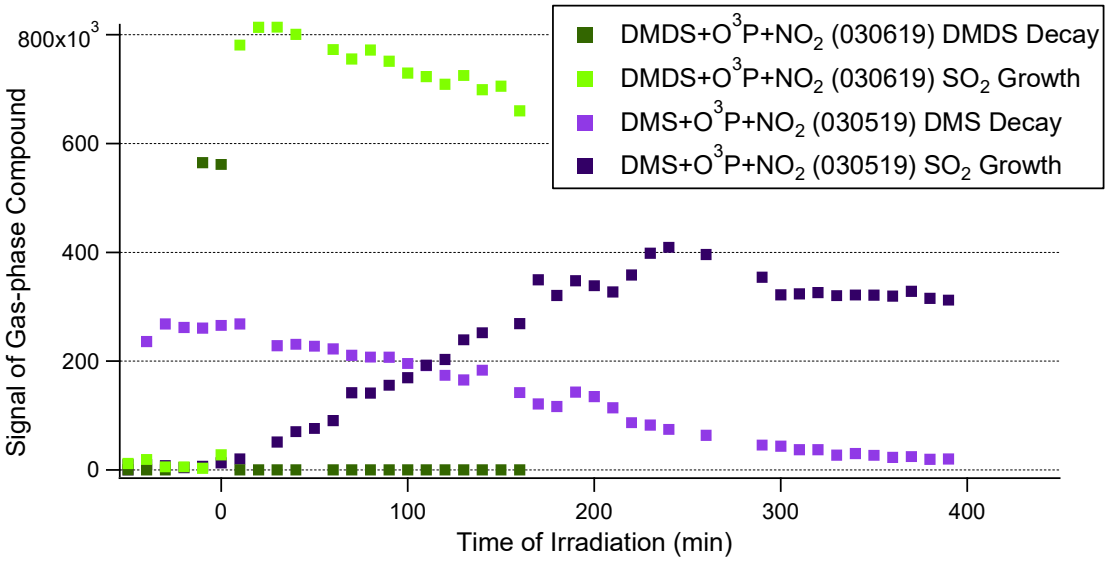

Figure 4-7: Precursor decay and sulfur dioxide formation during humid $O(^3P)$ oxidation experiments.

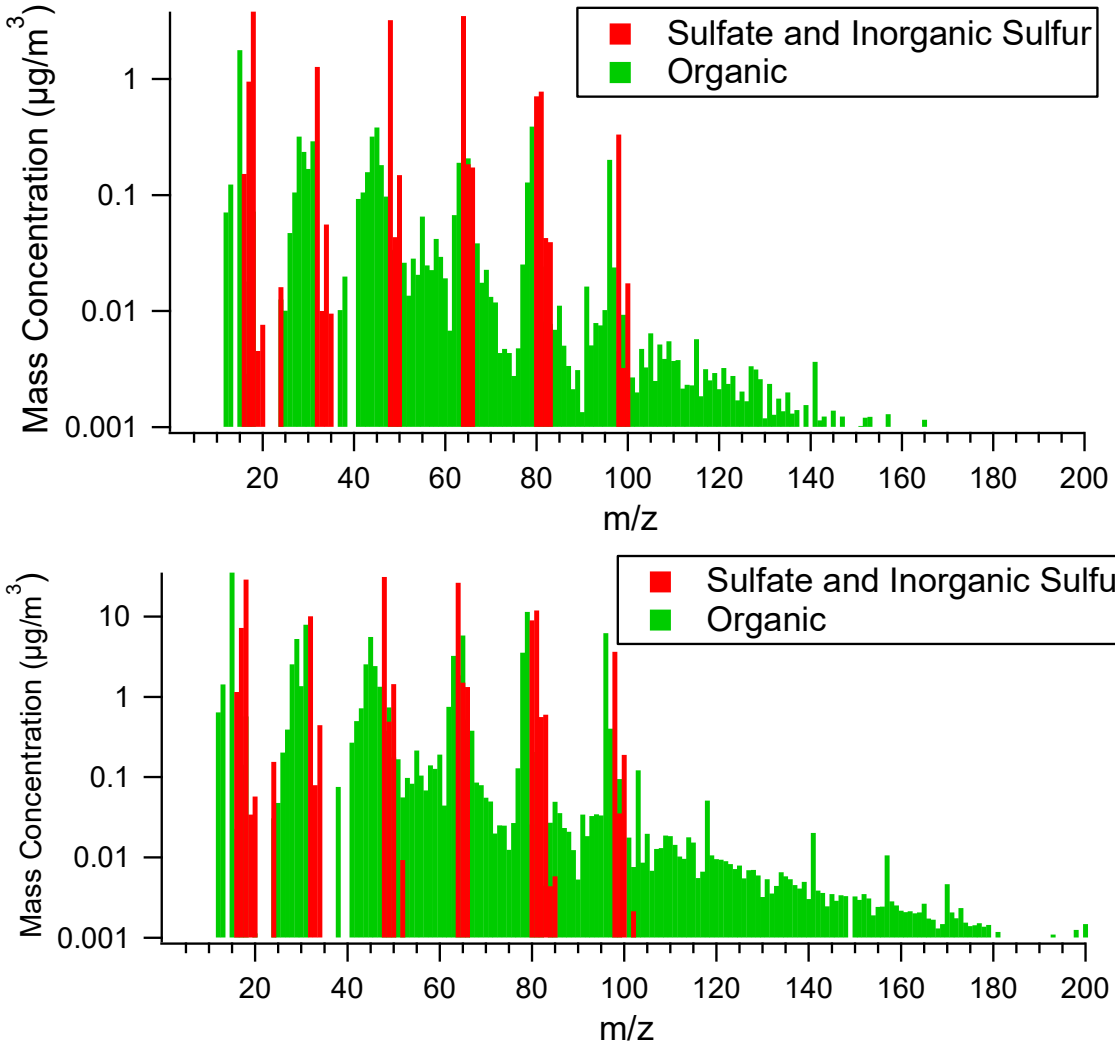

Figure 4-8: Average aerosol mass spectra, as measured by the AMS, for (top) $DMS + O(^3P) + NO_x + 40\%RH$ (030519) and (bottom) $DMDS + O(^3P) + NO_x + 40\%RH$ (030619)

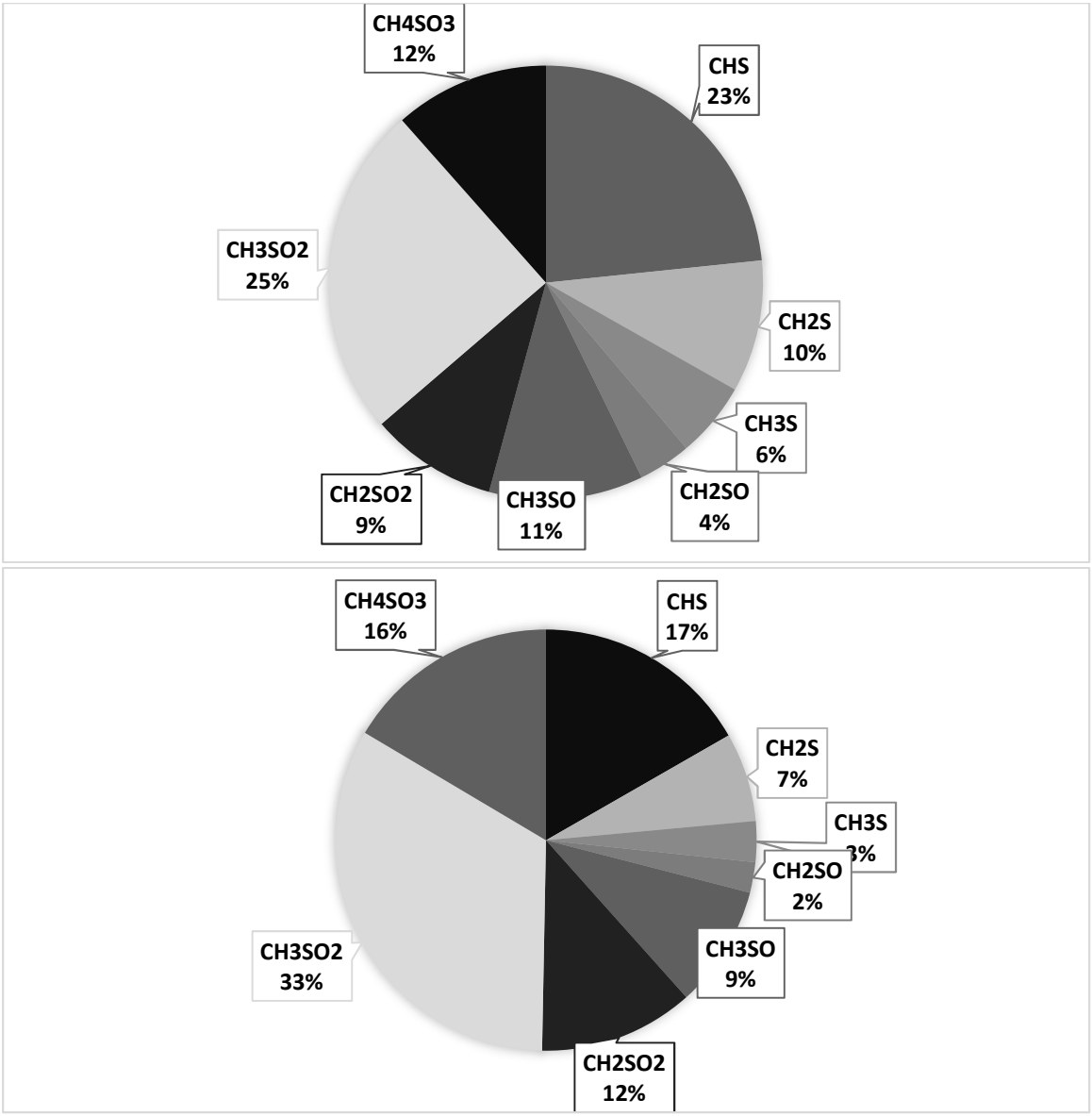

Figure 4-9: Fraction of each compound fragment that makes up the total sulfur-containing organic during the following oxidation experiments:

Top: $DMS + O(^3P) + NO_x + 40\%RH$ (030519)

Bottom: $DMDS + O(^3P) + NO_x + 40\%RH$ (030619)

Calculated by averaging the final 100 minutes of AMS data for each experiment.

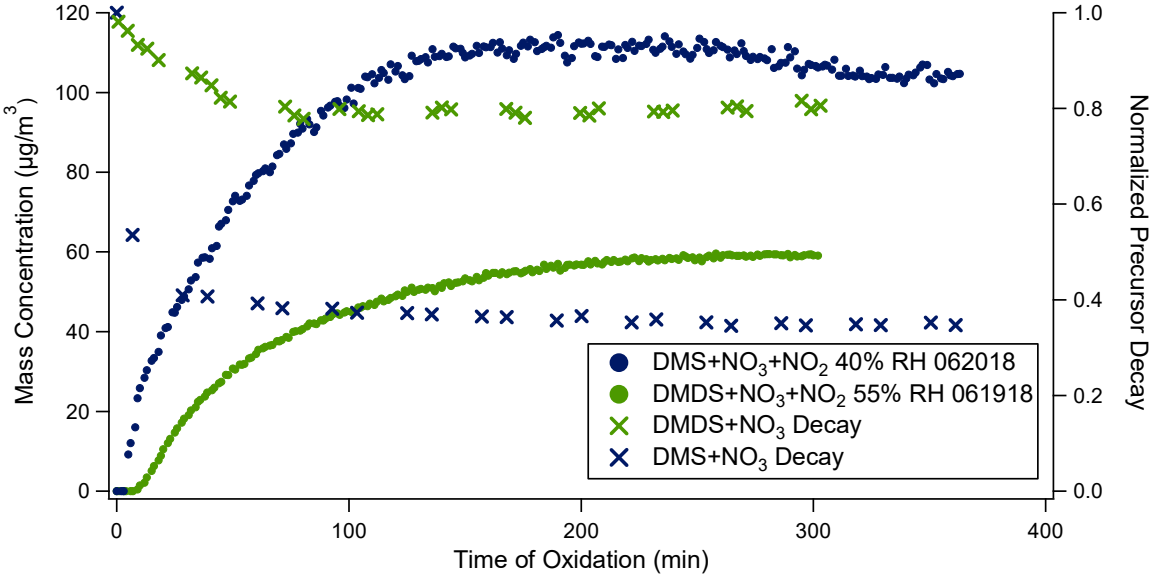

Figure 4-10: Mass concentration time series and normalized precursor decay (SIFT-MS) for nitrate radical oxidation of reduced sulfur compounds.

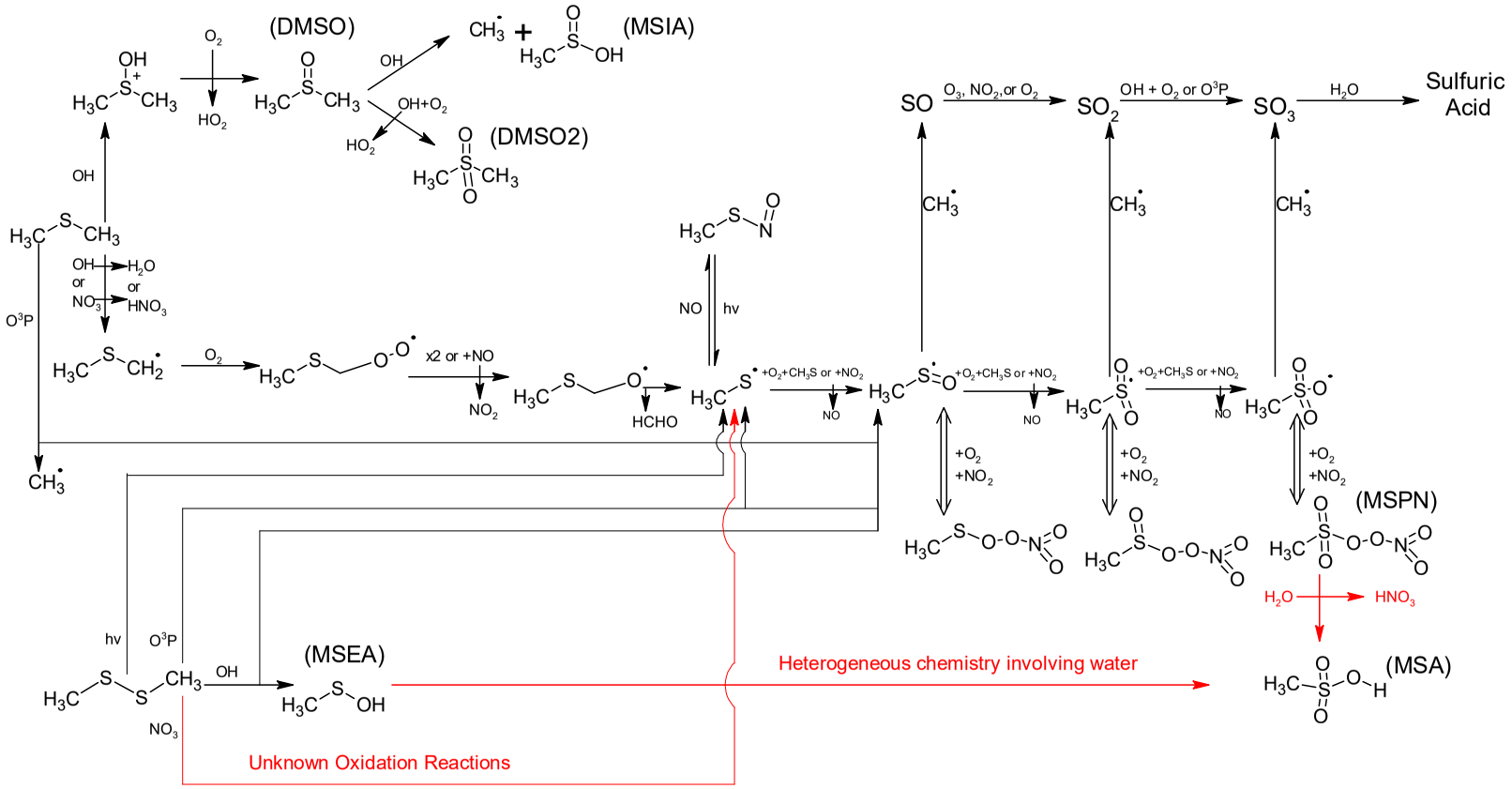

Figure 4-11: A possible mechanism by which aerosol forms through oxidation of DMS and DMDS by $OH, O(^3P)$, and NO_3. Black is representative of pathways that have previously been proposed and are supported by this research. Red represents changes to the previously proposed mechanisms based on the research presented here.

Chapter 5: Oxidation of Amines in the Presence and Absence of Reduced Sulfur Compounds

This chapter will discuss results from chamber experiments investigating the oxidation of amines (trimethylamine, butylamine, diethylamine) and ammonia under dry and humid conditions. Additionally, results from interaction experiments, involving oxidation of an amine and a reduced sulfur compound together, will be presented. Atmospheric implications of these results will be discussed.

5.1 Hydroxyl Radical Oxidation of Trimethylamine

Trimethylamine reacts with hydroxyl radical under dry and humid conditions to form approximately 80 and 95 $\frac{\mu g}{m^3}$ of aerosol, respectively (Figure 5-1). Aerosol yields were calculated to be similar at 37 and 41% (Table 5-1). The slightly higher mass concentration under humid conditions is likely due to condensation of water, as is evident by a lower density of 1.45$\frac{g}{cm^3}$ as compared to 1.55$\frac{g}{cm^3}$ (Table 5-1). If it is assumed that the 15 $\frac{\mu g}{m^3}$ concentration increase between dry and humid conditions, which makes up 16% of the total wet aerosol mass, is due to water condensation, a theoretical density of 1.48 $\frac{g}{cm^3}$ is calculated. This theoretical density value matches well with the measured value under humid conditions.

Gas-phase products of this reaction as measured by the SIFT-MS include oxidized compounds at m/z 74, 88, and 102 during the H_3O^+ ion scan and m/z 103, 117, and 131 during the NO^+ ion scan (Figure 5-2). This indicates the formation of gas phase products

with a molecular weight of 73, 87, and 101 $\frac{g}{mol}$, consistent with TMA oxidation products dimethylformamide, N-formyl-N-methylformamide, and N,N-diformylformamide and in agreement with previous research conducted by Price et al., 2014 as well as other studies (Lee et al., 2013, Pitts et al., 1978).

Particle-phase products, as measured by the HR-ToF-AMS, contain identical prominent peaks under dry and humid conditions, providing further evidence that water is simply condensing onto the particulate and not involved in any chemistry. The product fragments include the formation of high mass-to-charge ratio peaks such as m/z 88, 104, 133, 145, 161, and 191 (Figure 5-3 A). These fragments have been discussed in depth by Price et al., 2014 and are considered to be evidence of oligomer formation stemming from a $RO_2^{\cdot}$ radical formed through further oxidation of dimethylformamide. Other prominent peaks include m/z 76 and 122, fragments of $C_3H_9NO_6$ which is proposed by Price et al., 2014 to form through a reaction involving hydrogen rearrangement after TMA is oxidized by hydroxyl radical and oxygen. Simplified mechanisms of these particle forming pathways can be seen on Figure 5-14. The final notable peak is m/z 58, which is considered to be an amine aerosol indicator (Silva et al., 2008, McLafferty et al., 1993). Here, this peak fit to an oxidized nitrogen-containing organic fragment: C_2H_4NO. Bulk composition of the particulate formed during oxidation of TMA under dry and humid conditions, as seen on Figure 5-4 A and B, shows similar trends. Nearly 50% of the total non-water aerosol mass are made up of oxidized organics fragments, with an additional 15% made up of oxidized nitrogen-containing organic fragments. Reduced nitrogen-containing organic fragments contribute to approximately 20% of the total mass.

5.2 Dry Hydroxyl Radical Oxidation of Trimethylamine and Dimethyldisulfide

Under dry conditions, the TMA-DMDS interaction experiment forms a steadily increasing mass concentration of 186 $\frac{\mu g}{m^3}$ after 400 minutes (Figure 5-1). This is 1.4 times greater than the addition of the mass concentration formed during the two dry individual precursor experiments. As explained in previous chapters, the steady increase of aerosol concentration is a result of slow oxidation of sulfur dioxide to sulfuric acid. Gas-phase nitrogen containing products no longer include N-formyl-N-methylformamide and N,N-diformylformamide, compounds that were previously measured in TMA individual precursor experiments. A small increase in dimethylformamide, the first stable oxidation product of TMA, is detected.

HR-ToF-AMS data presents none of the high mass-to-charge ratio particle fragments that were formed during TMA oxidation (Figure 5-3 C). There are two important nitrogen-containing peaks to recognize: m/z 58, the amine aerosol indicator, and m/z 73, particulate dimethylformamide. Previously, during the TMA single precursor experiment, m/z 58 was fit to an oxidized nitrogen-containing organic fragment; here it is fit to C_3H_8N, a reduced fragment. The particulate dimethylformamide fragment at m/z 73 is the highest nitrogen-containing organic fragment and the only major oxidized nitrogen-containing fragment. In fact, less than 1% of the total aerosol mass consists of oxidized nitrogen-containing organic fragments while 45% of the mass consists of reduced nitrogen-containing organic fragments (Figure 5-4 E). This is in contrast with single precursor TMA oxidation experiments where oxidized nitrogen-containing organics made up

approximately 15% of the total aerosol mass while only 20% was made up of reduced nitrogen-containing organic fragments. This lack of highly oxidized gas- and particle-phase products suggests that DMDS products are inhibiting the oxidation and growth of amine oxidation products and oligomers.

Sulfur-containing particle fragments include peaks at m/z 96 and 79. As discussed in previous chapters, these peaks are indicative of methanesulfonic acid formation and can be used to estimate the fraction of mass that can be explained by methanesulfonic acid formation. This information is presented in Figure 5-4 E as well as Table 5-2. Nearly 30% of the total aerosol mass can be explained by the formation of methanesulfonic acid. 55% of the SO_x aerosol fragments can be explained by methanesulfonic acid, indicating that sulfuric acid is still an important aerosol product.

During individual precursor DMDS experiments, humidity and NO_2 were necessary in order to form methanesulfonic acid. This is the first occasion in this study where methanesulfonic acid formed under extreme dry conditions. Previous studies have shown that TMA or other amines can react with methanesulfonic acid and/or sulfuric acid to nucleate particles (Chen et al., 2015, 2017, Bork et al., 2014); these results were verified by injecting gas-phase TMA and methanesulfonic acid into the chamber. However, the formation of methanesulfonic acid under dry conditions suggests that TMA is not only important to methanesulfonic acid nucleation, it is also important to the formation of methanesulfonic acid.

Methanesulfonic acid is likely formed under dry conditions through a hydrogen-abstraction reaction between $CH_3SO_3^{\cdot}$ and the TMA precursor. This reaction would also

yield a $R^{\cdot}$ radical that can go on to form TMA oxidation products like dimethylformamide. The formation of methanesulfonic acid along with sulfuric acid can explain the lack of high mass-to-charge ratio oxidized nitrogen-containing organic fragments. Because TMA is basic, it can directly react with sulfuric acid and methanesulfonic acid to form a salt. This means TMA has essentially four competing initial reactions, only two of which would result in oxidation of TMA. This salt reaction explains the high fraction of reduced nitrogen-containing organic fragments. Some of TMA is allowed to oxidize and form dimethylformamide. As dimethylformamide is slightly basic, it will also react with acids to form salts. Glasoe et al., 2015 pointed out that amides are much less effective at reacting with sulfuric acid to form a salt, as compared to the more basic amines. However, given the excess acid in the reaction system, these amides are still able to play a role in particle formation here. This is consistent with the presence of gas- and particle-phase dimethylformamide in low concentrations as well as the lack of gas-phase N-formyl-N-methylformamide and N,N-diformylformamide. Because the high mass-to-charge ratio amine oligomer fragments require further oxidation of dimethylformamide, they are unable to form in the presence of acids.

The high mass-to-charge ratio non-oligomer peaks, m/z 76 and 122, do not require further oxidation of dimethylformamide in order to form. However, the TMA reaction mechanism suggests that there is a competition between hydrogen-rearrangement of $RO_2^{\cdot}$ to form these products, and $RO_2^{\cdot}$-$RO_2^{\cdot}$ reactions to further oxidize TMA and form $RO^{\cdot}$ radicals. Because of the higher concentration of $RO_2^{\cdot}$ radicals during the interaction experiment, the hydrogen-rearrangement pathways is suppressed. A mechanism for these

TMA-DMDS oxidation reactions can be seen on Figure 5-14. This mechanism notes multiple competing initial TMA reactions. While the reaction rates for most of these reactions are unknown, the combined initial reaction is expected to increase. This increase in initial reaction rate is captured by a comparison between the decay of TMA during a single precursor experiment to that of an interaction experiment (Figure 5-5). The interaction experiment results in a substantially faster decay of TMA than the individual precursor experiment, indicating that TMA is reacting with more than just hydroxyl radical.

To provide further evidence of the importance of TMA to methanesulfonic acid formation, an oxidant-free TMA-DMDS experiment was conducted with black lights on. This would allow DMDS to photodegrade and oxidize while the TMA precursor stayed intact. During this experiment, gas-phase TMA was consumed through a direct reaction with methanesulfonic or sulfuric acid, as indicated by the high fraction of reduced nitrogen-containing organic fragments (Figure 5-4 D). The formation of methanesulfonic acid, along with the presence of a prominent HR-ToF-AMS peak at m/z 73 and the formation of a small fraction of oxidized nitrogen-containing organics in the absence of an oxidant provide additional evidence that $CH_3SO_3^{\cdot}$ radical is reacting with TMA to form methanesulfonic acid and allow for TMA to oxidize to dimethylformamide.

Interestingly, in contrast with the dry DMDS individual precursor photodegredation experiment, this oxidant-free interaction experiment results in evidence of sulfuric acid formation. This suggests that the $CH_3SO_3^{\cdot}$ radical is in fact an important source of SO_3, and therefore H_2SO_4. In the absence of an amine, the concentration of sulfuric acid was not sufficient to grow particles to a size that is measurable by the SMPS. However, in the

presence of an amine and methanesulfonic acid, the particulate that forms is able to substantially grow to be measured by the SMPS.

5.3 Humid Hydroxyl Radical Oxidation of Trimethylamine and Dimethyldisulfide

In the presence of humidity, TMA and DMDS oxidized to form a steadily increasing mass concentration approaching 800 $\frac{\mu g}{m^3}$ after 375 minutes (Figure 5-1). This is 4.25 times higher than what formed during the dry reduced sulfur experiment and 5 times higher than the addition of the mass formed during the two single precursor humid experiments after allowing a similar amount of time for oxidation. Given all the DMDS and TMA is consumed, the aerosol yield is calculated to be 130%. Because the mass concentration has not leveled and SO_2 is still available, this would be a low aerosol yield estimation. The substantially higher mass concentration that formed during the humid interaction compared to the dry can likely be partially explained by condensation of water onto acidic particulate. However, given an increase in density, from 1.5 to nearly 1.8 $\frac{g}{cm^3}$, over the course of the experiment, water condensation is not the primary reason for this growth. Instead, it is likely that the presence of water vapor is speeding up and enhancing the formation of sulfuric acid, which has a density of 1.84 $\frac{g}{cm^3}$.

The aerosol composition provides further evidence of the increased prominence of sulfuric acid during the humid interaction experiment. The mass spectra shows the same lack of high mass-to-charge amine oligomer peaks that was seen in the dry interaction experiment as well as the presence of methanesulfonic acid and sulfuric acid peaks. The

fraction of total mass that can be explained by methanesulfonic acid is similar between the dry and humid experiment, as is the oxidized and reduce nitrogen-containing organic fractions (Figure 5-4 F). However, the fraction of sulfur containing inorganic fragment mass is higher under humid conditions and the fraction of this mass that can be explained by methanesulfonic acid is lower. Under dry conditions with hydroxyl radical present, 55% of the total sulfur-containing inorganic fragments can be explained by methanesulfonic acid formation. The remaining 45% can be assumed to be fragments of sulfuric acid. Similarly, under dry conditions with black lights on and in the absence of an oxidant, 50% of the total sulfur-containing inorganic fragments can be explained by methanesulfonic acid. In contrast, when humidity is present, this drops to 36%, indicating a higher fraction of sulfuric acid formation.

5.4 Humid Hydroxyl Radical Oxidation of Trimethylamine and Dimethylsulfide

TMA and DMS reacted with hydroxyl radical under humid conditions to form a mass concentration approximately 1.35 times higher than the addition of the two individual precursors, at 140 $\frac{\mu g}{m^3}$ after 400 minutes. This is nearly 6 times lower than the aerosol concentration formed during the similar DMDS interaction experiment. However, as noted in the previous chapters, DMS has a much slower initial reaction rate as compared to DMDS. Only one-third of the DMS precursor has decayed after 400 minutes. The SIFT-MS detects peaks consistent with the growth of dimethylformamide, N-formyl-N-methylformamide, and N,N-diformylformamide as well as dimethylsulfoxide,

dimethylsulfone, and methanesulfinic acid suggesting that these two compounds can at least partially oxidize in the presence of one another with minimal interaction.

While DMDS blocked TMA oligomer formation through acid-base reactions with sulfuric or methanesulfonic acid and the TMA oligomer precursors, DMS allows the formation of these amine oligomers (Figure 5-3 B). This is due to the slow initial reaction rate of DMS. DMS is not able to oxidize to an acid quick enough to consume TMA and first generation TMA oxidation products. In the absence of high acid concentrations, the branching ratio between acid-base reactions and reactions to form oligomers shifts towards the amine oligomer formation. Although the high mass-to-charge ratio peaks indicative of amine oligomer formation are still present in the DMS-TMA interaction experiment, the peaks at m/z 76 and 122 have diminished. This suggests that the additional radical species supplied by DMS oxidation is sufficient to prevent the hydrogen rearrangement discussed previously.

The presence of m/z 79 and 96 indicates methanesulfonic acid is able to form through reactions with TMA as described previously. A look at the high resolution data for m/z 58 (Figure 5-6) can be a useful indicator of a direct reaction between TMA and an acid. As discussed previously, during the individual precursor oxidation of TMA m/z 58 was fit to C_2H_4NO and during the DMDS-TMA interaction experiment this peak was fit to C_3H_8N. Here, we see both of these peaks present at m/z 58, indicating that sulfuric or methanesulfonic acid is still directly reacting with the amine precursor, but the amine is also still able to oxidize and form products.

The DMS-TMA interaction experiment results in aerosol that has smaller fraction of oxidized and larger fraction of reduced nitrogen-containing organic fragments as compared to the amine single precursor experiments (Figure 5-4 C). These fractions, as well as the methanesulfonic acid fraction, are much lower than those formed during the TMA-DMDS interaction experiment. This further implicates that the same amine-acid reaction described during the TMA-DMDS discussion is occurring here at a much slower rate.

5.5 Hydroxyl Radical Oxidation of Butylamine

Like trimethylamine, butylamine oxidized to form similar mass concentrations and compositions under both dry and humid conditions. Oxidation of butylamine results in a substantially lower mass concentration, at 14 $\frac{\mu g}{m^3}$ under humid conditions (Figure 5-7), as compared to trimethylamine. This low aerosol concentration is in agreement with a previous chamber study which recorded an aerosol yield of 7% (Tang et al., 2013). Also dissimilar to TMA oxidation, BA does not form the high mass-to-charge ratio particle fragments that are indicative to amine oligomer formation (Figure 5-9 A). Approximately 40% of the aerosol mass composition is made up of oxidized organic fragments, 5% of which also contain nitrogen (Figure 5-10 A). The remaining 60% of the aerosol mass is made up of reduced organic fragments, 17% of which also contain nitrogen.

SIFT-MS data shows mass-to-charge peaks consistent with the formation of C_4H_9NO (butyramide, H_3O^+: *m/z 88,* NO^+: *m/z* 117), $C_4H_7NO_2$ (acetoacetamide, H_3O^+: *m/z 102,* NO^+: *m/z* 131). Addition peaks at *m/z* 86 (H_3O^+) and 84 (NO^+) as well

as 100 (H_3O^+) and 99 (NO^+) may be evidence of C_4H_7NO (2-butenamide), and $C_4H_5NO_2$ (Figure 5-8). The mechanism by which these compounds form is currently unknown, but would require the formation of a C-C or C-N double bond. It is also possible that the presence of these peaks is due to fragmentation in the SIFT-MS. The SIFT uses a soft ionization source, however, fragmentation is still possible. Further investigation into the formation of these compounds, including the addition of 2-butenamide to the SIFT chemical library, is necessary prior to adding to the purposed mechanism, which can be seen on Figure 5-15.

This mechanism is based off of a nitrate radical BA oxidation mechanism proposed by Malloy et al. (2008) and a hydroxyl radical oxidation mechanism for aliphatic amines proposed by Schade et al. (1995). Several peaks with mass-to-charge values less than that of the precursor are also present and likely formed through a degradation reaction. Additionally, evidence of gas phase products with molecular weights of 127 and 141 are also present. These must be highly oxidized compounds that have possibly added a carbon to the precursor. There is currently not enough information to adequately propose a chemical formula for these compounds or a mechanism by which these compounds form.

5.6 Dry and Humid Hydroxyl Radical Oxidation of Butylamine and Dimethyldisulfide

Under dry conditions, BA and DMDS reacted to form 200 $\frac{\mu g}{m^3}$ of aerosol after 390 minutes of oxidation. After 450 minutes of oxidation under humid conditions, 680 $\frac{\mu g}{m^3}$ of aerosol formed; this is a mass concentration that is 6.2 times greater than the addition of

the mass formed during the two individual precursor experiments. The density of aerosol formed under dry conditions, 1.10 $\frac{g}{cm^3}$, is lower than that formed under humid conditions, 1.31 $\frac{g}{cm^3}$ (Table 5-1). Intuitively, it would be expected that when water vapor is present, the density would drop due to condensation of water on the particulate. Here, water is not only condensing onto the particulate, it is also involved in the formation of sulfuric acid. The increase in sulfuric acid, with a high density of 1.84 $\frac{g}{cm^3}$, combined with water condensation result in a subtle increase in aerosol density under humid condition.

The bulk composition of the aerosol formed under dry and humid conditions contains the same major peaks. Most notably, and not as prominent in the BA oxidation experiment, are peaks at *m/z* 30 and 72 (Figure 5-9 B). These peaks are fit to CH_4N and $C_4H_{11}N$. Similar to the TMA-DMDS interaction experiments, we are seeing the full BA fragment as a peak on the AMS. This, along with the presence of methanesulfonic acid peaks at *m/z* 79 and 96 as well as peaks consistent with sulfuric acid formation, indicate that a direct reaction between BA and an acid is occurring. Furthermore, the formation methanesulfonic acid during this interaction experiment under dry and humid conditions indicate that, just as in the TMA-DMDS interaction, BA can donate a hydrogen to the $CH_3SO_3^{\cdot}$ radical. This would imply that at least a small fraction of BA would further oxidize to form products. Less than 1% of the aerosol mass is made up of oxidized nitrogen containing organic fragments. Gas-phase mass spectra are not available for these experiments, however, based on what was measured in the TMA-DMDS experiments, it is likely that gas-phase BA oxidation products like C_4H_7NO are forming in much lower

concentrations due to the initial reaction competition, which can be seen on Figure 5-15. Some of these gas-phase oxidation products are likely able to react with an acid to form a salt, as was evident in the TMA interaction experiments.

Figures 5-10 C and D display the contribution of each compound family to the overall non-water aerosol mass composition and the fraction of each family that can be explained by methanesulfonic acid formation for the dry and humid BA-DMDS interaction experiments, respectively. The DMDS interaction experiments result in a mass composition that contains less than 5% oxidized organic fragment, more than half of which can be explained by methanesulfonic acid fragments. This is in stark contrast with the BA individual precursor experiment which consisted of 40% oxidized organic fragments. This further indicates the importance of a direct reaction between the amine and an acid.

A higher fraction of total methanesulfonic acid formed under dry conditions, at 30% of the total aerosol mass, as compared to humid conditions, at approximately 15% of the total aerosol mass. This drop in methanesulfonic acid's contribution to total mass under humid conditions coincides with an overall increase in the fraction of sulfur-containing inorganic fragments that cannot be explained by methanesulfonic acid formation. The unexplained fraction sulfur-containing inorganic fragments along with a higher aerosol density provide sufficient evidence to conclude that the formation of sulfuric acid is more prominent under humid conditions as compared to dry conditions. A similar, though not as prominent, trend occurred during the TMA-DMDS interaction experiments.

Under dry conditions, 96% of the sulfur-containing inorganic fragments can be explained by methanesulfonic acid formation, meaning very little sulfuric acid is forming.

The importance of the $CH_3SO_3^{\cdot}$ radical as a precursor to sulfuric acid formation was established during the TMA-DMDS dry photodegredation experiment. Here, with a minimal evidence of sulfuric acid formation, it can be said that $CH_3SO_3^{\cdot}$ radical is responsible for the bulk of the initial particulate sulfuric acid formation. Furthermore, different amines will react with the $CH_3SO_3^{\cdot}$ radical with varying strengths which will determine the branching ratio between methanesulfonic acid formation and initial sulfuric acid formation. Butylamine reacts with the $CH_3SO_3^{\cdot}$ radical more strongly to form methanesulfonic acid than trimethylamine does, as indicated by only 55% of the sulfur-containing inorganic fragments being explained by methanesulfonic acid during the dry TMA experiment. Eventually, as SO_2 slowly oxidizes, particulate sulfuric acid will continue to grow, as is evident by the continuous growth of aerosol in all reduced sulfur experiments.

Under humid conditions, the fraction of sulfur-containing inorganic fragments that can be explained by methanesulfonic acid formation drops to 33% for the BA-DMDS interaction and 36% for the TMA-DMDS interaction, indicating a higher fraction of sulfuric acid is forming. Logically, when water vapor is more readily available, as is the case under humid conditions, SO_3 should be able to react with H_2O to form higher concentrations of sulfuric acid in agreement with the trends that are seen here.

5.7 Humid Hydroxyl Radical Oxidation of Butylamine and Dimethylsulfide

Just as in the TMA-DMS interaction experiment, BA and DMS oxidized together to form salts as well as BA oxidation products. This interaction resulted in the formation

of 135 $\frac{\mu g}{m^3}$ of secondary aerosol, a value only 25% greater than the sum of the two individual precursor experiments. Approximately 10% of the dry aerosol mass can be explained by the formation of methanesulfonic acid (Figure 5-10 B). Oxidized nitrogen-containing organic fragments make up a low, but measurable fraction of the total mass, at 1%. An elevated fraction of oxidized organic fragments as compared to the DMDS interaction experiments further indicates the importance of BA oxidation, not just BA-acid salt formation, to overall aerosol formation. The slower reaction rate of DMS allows time for BA, which has an initial reaction rate nearly 10 times faster than that of DMS, to form oxidation products. This is not possible during DMDS interaction experiments because the initial DMDS reaction rate is 50 times faster than that of DMS.

5.8 Hydroxyl Radical Oxidation of Diethylamine

Oxidation of DEA under dry and humid conditions resulted in minimal aerosol formation, less than 6 $\frac{\mu g}{m^3}$ after 400 minutes. Approximately 80% of the gas-phase precursor was consumed during the experiments. Gas-phase oxidation products (Figure 5-11) include compounds with a molecular weight 101 (diacetamide, $C_4H_7NO_2$), 87 (C_4H_9NO), and 71 (C_3H_5NO), as is evident by H^+ peaks at *m/z* 102, 88, and 72, respectively and NO^+ peaks at 131, 117, and 71, respectively. Peaks at *m/z* 131 and 117 are a result of NO^+ addition, while *m/z* 71 is a result of a charge transfer. A cluster of H^+ peaks around *m/z* 45 along with a cluster of NO^+ peaks around 43 and 44 provide evidence of acetaldehyde, ethylamine, and/or ethanimine formation. Ethylamine was also measured in the gas-phase

by the AIM. Many of these products are in agreement with previous studies (Nielsen et al., 2012, Lee et al., 2013). Given the low aerosol concentrations, no unique peaks that may provide insight into particle formation were identified. Nonetheless, a possible gas-phase DEA oxidation mechanism, partially based off of the mechanism purposed by Nielsen et al. (2012) can be seen on Figure 5-16

5.9 Hydroxyl Radical Oxidation of Diethylamine: Interaction Experiments

The interaction between DEA and the reduced sulfur compounds follow the same trends as those recorded previously in this chapter for TMA and BA. Oxidation of DEA in the presence of DMS results in approximately 20 $\frac{\mu g}{m^3}$ of aerosol after 500 minutes (Figure 5-12), a concentration two-times greater than the sum of the concentration formed through oxidation of the individual precursors. The DMDS interaction experiment resulted in 650 $\frac{\mu g}{m^3}$ of aerosol under dry conditions and nearly 2400 $\frac{\mu g}{m^3}$ under humid conditions; this is approximately 7 and 24 times higher than the sum of concentrations formed during individual precursor experiments. All mass concentrations continue to increase the duration of the experiment due to slow oxidation of SO_2 and formation of sulfuric acid.

All DEA interaction experiments form aerosol with a high fraction of reduced nitrogen-containing organic fragments (Table 5-2), including full diethylamine and ethylamine fragments. Less than 1% of the aerosol fragments consist of oxidized nitrogen-containing organics. Again, a direct reaction between the amine and the acidic compounds formed through oxidation of reduced sulfurs is one particle-forming pathway. The DEA-

DMS interaction experiment has a higher fraction of oxidized organic fragments; as in previous DMS interaction experiments, this can be explained by the slow initial reaction rate of DMS. The percentage of inorganic sulfur containing organic fragments that can be explained by methanesulfonic acid formation for DEA-DMDS dry and humid conditions was similarly low at 14% and 18%, respectively. These low percentages indicate a higher fraction of sulfuric acid formation.

5.10 Hydroxyl Radical Oxidation of Ammonia: Interaction Experiments

Due to the slow initial reaction rate of ammonia with hydroxyl radical, no aerosol formed during the individual precursor oxidation experiment. Under humid conditions, the ammonia-DMS experiment formed 30 $\frac{\mu g}{m^3}$ after 320 minutes of oxidation and the ammonia-DMDS experiment resulted in nearly 2100 $\frac{\mu g}{m^3}$ of particulate after 280 minutes (Table 5-1). Under dry conditions, hydroxyl radical oxidation of ammonia and DMDS formed 315 $\frac{\mu g}{m^3}$ of aerosol after 350 minutes. Gas-phase ammonia data was unable to be measured for these experiments, however, injections of approximately 200 ppb were made in all cases. A high fraction of ammonium fragments (Table 5-2) along with evidence of methanesulfonic acid formation suggest ammonia is able to donate a hydrogen to form methanesulfonic acid as well as directly react with the acid products of DMS and DMDS in the same manner as the amines. 64% of the inorganic sulfur-containing fragments can be explained by methanesulfonic acid formation, implying that in the presence of ammonia, the branching ratio of $CH_3SO_3^{\cdot}$ shifts towards methanesulfonic acid as opposed to sulfuric acid formation.

5.11 Conclusions and Implications

The work presented here represents, to date, the only aerosol aging study focused on the oxidation of amines in the presence of reduced sulfur compounds. Previous work has established that amines and methanesulfonic or sulfuric acid can directly react and are atmospherically important to new particle formation and particle growth (Smith et al., 2010, Zhau et al., 2011, Zhang et al., 2012). This work has provided further evidence that amines can directly react with sulfuric and methanesulfonic acid to nucleate particles. Additionally, these particles can grow well above 40 nm and are highly hydrophilic, making them important to cloud condensation nuclei (Hodshire et al., 2019, Petters et al., 2007). In some cases, the interaction between amines and reduced sulfur compound results in aerosol yields of 500%, making them a potentially important source of particulate pollution, and therefore human health (Pope et al. 2006), in areas where both amines and reduced sulfurs are present, like agricultural land, coastlines, and marine environments (Trabue et al., 2008, van Pinxteren et al., 2019, Schade et al., 1995, Ge et al. 2011, Fitzgerald et al. 1991).

The results of this work suggest that amines and ammonia are not only involved in acid-base reactions with methanesulfonic acid to form particulate, they are also important to the formation of methanesulfonic acid via hydrogen donation to the $CH_3SO_3^{\cdot}$ radical. Each amine reacts with the $CH_3SO_3^{\cdot}$ radical with a different strength, which determines the branching ratio between sulfuric and methanesulfonic acid formation. The effect each individual amine has on this branching ratio can be qualitatively determined by estimating

the percentage of total inorganic sulfur-containing fragments that can be explained by methanesulfonic acid formation for each amine-DMDS interaction experiment. This information can be found on Table 5-2.

Butylamine under dry conditions, with 96% of the total inorganic sulfur-containing fragments explained by methanesulfonic acid, is very willing to donate a hydrogen to the $CH_3SO_3^{\cdot}$ radical and form methanesulfonic acid. On the other hand, only 14% of the sulfur-containing inorganic fragments can be explained by methanesulfonic acid for the DEA-DMDS dry oxidation experiment, indicating that diethylamine is less willing to give up a hydrogen to form methanesulfonic acid. After investigating the basicity, initial reaction rate, and structure of each of these amines, there is no obvious explanation for why one amine would be more willing to give up a hydrogen than another. Instead, it is likely a combination of these, and possibly other, chemical and physical properties. Future studies could focus on the importance of amine structure to the formation of methanesulfonic acid by running interaction experiment with, for example, ethylamine, diethylamine, and trimethylamine.

As discussed in the previous chapter, it is important to obtain a more complete understanding of the branching between sulfuric and methanesulfonic acid because, on a unit-mass basis, methanesulfonic acid is more important than sulfuric acid to the indirect cooling effect and of similar importance to the direct cooling effect (Hodshire et al., 2019). In chapter 4, it was determined that the presence of humidity and NO_x play a role in the fraction of total aerosol that is made up of sulfuric versus methanesulfonic acid. Here, it has been determined that the presence of amines can also play a role in the branching ratio

between sulfuric and methanesulfonic acid, further complicating the issue. However, it is important to note that in the presence of humidity in all cases, the total inorganic sulfur-containing fragments explained by methanesulfonic acid drops to between 18% and 36%, indicating that under atmospherically relevant conditions, this branching ratio shifts consistently in favor of sulfuric acid.

It is likely that the reduced sulfur radical reaction with amine precursor is not a unique case in the atmosphere. Other compound families are sure to interact with each other as well. The mass concentrations that formed during interaction experiments were substantially higher than the sum of the individual precursor experiments, suggesting that the current method of estimating mass concentrations one compound at a time is inadequate. Further research into other potentially important co-emitted compounds is necessary in order to obtain a more realistic yield estimation.

5.12 References

Bork, N., Elm, J., Olenius, T., Vehkamaki, H. (2014). Methane sulfonic acid-enhanced formation of molecular clusters of sulfuric acid and dimethyl amine. Atmospheric Chemistry and Physics 14:12023-12030.

Chen, H. H., Ezell, M. J., Arquero, K. D., Varner, M. E., Dawson, M. L., Gerber, R. B., Finlayson-Pitts, B. J. (2015). New particle formation and growth from methanesulfonic acid, trimethylamine and water. Physical Chemistry Chemical Physics 17:13699-13709.

Chen, H. H. and Finlayson-Pitts, B. J. (2017). New Particle Formation from Methanesulfonic Acid and Amines/Ammonia as a Function of Temperature. Environmental Science & Technology 51:243-252.

Fitzgerald, J. W. (1991). Marine aerosols: A review. Atmospheric Environment, Part A 25A:533-545.

Ge, X., Wexler, A. S., Clegg, S. L. (2011). Atmospheric amines - Part I. A review. Atmospheric Environment 45:524-546.

Glasoe, W. A., Volz, K., Panta, B., Freshour, N., Bachman, R., Hanson, D. R., McMurry, P. H., Jen, C. (2015). Sulfuric acid nucleation: An experimental study of the effect of seven bases. Journal of Geophysical Research-Atmospheres 120:1933-1950.

Hodshire, A. L., Campuzano-Jost, P., Kodros, J. K., Croft, B., Nault, B. A., Schroder, J. C., Jimenez, J. L., Pierce, J. R. (2019). The potential role of methanesulfonic acid (MSA) in aerosol formation and growth and the associated radiative forcings. Atmospheric Chemistry and Physics 19:3137-3160.

Lee, D. and Wexler, A. S. (2013). Atmospheric amines - Part III: Photochemistry and toxicity. Atmospheric Environment 71:95-103.

Malloy, Q. G. J., Qi, L., Warren, B., Cocker, D. R., Erupe, M. E., Silva, P. J. (2009). Secondary organic aerosol formation from primary aliphatic amines with NO3 radical. Atmospheric Chemistry and Physics 9:2051-2060.

McLafferty, F. W. (1993). Interpretation of mass spectra. University Science Books, Mill Valley, Calif.

Nielsen, C. J., D'Anna, B., Bossi, R., Gunkan, A. J. C., Dithmer, L., Glasius, M., Hallquist, M., Hansen, A. M. K., Lutz, A., Salo, K., Maguta, M. M., Nguyen, Q., Mikoviny, T., Muller, M., Skov, H., Sarrasin, E., Stenstrom, Y., Tang, Y., Westerlund, J., Wisthaler, A. (2012). Atmospheric Degradartion of Amines

(ADA): Summary report from atmospheric chemistyr studies of amines, nitrosamines, nitramines and amides, University of Oslo, Oslo.

Petters, M. D. and Kreidenweis, S. M. (2007). A single parameter representation of hygroscopic growth and cloud condensation nucleus activity. Atmospheric Chemistry and Physics 7:1961-1971.

Pitts, J. N., Grosjean, D., Vancauwenberghe, K., Schmid, J. P., Fitz, D. R. (1978). Photo-oxidation of Aliphatic-Amines under Simulated Atmospheric Conditions – Formation of Nitrosamines, Nitramines, Amides, and Photo-Chemical Oxidant. Environmental Science & Technology 12:946-953.

Pope, C. A., III and Dockery, D. W. 2006 Critical Review - Health Effects of Fine Particulate Air Pollution: Lines that Connect. Journal of the Air & Waste Management Association.

Price, D. J., Clark, C. H., Tang, X., Cocker, D. R., Purvis-Roberts, K. L., Silva, P. J. (2014). Proposed chemical mechanisms leading to secondary organic aerosol in the reactions of aliphatic amines with hydroxyl and nitrate radicals. Atmospheric Environment 96:135-144.

Schade, G. W. and Crutzen, P. J. (1995). Emissions of Aliphatic-Amines from Animal Husbandry and their Reactions – Potential source of N2O and HCN. Journal of Atmospheric Chemistry 22:319-346.

Silva, P. J., Erupe, M. E., Price, D., Elias, J. (2008). Trimethylamine as Precursor to Secondary Organic Aerosol Formation via Nitrate Radical Reaction in the Atmosphere. Environmental Science & Technology 42:4689-4696.

Smith, J. N., Barsanti, K. C., Friedli, H. R., Ehn, M., Kulmala, M., Collins, D. R., Scheckman, J. H., Williams, B. J., McMurry, P. H. (2010). Observations of aminium salts in atmospheric nanoparticles and possible climatic implications. Proceedings of the National Academy of Sciences of the United States of America 107:6634-6639.

Tang, X. C., Price, D., Praske, E., Lee, S. A., Shattuck, M. A., Purvis-Roberts, K., Silva, P. J., Asa-Awuku, A., Cocker, D. R. (2013). NO3 radical, OH radical and O-3-initiated secondary aerosol formation from aliphatic amines. Atmospheric Environment 72:105-112.

Trabue, S., Scoggin, K., Mitloehner, F., Li, H., Burns, R., Xin, H. (2008). Field sampling method for quantifying volatile sulfur compounds from animal feeding operations. Atmospheric Environment 42:3332-3341.

van Pinxteren, M., Fomba, K. W., van Pinxteren, D., Triesch, N., Hoffmann, E. H., Cree, C. H. L., Fitzsimons, M. F., von Tumpling, W., Herrmann, H. (2019). Aliphatic amines at the Cape Verde Atmospheric Observatory: Abundance, origins and sea-air fluxes. Atmospheric Environment 203:183-195.

Zhang, R. Y., Khalizov, A., Wang, L., Hu, M., Xu, W. (2012). Nucleation and Growth of Nanoparticles in the Atmosphere. Chemical Reviews 112:1957-2011.

Zhao, J., Smith, J. N., Eisele, F. L., Chen, M., Kuang, C., McMurry, P. H. (2011). Observation of neutral sulfuric acid-amine containing clusters in laboratory and ambient measurements. Atmospheric Chemistry and Physics 11:10823-10836.

5.13 Tables

Experiment	Elapsed Time (min)	Amine Consumed ΔHC_1 ppb	Reduced Sulfur Consumed ΔHC_2 (ppb)	Mass Formed ΔM_o $(\mu g/m^3)$	Density (g/cm^3)	Volume Fraction Remaining	Aerosol Yield $\frac{\Delta M_o}{\sum \Delta HC}$ (%)
TMA+OH (dry) 032019	300	95	-	82	1.55	0.84	37.1
TMA+OH (35%RH) 032119	390	100^a	-	95	1.45	0.90	40.8
TMA+DMS+OH (27%RH) 032219	430	NA	NA	143+	1.47	0.70-0.84	NA
TMA+DMDS+UV On (dry) 032319	480	NA	NA	50+	1.48	0.50-0.70	NA
TMA+DMDS+OH (dry) 032519	430	100	100	186+	1.55-1.40	0.20-0.75	30.8*
TMA+DMDS+OH (30%RH) 032419	375	100	100	790+	1.58-1.80	0.45-0.62	130.8*
DEA+OH (dry) 031419	380	NA	-	<2	-	-	NA
DEA+OH (30%RH) 031519	450	NA	-	<2	-	-	NA
DEA+DMS+OH (30%RH) 031619	505	NA	NA	20+	1.40-1.30	0.30-0.50	NA
DEA+DMDS+OH (dry) 031719	455	100^b	100^b	647+	1.30	0.90-0.95	98.1*
DEA+DMDS (30%RH) 031819	360	100^b	100^b	2388+	1.60-1.35	0.80-0.87	362.2*
BA+OH (30%RH) 040219	440	NA	-	14	1.34	-	NA
BA+DMS+OH (30%RH) 040319	475	NA	NA	135+	1.20	-	NA
BA+DMDS+OH (dry) 040519	390	100^b	100^b	200+	1.10	-	30.3*
BA+DMDS+OH (30%RH) 040419	455	100^b	100^b	682+	1.31	-	88.3*
NH_3+DMS+OH (45%RH) 031319	320	NA	NA	30+	1.74	0.40-0.50	NA
NH_3+DMDS+OH (dry) 031219	350	NA	NA	315+	1.6	0.24-0.70	NA
NH_3+DMDS+OH (35%RH) 031119	280	NA	NA	2090+	1.95-1.80	0.55-0.65	NA

Table 5-1: Physical properties and yield calculations for all amine and amine-reduced sulfur interaction oxidation experiments. In some cases, physical properties of the aerosol changed during the course of the experiment, as indicated by a range of values.

NA: Data not currently available.
a: Data currently not available, upper estimate based on TMA+OH Dry 030219 experiment.
b: Data currently unavailable, upper estimate of precursor decay based on data from TMA+DMDS interaction experiments.
+: Aerosol mass concentration has not leveled off.
*: Low estimate of yield due to the continuous growth of aerosol.

Experiment	Reduced Organic Fragments (Fraction explained by MSA)	Oxidized Organic Fragments (Fraction explained by MSA)	Sulfur-Containing Organic Fragments (Fraction explained by MSA)	Sulfur-Containing Inorganic Fragments (Fraction explained by MSA)	"Other" Fragments (Fraction explained by MSA)	Reduced Nitrogen-Containing organics or ammonium fragments*	Oxidized Nitrogen-Containing organics
TMA+OH (dry) 032019	0.11	0.48	0.00	0.00	0.08	0.18	0.15
TMA+OH (35%RH) 032119	0.08	0.46	0.00	0.00	0.11	0.21	0.14
TMA+DMS+OH (27%RH) 032219	0.09 (0.01)	0.43 (0.005)	0.01 (0.005)	0.02 (0.015)	0.11 (0.01)	0.23	0.11
TMA+DMDS+UV On (dry) 032319	0.21 (0.04)	0.22 (0.02)	0.03 (0.02)	0.09 (0.06)	0.07 (0.03)	0.37	0.02
TMA+DMDS+OH (dry) 032519	0.25 (0.07)	0.06 (0.03)	0.04 (0.03)	0.16 (0.09)	0.05 (0.05)	0.44	0.00
TMA+DMDS+OH (30%RH) 032419	0.19 (0.06)	0.03 (0.03)	0.03 (0.03)	0.22 (0.08)	0.09 (0.05)	0.45	0.00
DEA+OH (dry) 031419	-	-	-	-	-	-	-
DEA+OH (30%RH) 031519	-	-	-	-	-	-	-
DEA+DMS+OH (30%RH) 031619	0.25 (0.02)	0.10 (0.01)	0.01 (0.01)	0.09 (0.02)	0.20 (0.01)	0.36	0.00
DEA+DMDS+OH (dry) 031719	0.21 (0.02)	0.03 (0.01)	0.01 (0.01)	0.16 (0.02)	0.07 (0.01)	0.52	0.00
DEA+DMDS (30%RH) 031819	0.17 (0.02)	0.04 (0.01)	0.01 (0.01)	0.15 (0.03)	0.07 (0.02)	0.57	0.00
BA+OH (30%RH) 040219	0.41	0.37	0.00	0.00	0.00	0.17	0.05
BA+DMS+OH (30%RH) 040319	0.25 (0.02)	0.08 (0.01)	0.01 (0.01)	0.08 (0.03)	0.05 (0.02)	0.51	0.01
BA+DMDS+OH (dry) 040519	0.26 (0.08)	0.04 (0.03)	0.04 (0.04)	0.10 (0.10)	0.04 (0.04)	0.52	0.00
BA+DMDS+OH (30%RH) 040419	0.20 (0.04)	0.03 (0.02)	0.02 (0.02)	0.16 (0.05)	0.07 (0.03)	0.52	0.00
NH_3+DMS+OH (45%RH) 031319	-	-	-	-	-	-	-
NH_3+DMDS+OH (dry) 031219	0.12 (0.12)	0.05 (0.05)	0.07 (0.07)	0.27 (0.18)	0.09 (0.09)	0.40*	0.00
NH_3+DMDS+OH (35%RH) 031119	0.06 (0.06)	0.03 (0.03)	0.03 (0.03)	0.38 (0.09)	0.15 (0.06)	0.35*	0.00

Table 5-2: Average mass fraction of aerosol belonging to each compound family, based on final 100 minutes of each experiment, along with estimated fraction explained by the formation of methanesulfonic acid. All fractions are rounded estimates and may add up to greater than or less than 1. Methanesulfonic acid mass fraction estimations are based on calculations presented in Chapter 4 of this thesis. Because of the high background concentration of OH and H2O, the mass fraction of "other" fragments should be taken with a grain of salt. Sum of values in parenthesis will give total fraction of aerosol explained by methanesulfonic acid for each experiment.

5.14 Figures

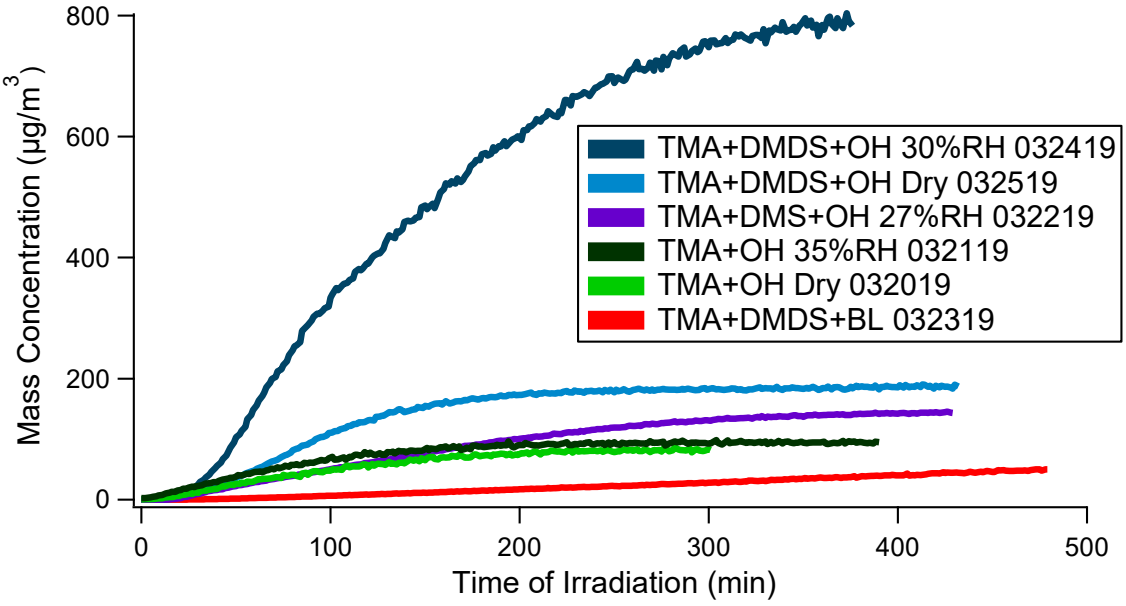

Figure 5-1: Wall-loss corrected mass concentration time series for all trimethylamine individual precursor and interaction oxidation experiments.

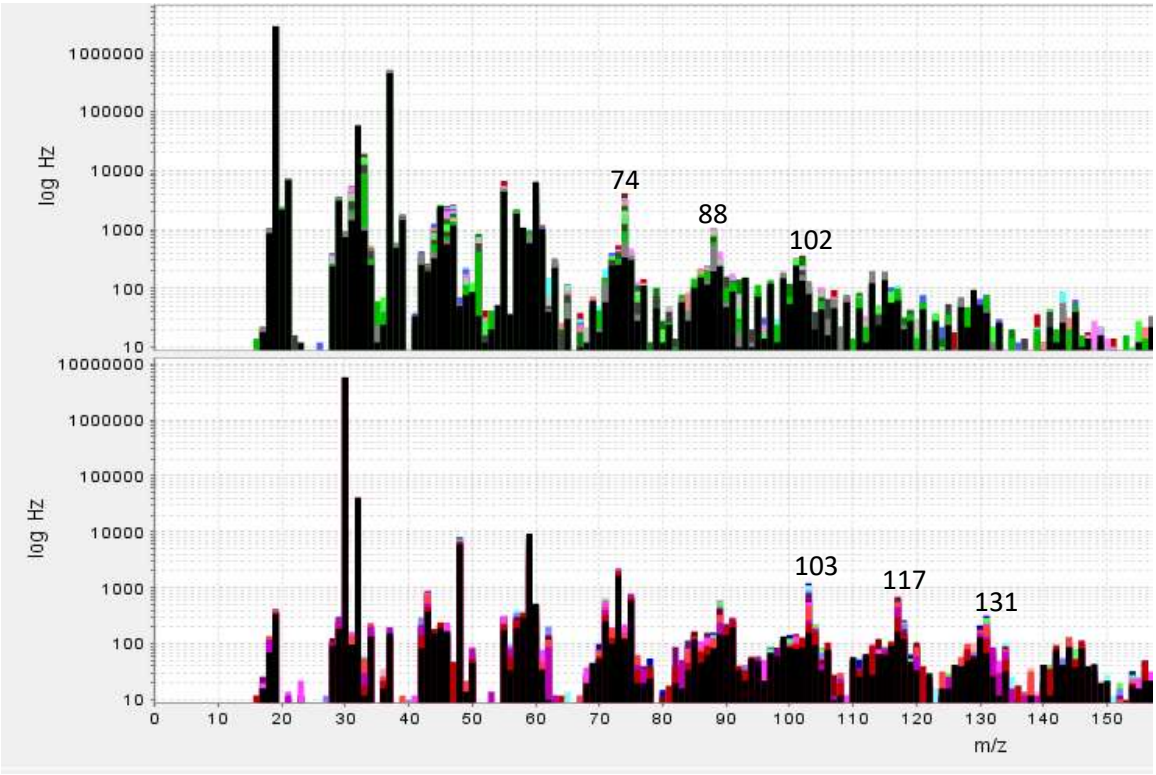

Figure 5-2: Gas-phase mass spectra showing oxidation products that formed during hydroxyl radical oxidation of trimethylamine (060118). Two reagent ions were used to measure products: H_3O^+(top) and NO^+ (bottom). The growth of a compound is indicated by the stacking of colors at any given *m/z*. Black indicates background. Several important products are pointed out.

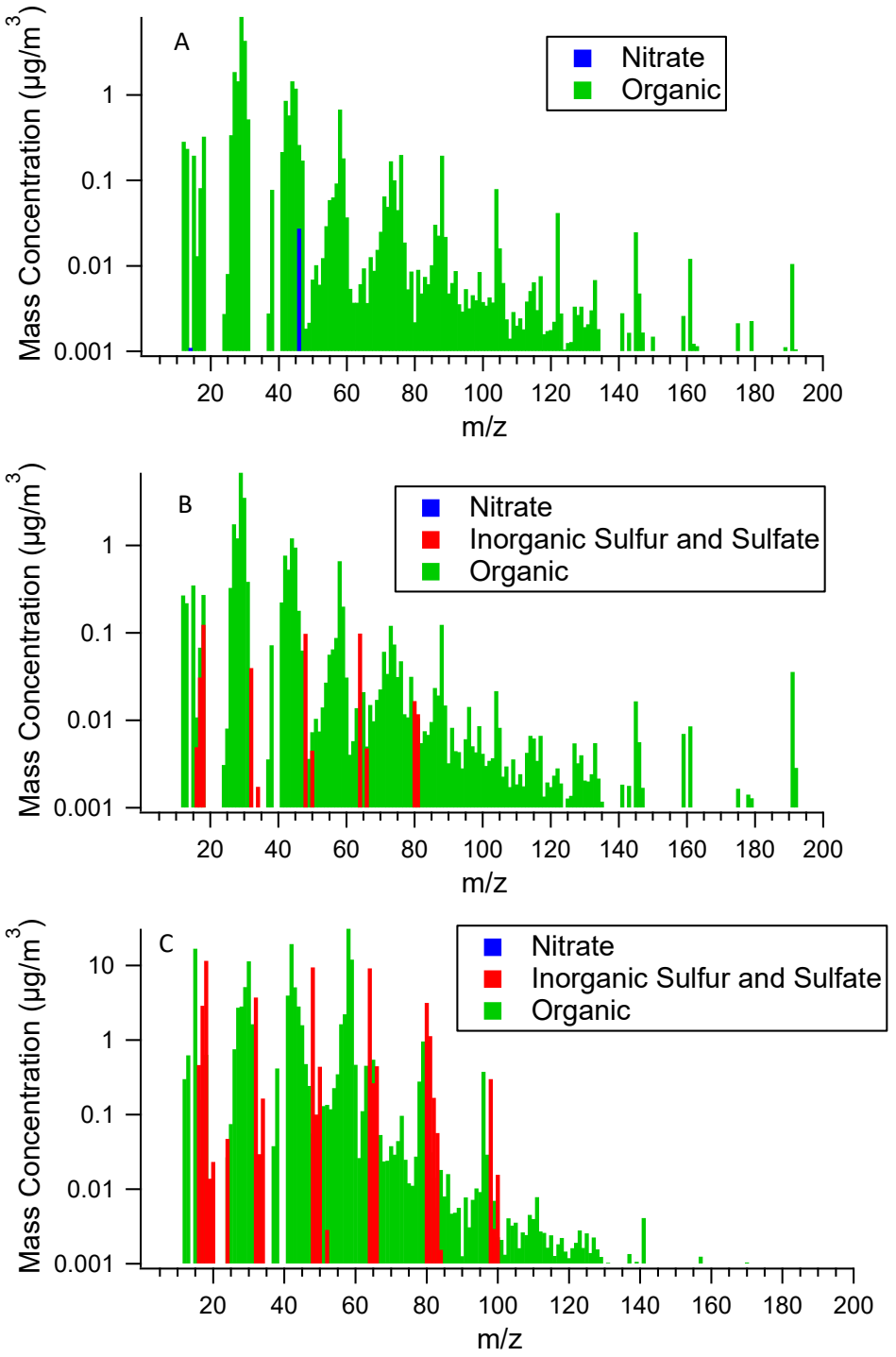

Figure 5-3: AMS average mass spectra for A) TMA+OH, B) TMA+DMS+OH, and C) TMA+DMDS+OH

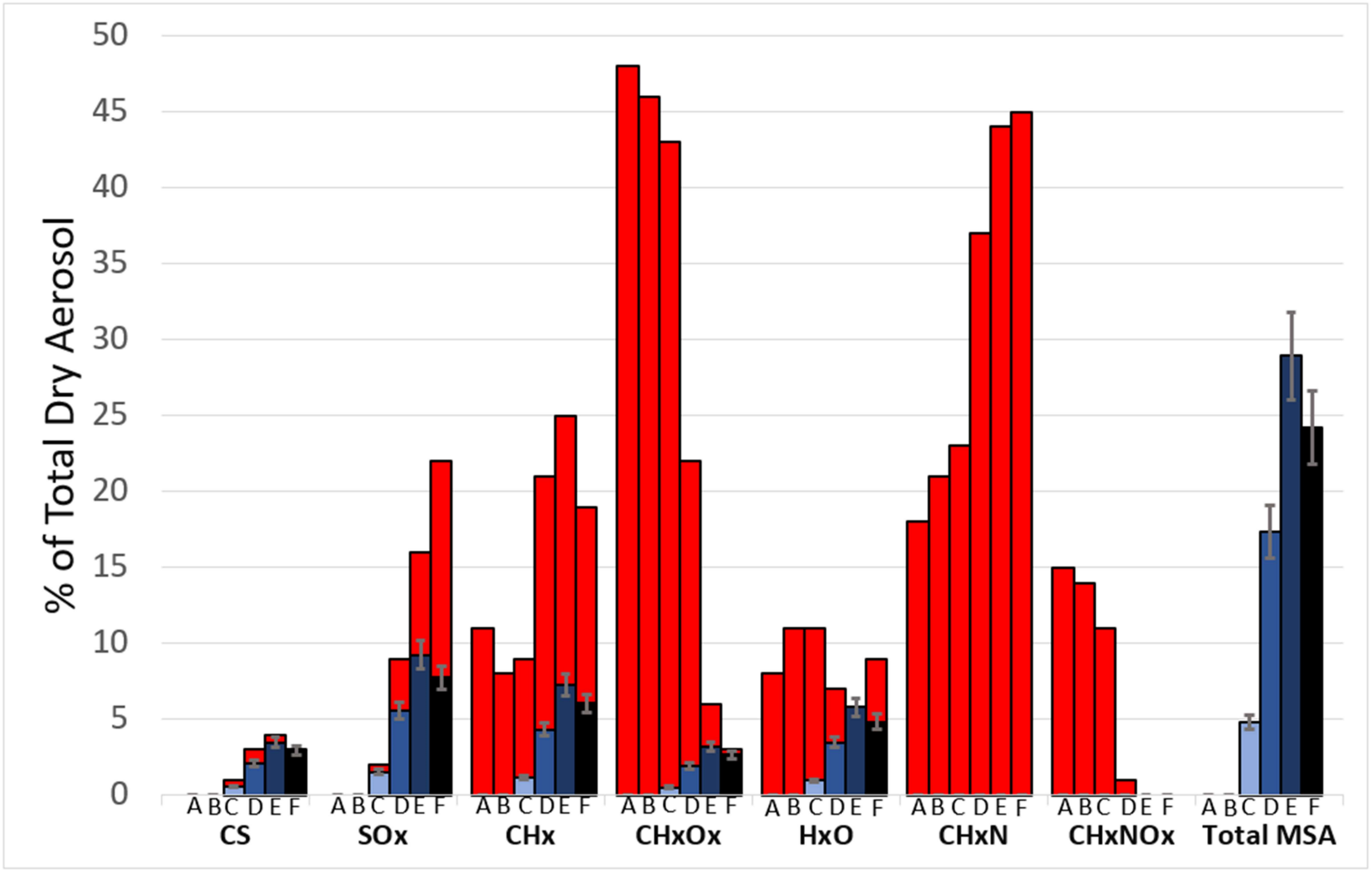

Figure 5-4: Average mass fraction of aerosol belonging to each compound family along with estimated fraction explained by the formation of methanesulfonic acid (in shades of blue) for A) TMA+OH, B) TMA+OH+27%RH, C) TMA+DMS+OH, D) TMA+DMDS+UV, E) TMA+DMDS+OH, F) TMA+DMDS+OH+30%RH. Error bars of +/- 20% of total MSA mass fraction are based on calculation differences between use of aerosol fragment CH_4SO_3 versus CH_3SO_2 to estimate mass fraction of MSA, as noted in Chapter 4 of this thesis.

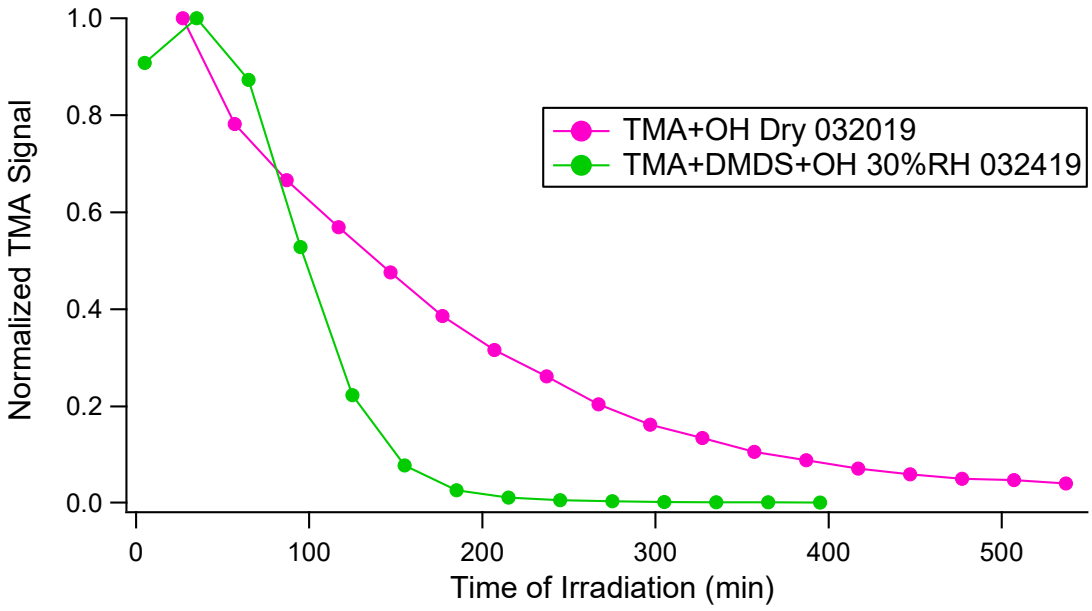

Figure 5-5: Comparison between decay rate of trimethylamine in the presence and absence of dimethyldisulfide, as measured by the SIFT-MS.

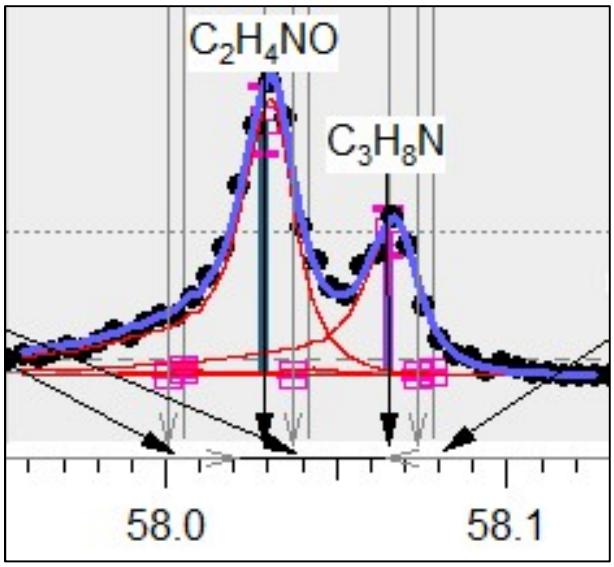

Figure 5-6: A high resolution look at amine aerosol indication *m/z* 58 for the DMS+TMA+OH experiment, as measured by the HR-ToF-AMS. Two nitrogen-containing peaks are present, one oxidized and one reduced.

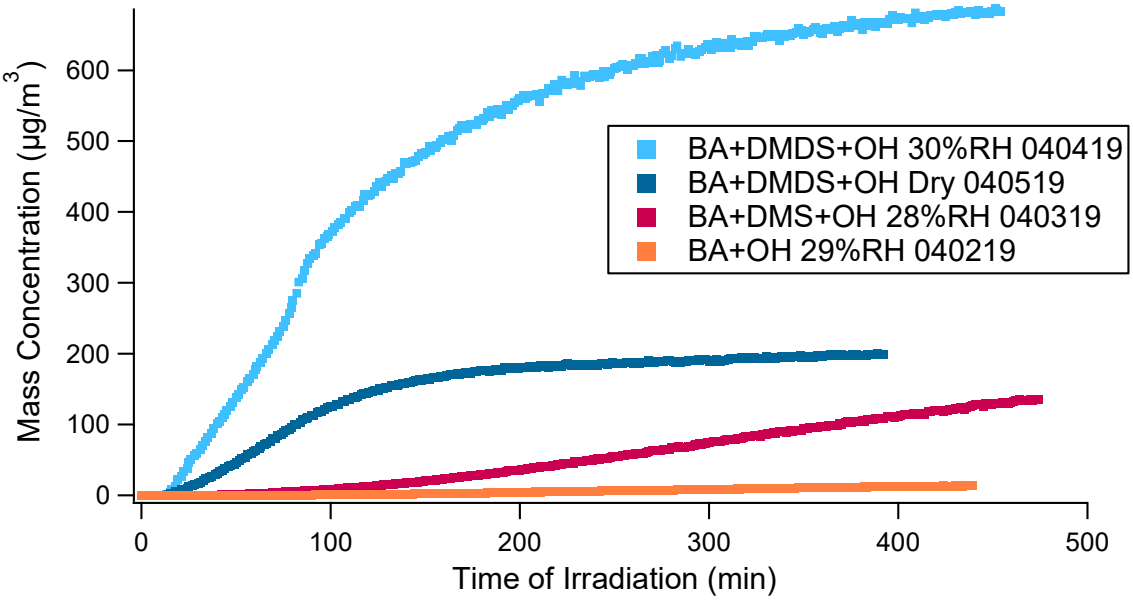

Figure 5-7: Wall-loss corrected mass concentration time series for all butylamine oxidation experiments.

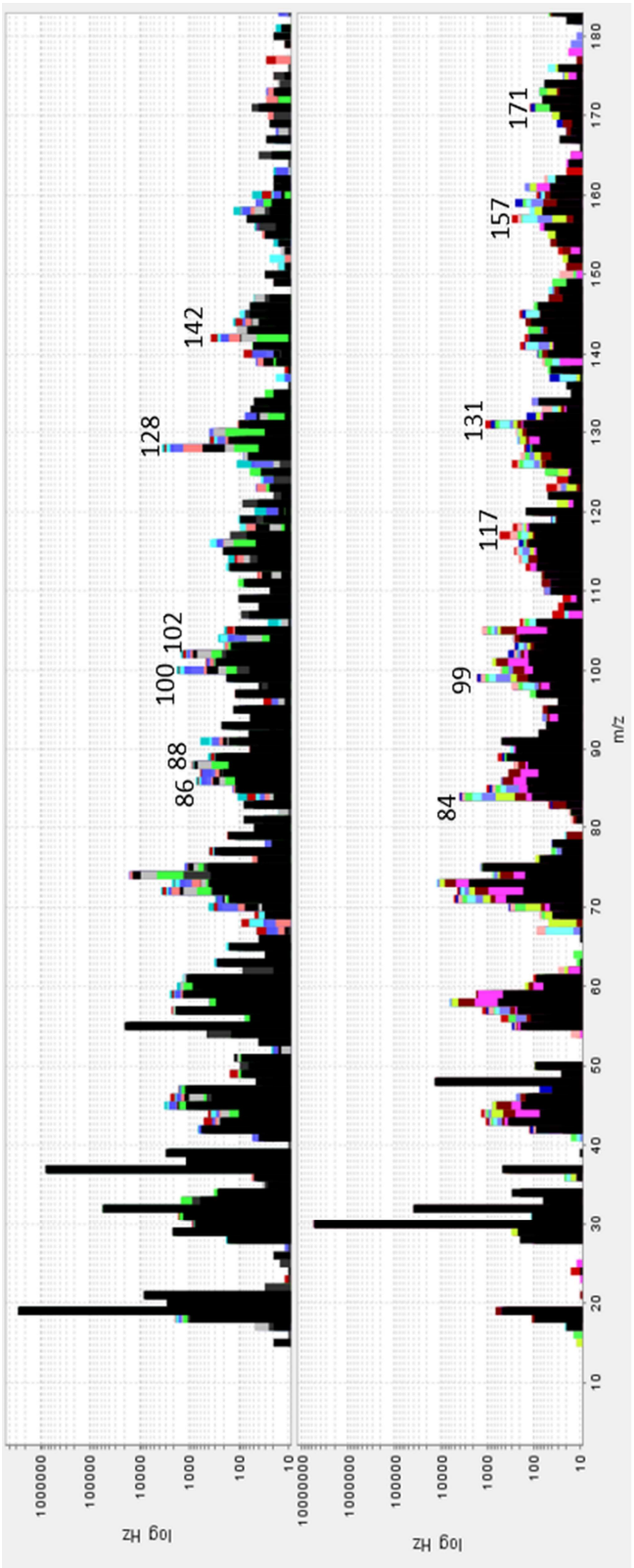

Figure 5-8: Gas-phase mass spectra showing oxidation products that formed during hydroxyl radical oxidation of butylamine (052918). Two reagent ions were used to measure products: H_3O^+(top) and NO^+ (bottom). The growth of a compound is indicated by the stacking of colors at any given *m/z*. Black indicates background. Several important products are pointed out.

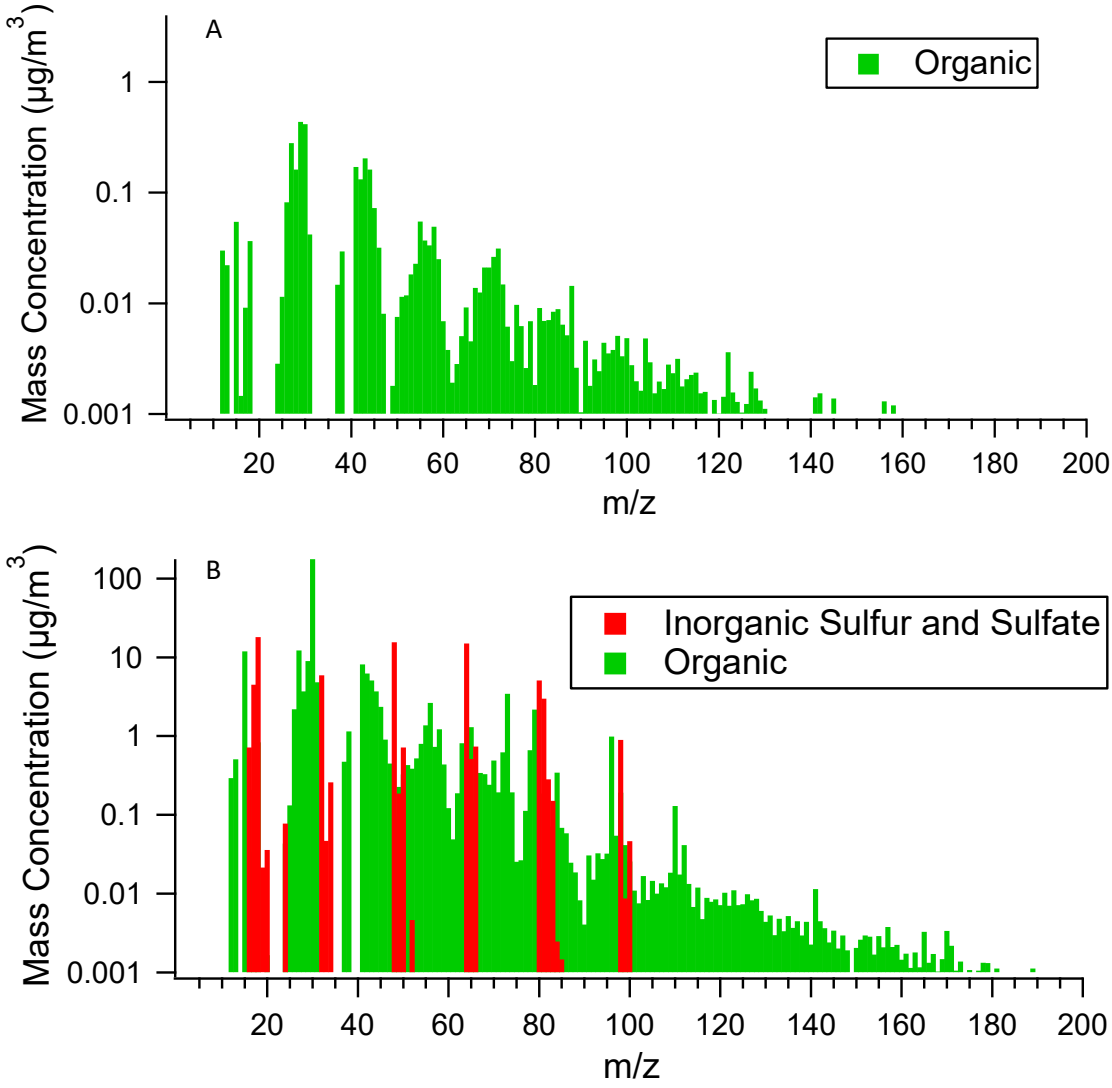

Figure 5-9: Aerosol mass spectra for (A) BA+OH and (B) BA+DMDS+OH oxidation.

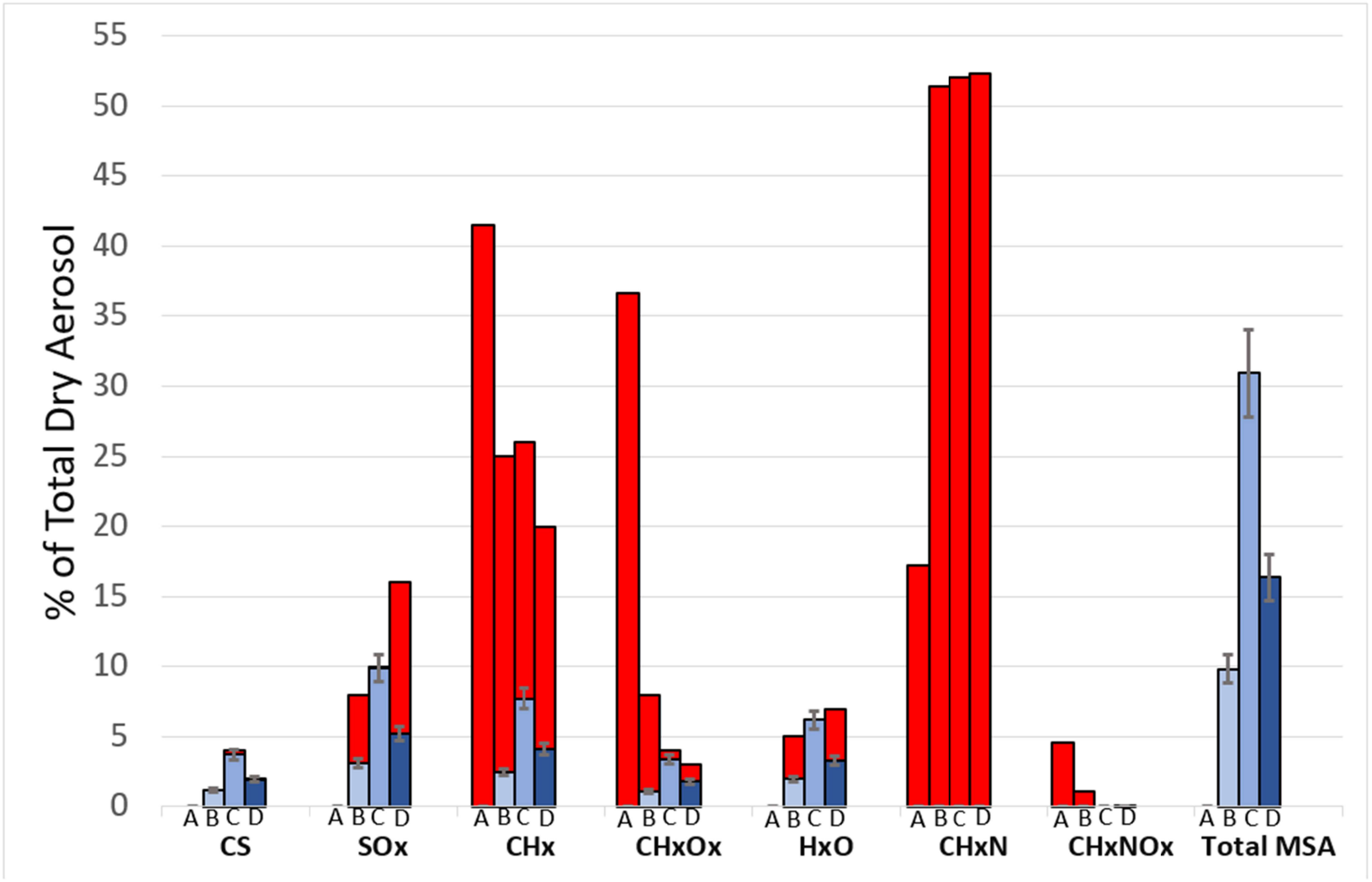

Figure 5-10: Average mass fraction of aerosol belonging to each compound family along with estimated fraction explained by the formation of methanesulfonic acid (in shades of blue) for A) BA+OH+30%RH, B) BA+DMS+OH+30%RH, C) BA+DMDS +OH, D) BA+DMDS+OH+30%RH. Error bars described in Figure 5-4.

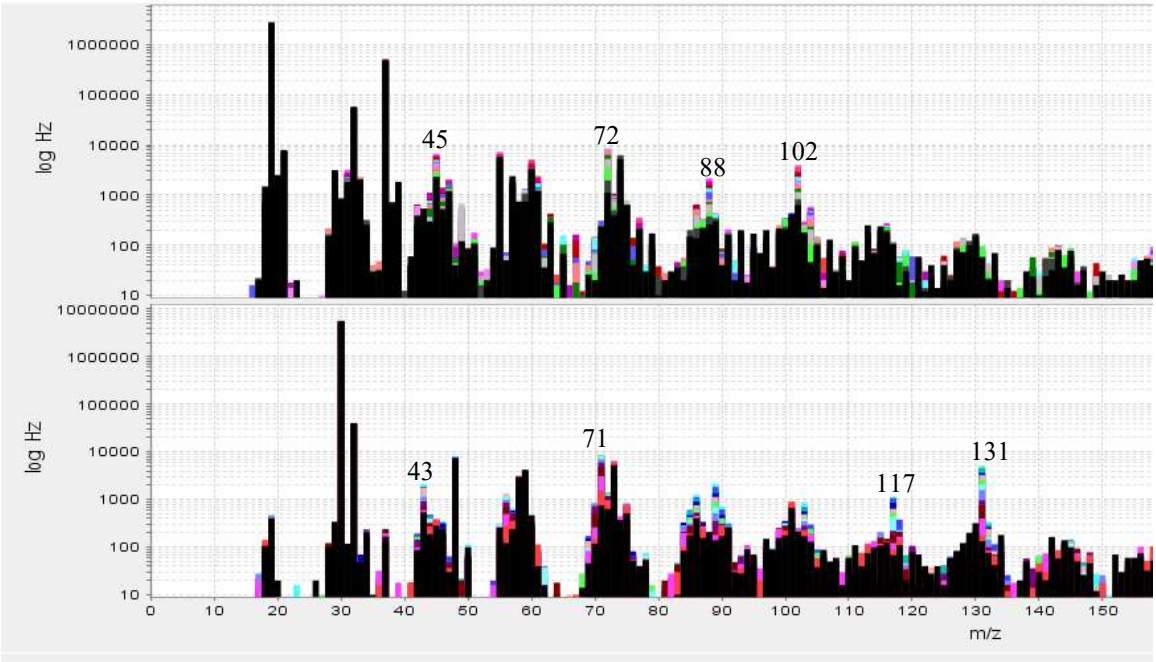

Figure 4-11: Gas-phase mass spectra showing oxidation products that formed during hydroxyl radical oxidation of diethylamine (052318). Two reagent ions were used to measure products: H_3O^+(top) and NO^+ (bottom). The growth of a compound is indicated by the stacking of colors at any given *m/z*. Black indicates background. Several important products are pointed out.

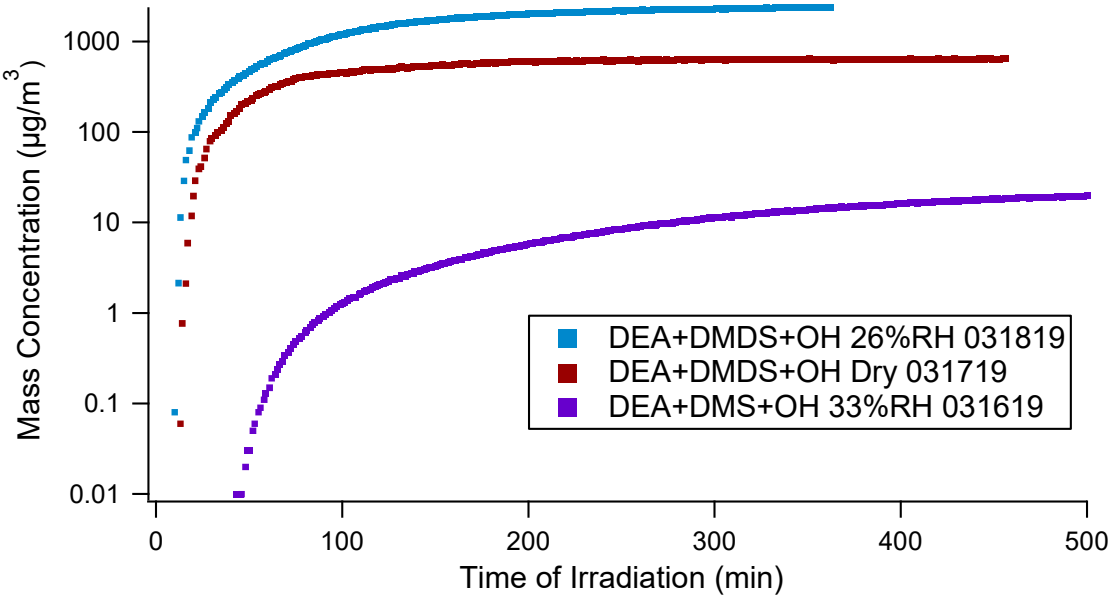

Figure 4-12: Mass concentration time series for DEA interaction experiments. Concentration is in log scale.

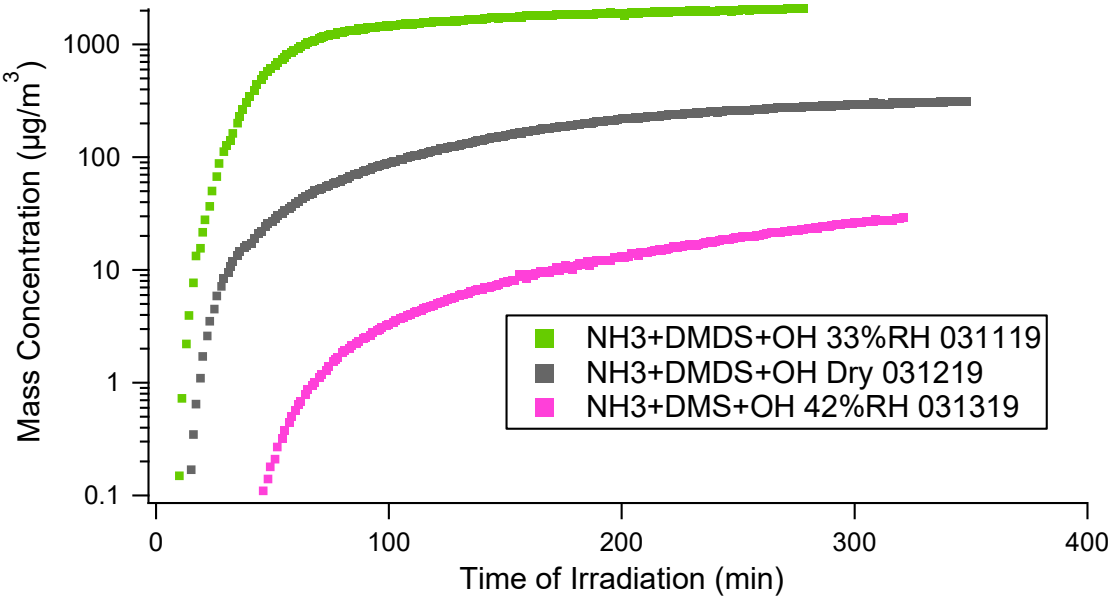

Figure 5-13: Mass concentration time series for ammonia interaction experiments. Concentration is in log scale.

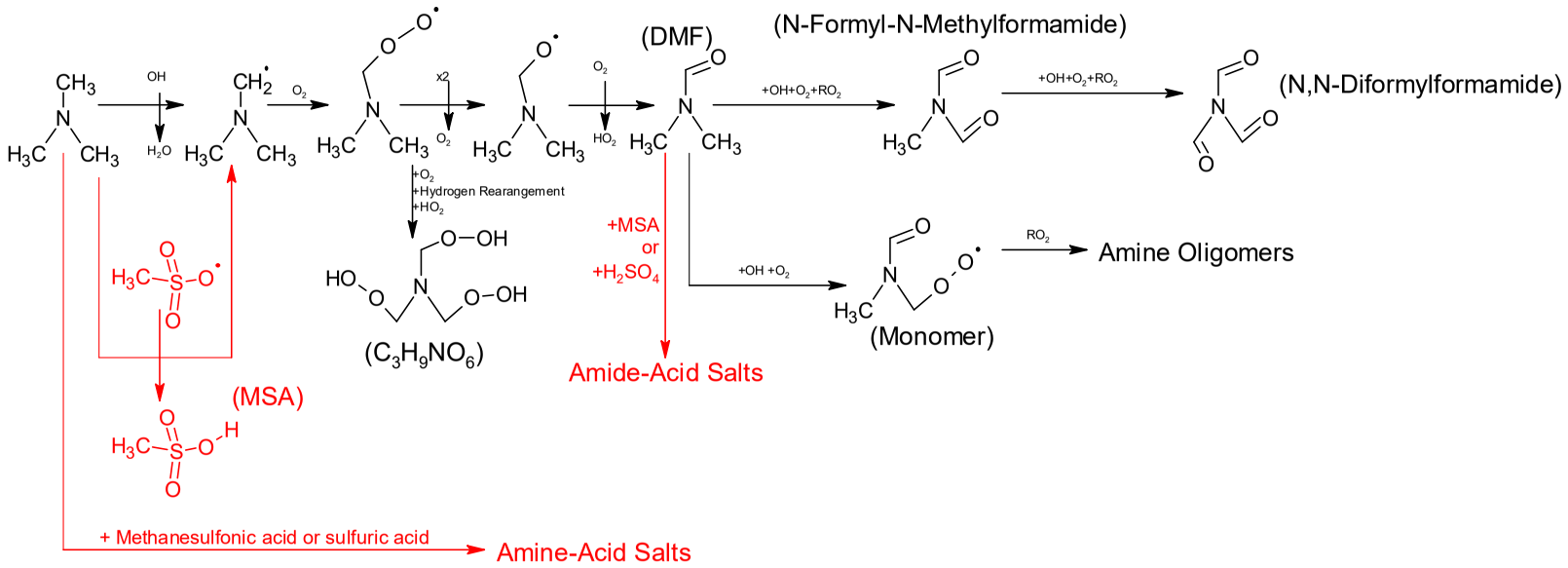

Figure 5-14: Simplified mechanism for oxidation of TMA by hydroxyl radical (black), along with ways in which TMA and TMA oxidation products interact with reduced sulfur oxidation products (red).

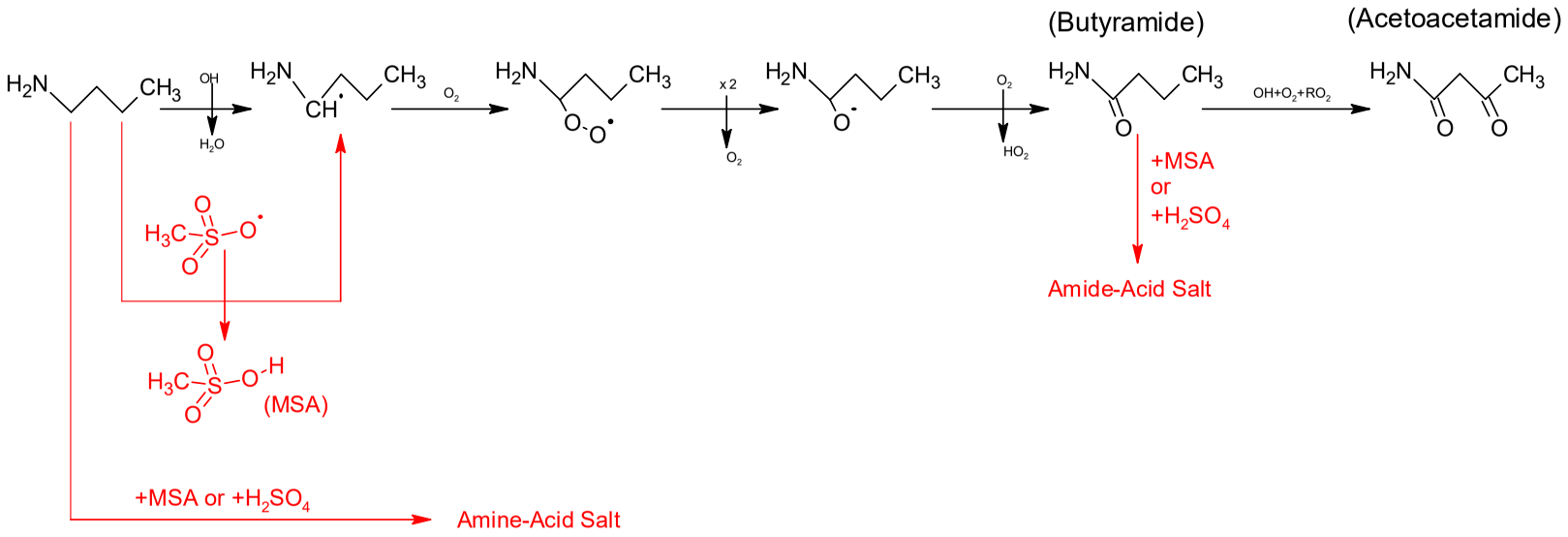

Figure 5-15: Simplified mechanism for oxidation of BA by hydroxyl radical (black), along with ways in which BA and BA oxidation products interact with reduced sulfur oxidation products (red). It is likely that BA also oxidizes and falls apart to form more products (in a similar manner that can be seen in Figure 5-16) however, these pathways were left out due to lack of evidence found here and lack of previous studies investigating BA oxidation products.

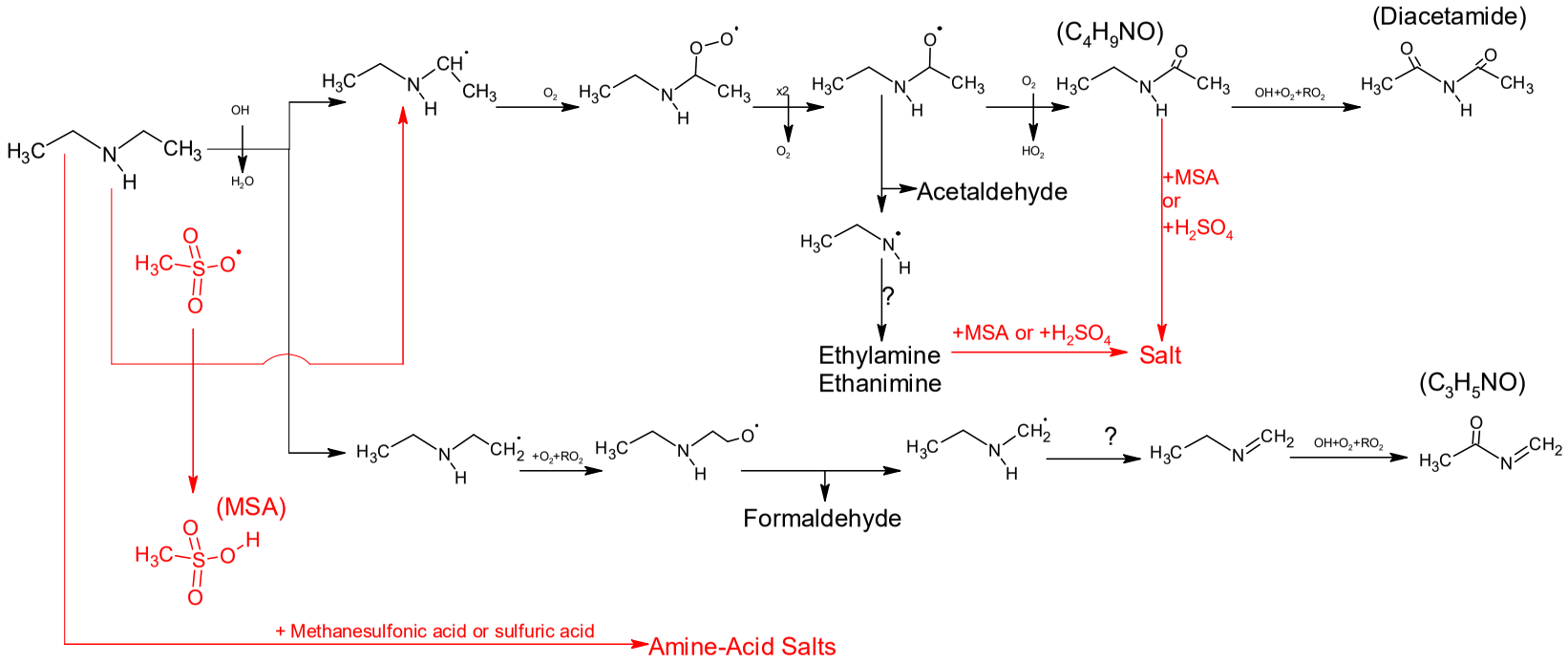

Figure 5-16: Simplified mechanism for oxidation of DEA by hydroxyl radical (black), along with ways in which DEA and DEA oxidation products interact with reduced sulfur oxidation products (red).

Chapter 6: Summary of Major Findings and Suggested Future Work

This chapter will briefly discuss the major outcomes of the research covered in this thesis. Additionally, recommendations on future work will be made.

6.1 Summary of Major Findings

Perhaps the most useful information that was provided in this thesis is the methodology to run amines and reduced sulfur compounds (or any compounds that form acids or bases) in a chamber setting. Similar methodology could be applied to flow tubes. Additionally, the procedure provided in this thesis may become important as chamber studies continue to study lower vapor pressure volatile organic compounds, as these compound are more likely to be involved in gas-wall partitioning and could off-gas during subsequent experiments. The information provided in Chapter 2 of this thesis will allow future generations of researcher to by-pass several years of struggle to obtain repeatable, contamination-free experimental results and instead focus on the project at hand.

Beyond outlining the methodology to properly run these chamber experiments, this thesis also provided information that lead to a deeper understanding of oxidation of reduced sulfur compound and amines, both individually and together, under the most atmospherically relevant conditions to date. By running reduced sulfur oxidation experiments under extreme dry as well as humid conditions, it has been determined that water vapor plays a major role in the composition of the aerosol that forms. Under dry conditions, sulfur-containing organic particulate of an unknown structure and previously

unrecorded composition forms along with sulfuric acid. When water vapor is present, even as low as 2% relative humidity, the unknown particulate does not form in abundance. Instead the aerosol consists primarily of sulfate fragments, likely because of sulfuric acid formation. It has also been determined that the presence of NO_x as well as water vapor is necessary in order to form a substantial concentration of methanesulfonic acid. Previously, the reduced sulfur oxidation mechanism did not include water vapor as an important component of methanesulfonic acid formation. Updated oxidation mechanisms have been developed and are included here. A process to estimate the fraction of dry aerosol that is made up methanesulfonic acid was also developed. Low estimates of aerosol yields have been calculated for all reduced sulfur oxidation experiments. These represent the most atmospherically relevant yield calculations to date.

By running amines under both dry and humid conditions, it was determined that water vapor does not play a major role in the composition or mass formation of secondary aerosol from amine oxidation. Amine-reduced sulfur interaction experiments gave insight into how these compound may be reacting together in the atmosphere where they are often co-emitted, especially around agricultural areas. Amines and amine oxidation products can directly react with reduced sulfur oxidation products, like methanesulfonic acid and sulfuric acid, to form aerosol. Additionally, amines can react with sulfur-containing organic radical species, resulting in the formation of amine radicals and methanesulfonic acid. Mechanisms have been developed for these interactions. The fraction of methanesulfonic acid that forms during an interaction

experiment depends on the amine present. Aerosol yield ranging from 30% to 360% were calculated for some of these interaction experiments. Aerosol yields are consistently around 3 times higher under humid conditions as compared to dry conditions, indicating humidity plays a major role in particle growth.

As noted in previous chapters, the results of these studies have important health and climate implications, in particular around agricultural areas where both of these compound families have been measured in the mid to upper ppb levels. Additionally, these studies highlight the importance of running oxidation experiments under atmospherically relevant conditions. Often times chamber experiments are run under dry conditions in order to simplify things. As is evident here, running dry experiments may result in the formation of atmospherically irrelevant chemistry. Furthermore, while flow tubes offer a quick and relatively inexpensive way to study the oxidation of an aerosol precursor, the extreme high concentrations that are used again likely result in atmospherically irrelevant chemistry, as is evident by the lack of consistency between various flow tube and chamber studies. Finally, this thesis research suggests that running traditional single-precursor experiments does not give a full picture of what is happening in the atmosphere and may result in models over- or under-estimating secondary aerosol formation.

6.2 Future work

The research presented here is ongoing. Results measured during a recent intensive chamber study by collaborators at the USDA and Claremont Colleges study are expected to arrive in the coming months. This will include gas-phase concentration data for sulfur dioxide, methanesulfonic acid, and sulfuric acid as well as particle-phase sulfuric acid and methanesulfonic acid. These new data sets will be applied to the research presented in this thesis to more accurately calculate aerosol yields and specific product yields. This will create a more robust and useful set of results.

Beyond this ongoing research, the results presented in this thesis have brought up several new research ideas listed below:

- A comprehensive field and chamber study focused on secondary aerosol formation from agricultural emissions. The research presented in this thesis has provided information of how two common agricultural pollutants react in the atmosphere, however, it is unknown if evidence of these interactions is also seen in the ambient. By deploying the SIFT-MS and the HR-ToF-AMS, or similar instruments, it would be possible to obtain sufficient evidence to determine if the interactions studied in this thesis are occurring around agricultural land. If it is determined that the interactions are not occurring, a deeper investigation into what is causing secondary aerosol formation around agricultural land is necessary. This could include gathering agricultural samples (hay, waste, pesticides, etc.) and allowing them to off-gas and oxidize in a chamber setting in an attempt to replicate secondary aerosol formation observed in the ambient and pin-point

important secondary aerosol precursors. In separate chamber studies, the major gas-phase compound measured during the off-gassing chamber study could be directly injected to try to replicate the aerosol formed during off-gassing study to determine if these gasses in high concentration are the primary source of secondary aerosol or there are compounds at lower concentration that are substantially contributing to the mass formed. In general, a deeper understanding of agricultural air quality is necessary, given approximately 10% of land worldwide is agricultural land. Pinpointing the sources of secondary aerosol, or hazardous gasses, may allow for future research in how to mitigate or treat the sources of these precursors to prevent adverse environment and human health effects.

- A temperature and NO_x sensitivity focused on oxidation of reduced sulfur compounds in an environmental chamber. Previous flow tube studies have indicated that temperature plays a major role in the branching ratio between DMS-OH addition (leading to the formation of DMSO) and DMS-OH abstraction (leading to the formation of MSA and sulfuric acid). To obtain a more complete and atmospherically relevant understanding of the effect of temperature on the aerosol forming potential of both DMS and DMDS, these compounds should be oxidized in a chamber setting at various temperatures. Additionally, previous studies, as well as this one, have pointed out the importance of NO_x to methanesulfonic acid formation. This study represents the most atmospherically relevant NO_x concentrations investigated in a chamber, at 100 ppb. Several

experiments were attempted at 10 and 20 ppb, however the NO_x depleted too quickly to obtain useful results. To investigate the effects of atmospherically relevant and available NO_x concentrations, a continuous injection method could be developed in order to supply the chamber with a constant NO_x and relevant concentration. This would provide further insight in to the true importance of reduced sulfur compounds as precursors to methanesulfonic and sulfuric acid.

- A more general multiple precursor oxidation study. The results of this study suggest that traditional single-precursor yield calculations may adequately capture true potential of any given compound to form aerosol in the atmosphere. More multiple precursor experiments, either involving commonly co-emitted compounds or commonly studied compounds, should be conducted in order to determine if the traditional single-precursor experiments are sufficient in estimating aerosol yields. If there is a major difference between single-precursor yield and multiple precursor yields, it may be necessary to switch to more complicated chamber experiments, perhaps utilizing the surrogate atmosphere developed previously, to obtain relevant yields.
- An in depth comparison between oxidation flow reaction (OFR) experiments and chamber oxidation experiments. Because OFRs are becoming a more common way to study oxidation of an aerosol precursor, it is necessary to ensure the results from OFRs match well with those from chamber experiments.

And with that, I will bring this thesis to a close. Have a nice day and don't panic!